

Diss. ETH N° 18930

**HUMAN MONOCLONAL ANTIBODIES  
FOR THE TARGETING OF MATRIX METALLOPROTEINASES**

A dissertation submitted to  
ETH ZURICH

for the degree of  
**Doctor of Sciences**

presented by  
**STEFANIE PFAFFEN**

Dipl. Pharm. Sciences ETH Zurich  
Born on May 29, 1980  
Citizen of Switzerland

Accepted on the recommendation of

Prof. Dr. Dario Neri, examiner  
Prof. Dr. Roger Schibli, co-examiner

2010



**Für meine Eltern**



# TABLE OF CONTENTS

<b>SUMMARY</b>	<b>11</b>
<b>ZUSAMMENFASSUNG</b>	<b>13</b>
<b>1 INTRODUCTION</b>	<b>15</b>
<b>1.1 <i>Antibodies</i></b>	<b>15</b>
1.1.1 Monoclonal antibodies	15
1.1.2 Antibody formats	16
1.1.3 Antibody alternatives	21
1.1.3.1 <i>Scaffolds</i>	21
<b>1.2 <i>Generation of antibodies in vitro</i></b>	<b>24</b>
1.2.1 Selection methodologies	24
1.2.2 Phage display	24
1.2.2.1 <i>ETH-2 Gold antibody library</i>	27
1.2.2.2 <i>In vitro affinity maturation by site-directed mutagenesis</i>	29
1.2.3 Iterative colony filter screening	30
1.2.4 Yeast surface display	31
1.2.5 Ribosome display	32
<b>1.3 <i>Tumor targeting</i></b>	<b>35</b>
1.3.1 The concept	35

<b>1.4</b>	<b><i>Matrix metalloproteinases (MMPs)</i></b>	<b>36</b>
1.4.1	The MMP family	36
1.4.1.1	<i>MMP-1</i>	38
1.4.1.2	<i>MMP-2</i>	39
1.4.1.3	<i>MMP-3</i>	39
1.4.2	Regulation of MMP activity	40
1.4.3	MMPs and Tissue Inhibitors of MMPs (TIMPs) in cancer	41
1.4.4	MMPs in inflammatory and vascular diseases	45
1.4.4.1	<i>Arthritis</i>	45
1.4.4.2	<i>Cardiovascular and vascular diseases</i>	46
1.4.4.3	<i>Oral diseases</i>	47
1.4.5	MMPs and potential pharmaceutical interventions	48
1.4.5.1	<i>Inhibition of MMPs</i>	48
1.4.5.2	<i>Imaging of MMPs</i>	51
1.4.5.3	<i>Targeting of MMPs for pharmacodelivery applications</i>	53
1.4.5.4	<i>MMP-specific prodrug design or MMP activated drug delivery</i>	54
<b>1.5</b>	<b><i>Aim of the thesis</i></b>	<b>57</b>
<b>2</b>	<b>RESULTS</b>	<b>59</b>
<b>2.1</b>	<b><i>Production and characterization of MMP- 1A, MMP-2 and MMP-3</i></b>	<b>59</b>
2.1.1	Cloning, expression, purification and activity measurements of recombinant catalytic domains of MMP-1A, MMP-2 and MMP-3	59

<b>2.2</b>	<b><i>Generation and characterization of scFv antibody fragments specific to MMP-1A, MMP-2 and MMP-3</i></b>	<b>61</b>
2.2.1	Antibody phage display selections	61
2.2.1.1	<i>An overview</i>	61
2.2.1.2	<i>Affinity maturation libraries</i>	62
2.2.1.3	<i>Generation of high-affinity antibodies specific to MMP-1A</i>	64
2.2.1.4	<i>Generation of high-affinity antibodies specific to MMP-2</i>	69
2.2.1.5	<i>Generation of high-affinity antibodies specific to MMP-3</i>	70
2.2.2	<i>In vitro</i> characterization of three scFv fragments specific to MMP-1A, MMP-2 and MMP-3	73
2.2.2.1	<i>Affinity measurements and specificity of scFv(SP1), scFv(SP2) and scFv(SP3)</i>	73
2.2.2.2	<i>Immunofluorescence with SP1, SP2 and SP3 on cancer and arthritic sections</i>	75
2.2.2.3	<i>Confocal laser scanning microscopy studies with the scFv fragments SP1, SP2 and SP3</i>	78
<b>2.3</b>	<b><i>Generation and characterization of antibodies in the small immunoprotein format</i></b>	<b>79</b>
2.3.1	Production and <i>in vitro</i> characterization of SIP antibodies specific to MMP-1A, MMP-2 and MMP-3	79
2.3.2	Quantitative biodistribution studies	82
2.3.2.1	<i>Biodistribution studies with SIP(5E) specific to MMP-1A and SIP(9H) specific to MMP-3</i>	82
2.3.2.2	<i>Biodistribution studies with SIP(SP1), SIP(SP2) and SIP(SP3) in F9 tumor-bearing mice</i>	83

<b>3</b>	<b><u>DISCUSSION</u></b>	<b>90</b>
<b>4</b>	<b><u>MATERIAL AND METHODS</u></b>	<b>93</b>
<b>4.1</b>	<b><u>Cell lines</u></b>	<b>93</b>
<b>4.2</b>	<b><u>Production and characterization of the antigens</u></b>	<b>94</b>
4.2.1	Cloning and expression of the murine MMP-1A catalytic domain	94
4.2.2	Cloning and expression of the murine MMP-2 catalytic domain	94
4.2.3	Cloning and expression of the murine MMP-3 catalytic domain	94
4.2.4	Activity assay for the catalytic domains of MMP-1A MMP-2 and MMP-3	95
<b>4.3</b>	<b><u>Isolation and characterization of the scFv fragments</u></b>	<b>96</b>
4.3.1	Selection of antibodies from the ETH-2-Gold library by phage display	96
4.3.2	Sequencing of scFv antibody genes	96
4.3.3	Characterization of antibody scFv fragments	96
4.3.4	Construction of affinity maturation libraries	96
4.3.5	Immunofluorescence on frozen tissue sections	97
4.3.6	Immunocytochemistry /confocal laser scanning microscopy with murine F9 teratocarcinoma cells	97
4.3.7	Immunohistochemistry on frozen tissue sections	98



4.4	<b><u>Generation and characterization of the SIP antibodies</u></b>	<b>99</b>
4.4.1	Cloning, expression, and purification of antibodies in the SIP format	99
4.4.2	Characterization of the SIP antibodies	99
4.4.3	Immunofluorescence analysis of frozen tissue sections	99
4.4.4	Radioiodination of SIP antibodies	100
4.4.5	Biodistribution of tumor bearing mice with the radiolabeled SIP antibodies	100
4.4.6	Microautoradiography	100
4.4.7	Immunofluorescence analysis of <i>in vivo</i> injected antibodies	101
4.4.8	Deglycosylation	101
4.4.9	Murine blood plasma analysis by surface plasmon resonance measurements	101
4.4.10	Biodistribution of healthy mice with radiolabeled SIP antibodies	102
<b>5</b>	<b><u>SUPPLEMENTARY MATERIAL</u></b>	<b>103</b>
<b>5.1</b>	<b><u>scFv(SP1)</u></b>	<b>103</b>
5.1.1	Nucleotide sequence	103
5.1.2	Amino acid sequence	103
<b>5.2</b>	<b><u>scFv(5E)</u></b>	<b>104</b>
5.2.1	Nucleotide sequence	104
5.2.2	Amino acid sequence	104
<b>5.3</b>	<b><u>scFv(SP2)</u></b>	<b>105</b>
5.3.1	Nucleotide sequence	105
5.3.2	Amino acid sequence	105
<b>5.4</b>	<b><u>scFv(SP3)</u></b>	<b>106</b>
5.4.1	Nucleotide sequence	106
5.4.2	Amino acid sequence	106

<b>5.5</b>	<b><u>scFv(9H)</u></b>	<b><u>107</u></b>
5.5.1	Nucleotide sequence	107
5.5.2	Amino acid sequence	107
<b>6</b>	<b><u>REFERENCES</u></b>	<b><u>108</u></b>
<b>7</b>	<b><u>ABBREVIATIONS</u></b>	<b><u>121</u></b>
<b>8</b>	<b><u>CURRICULUM VITAE</u></b>	<b><u>125</u></b>
<b>9</b>	<b><u>ACKNOWLEDGEMENTS</u></b>	<b><u>128</u></b>

## SUMMARY

The antibody-based delivery of therapeutic agents to the tumor site is an emerging field of modern anti-cancer research, which aims at concentrating bioactive molecules onto neoplastic lesions while sparing normal tissues (Weiner, 2006; Carter, 2006; Schrama et al, 2006). Although originally monoclonal antibodies specific to membrane antigens on cancer cells have been used for tumor targeting applications, alternative targets such as markers of angiogenesis (Neri and Bicknell, 2005), stromal antigens (Rybak et al, 2007; Schliemann and Neri, 2007; Hofheinz et al, 2003) and intracellular proteins released at sites of necrosis (Street et al, 2006) are increasingly being considered. In this context, we and others have shown that the antibody-based targeting of enzymes, which are up-regulated at the tumor site, represents an additional attractive avenue for pharmacodelivery applications (Ahlskog et al, 2009; Chrastina et al, 2003).

Matrix metalloproteinases (MMPs), a group of more than 20 zinc-containing endopeptidases, are up-regulated in many diseases, but the use of MMP inhibitors for therapeutic purposes has often been disappointing, possibly for the limited specificity of the drugs used in clinical trials. In principle, individual MMPs could be specifically drugged by monoclonal antibodies, either by inhibition of their catalytic activity or by antibody-based pharmacodelivery strategies (Overall and Kleifeld, 2006).

This thesis describes the isolation and affinity maturation of recombinant antibodies specific to the murine catalytic domains of MMP-1A, MMP-2 and MMP-3. Furthermore, we cloned, produced and characterized these high-affinity monoclonal antibodies in SIP (small immunoprotein) mini-antibody format using biochemical and immunochemical methods. In addition, comparative biodistribution analysis of their tumor targeting properties at different time points (3 h, 24 h, 48 h) were performed in mice bearing subcutaneous F9 tumors using radioiodinated protein preparations.

The new anti-MMP antibodies allowed a systematic comparative immunofluorescence analysis of the expression patterns of their cognate antigens in a variety of healthy, cancerous and arthritic murine tissues. While all three MMPs were strongly expressed in tumor and arthritis specimens, MMP-1A was completely undetectable in the normal tissues tested, whereas MMP-2 and MMP-3 exhibited a weak expression in certain normal tissues (e.g., liver). However, in biodistribution experiments, only antibodies specific to MMP-3 selectively accumulated at the tumor site after intravenous injection, while being rapidly

cleared out from other organs. By contrast, antibodies specific to MMP-1A and MMP-2, showed no preferential accumulation at the tumor site.

Antibodies specific to MMP-3 may serve as vehicles for the efficient and selective delivery of imaging agents or therapeutic molecules to sites of disease.

# ZUSAMMENFASSUNG

Die zielgerichtete Anreicherung von therapeutischen Stoffen in Tumoren mit Hilfe von Antikörpern ist ein wichtiges Feld der modernen Krebsforschung. Bioaktive Stoffe können so hauptsächlich zum Tumor gebracht werden, während gesundes Gewebe und Organe ausgespart werden (Weiner, 2006; Carter, 2006; Schrama et al, 2006). Obwohl für diese zielgerichtete Akkumulation von Therapeutika ursprünglich monoklonale Antikörper gegen auf Krebszellen befindliche Membranantigene verwendet wurden, werden nun vermehrt andere Proteine als Zielmoleküle in Erwägung gezogen, wie z.B. Angiogenesemarker (Neri and Bicknell, 2005), stromale Antigene (Rybak et al, 2007; Schliemann and Neri, 2007; Hofheinz et al, 2003) oder intrazelluläre Proteine, die an nekrotischen Stellen auch extrazellulär zugänglich werden (Street et al, 2006). In diesem Zusammenhang haben wir und andere Gruppen gezeigt, dass im Tumor überexprimierte Enzyme auch eine äusserst attraktive Möglichkeit für die zielgerichtete Krebstherapie darstellen können (Ahlskog et al, 2009; Chrastina et al, 2003).

Matrixmetalloproteinasen (MMPs) sind eine Gruppe von mehr als 20 zinkhaltigen Endopeptidasen, die bei verschiedensten Krankheiten überreguliert und überexprimiert sind. Trotzdem war der Gebrauch von kleinen organischen Molekülen als Inhibitoren solcher MMPs in klinischen Studien enttäuschend, vor allem wegen ihrer unzulänglichen Spezifität. Monoklonale Antikörper stellen eine Alternative dar, einerseits als spezifische Inhibitoren, andererseits aber auch als Antikörper-Konjugate, um therapeutische Stoffe zielgerichtet zu den von Krankheit befallenen Geweben oder Organen zu bringen (Overall and Kleifeld, 2006).

Diese Doktorarbeit beschreibt die Isolation und Affinitätsmaturierung von rekombinanten Antikörpern gegen die murinen katalytischen Domänen der Enzyme MMP-1A, MMP-2 und MMP-3. Des Weiteren wurden diese hochaffinen monoklonalen Antikörper mit Hilfe biochemischer und immunochemischer Methoden ins Miniantikörperformat kloniert, produziert und charakterisiert. Wir führten zudem eine vergleichende Biodistributionsanalyse mit den radioaktiv markierten MMP-Antikörpern durch und verglichen ihre unterschiedliche Verteilung in Mäusen mit subkutanem F9 Tumor zu verschiedenen Zeitpunkten (3 Stunden, 24 Stunden und 48 Stunden).

Die hergestellten MMP-Antikörper erlaubten eine systematische und vergleichende Immunfluoreszenzanalyse, in der das Expressionsmusters des jeweiligen Antigens in einer

Vielzahl von gesunden, krebsbefallenen und arthritischen murinen Geweben untersucht wurde. Während alle drei Matrixmetalloproteinasen in Tumor- und Arthritisgeweben stark überexprimiert waren, konnte MMP-1A in gesunden Geweben nicht entdeckt werden. MMP-2 und MMP-3 hingegen zeigten eine schwache Expression in gewissen gesunden Geweben (wie z.B. in der Leber). In der Biodistribution wiesen nur MMP-3-Antikörper eine selektive Anreicherung im Krebsgewebe auf, während sie aus den anderen gesunden Organen rasch ausgeschieden wurden. Im Gegensatz dazu zeigten MMP-1A- und MMP-2- Antikörper keine bevorzugte Anreicherung im subkutanen F9-Tumor.

Die beschriebenen MMP-3-Antikörper können demzufolge in Zukunft als Vehikel für die effiziente und zielgerichtete Lieferung von Stoffen für bildgebende Verfahren oder von therapeutischen Molekülen zum Ort der Krankheit dienen.

# 1 INTRODUCTION

## 1.1 Antibodies

### 1.1.1 Monoclonal antibodies

In pharmaceutical biotechnology, antibodies are indisputably the best-established class of binding molecules that can be rapidly isolated with high affinity and specificity to virtually any antigen of choice. Indeed, 35 years after the advent of hybridoma technology (Kohler and Milestein, 1975) antibodies are nowadays routinely used in biomedical research for analytical and separation purposes, are essential ingredients in many diagnostic procedures, and represent the fastest growing sector in the field of the therapeutic proteins. Engineered antibodies and fragments thereof generate more than 30% of all revenues in the biotechnology market and are expected to reach \$ 26 billion by 2010 (Chames et al, 2009). Not only the high affinity and specificity, but also the variety of mechanism of actions (e.g., neutralization, interfering with cell signaling, antibody-dependent cellular toxicity and/or complement activation) and favorable pharmacokinetic profiles contribute to the great success of this class of drug. Table 1.1 gives an overview of monoclonal antibodies approved by FDA for therapy.

**Table 1.1: Monoclonal antibodies approved for therapeutic use (adapted from Chames et al, 2009)**

Generic name	Trade name	Antibody format	Antigen	Approved indication	FDA approval
<b>MuromomAb</b>	Orthoclone	Murine, IgG2a	CD3	Allograft rejection in allogeneic renal transplantation	86/06/19
<b>AbciximAb</b>	Reopro	Chimeric, IgG1(Fab)	GPIIb / IIIa	Maintenance of coronary patency	94/12/22
<b>RituximAb</b>	MABthera	Chimeric, IgG1	CD20	CD20-positive B-cell non-Hodgkin's lymphoma	97/11/26
<b>DaclizumAb</b>	Zenapax	Humanized, IgG1	CD25 (II2r)	Allograft rejection	97/12/10
<b>BasiliximAb</b>	Simulect	Chimeric, IgG1	CD25 (II2r)	Allograft rejection	98/05/12
<b>PalivizumAb</b>	Synagis	Humanized, IgG1	Protein F	Respiratory syncytial virus (RSV inhibitor) in children	98/06/19
<b>InfliximAb</b>	Remicade	Chimeric, IgG1	TNF $\alpha$	Crohn's disease and rheumatoid arthritis	98/08/24
<b>TrastuzumAb</b>	Herceptin	Humanized, IgG1	Her2 / Neu	Metastatic breast cancer	98/90/25
<b>GemtuzumAb</b>	Mylotarg	Humanized, IgG4; immunotoxin	CD33	CD-33-positive acute myeloid leukemia	00/05/17
<b>AlemtuzumAb</b>	MABcampath	Humanized, IgG1	CD52	B-cell chronic lymphocytic leukemia	01/05/07
<b>IbritumomAb</b>	Zevalin <sup>90</sup> Y	Mouse, IgG1, radiolabeled	CD20	B-cell non-Hodgkin's lymphoma	02/02/19

<b>AdalimumAb</b>	Trudexa	Human, IgG1	TNF $\alpha$	Crohn's disease and rheumatoid arthritis	02/12/31
<b>OmalizumAb</b>	Xolair	Humanized, IgG1	IgE	Treatment of asthma	03/06/20
<b>TositumomAb</b>	Bexxar	Murine, IgG2a, radiolabeled <sup>131</sup> I	CD20	CD20-positive B-cell non-Hodgkin's lymphoma	03/06/27
<b>EfalizumAb</b>	Raptiva	Humanized, IgG1	CD11a	Moderate to severe plaque psoriasis	03/10/27
<b>CetuximAb</b>	Erbix	Chimeric, IgG1	EGFR	Metastatic colorectal and head and neck carcinoma	04/02/12
<b>BevacizumAb</b>	Avastin	Humanized, IgG1	VEGF-A	Metastatic colorectal and non-small cell lung carcinoma	04/02/26
<b>NatalizumAb</b>	Tysabri	Humanized, IgG4	Integrin- $\alpha$ 4	Multiple sclerosis	04/11/23
<b>RanibizumAb</b>	Lucentis	Humanized, IgG1 (Fab)	VEGF-A	Wet-type age-related macular degeneration	06/06/30
<b>PanitumomAb</b>	Vectibis	Human, IgG2	EGFR	Metastatic colorectal carcinoma	06/0/27
<b>EculizumAb</b>	Soliris	Humanized, IgG2/4	C5	Paroxysmal nocturnal haemoglobinuria	07/03/16
<b>CertolizumAb pegol</b>	Cimiza	Humanized, IgG1, PEGylated Fab	TNF $\alpha$	Crohn's disease	08/04/18

### 1.1.2 Antibody formats

Since 1975, when Kohler and Milestein developed the hybridoma technology to efficiently produce monoclonal antibodies (mAbs) (Kohler and Milestein, 1975), it has been widely believed that these molecules could be ideal reagents for imaging and therapy. However, the early excitement was rapidly replaced by disappointment when it became clear that these molecules were facing serious problems when used as therapeutics:

- 1) The first antibodies were of murine origin and when injected into patients, they were recognized as foreign and were eliminated by the immune system **[Figure 1.1]**.
- 2) The antibodies could not interact properly with the components of the immune system because of their murine nature and, therefore, the biological efficacy of these antibodies was severely restricted for some applications.

In the early 90s, Winter and Milestein cloned the genes of IgG molecules and, as a result, the genes of any mAb of interest could be cloned in eukaryotic expression vectors (Winter and Milestein, 1991) and could be produced by various cell lines. This achievement could solve problems in the mAb production caused by the instability of many hybridoma cell lines (Chames and Baty, 2000).



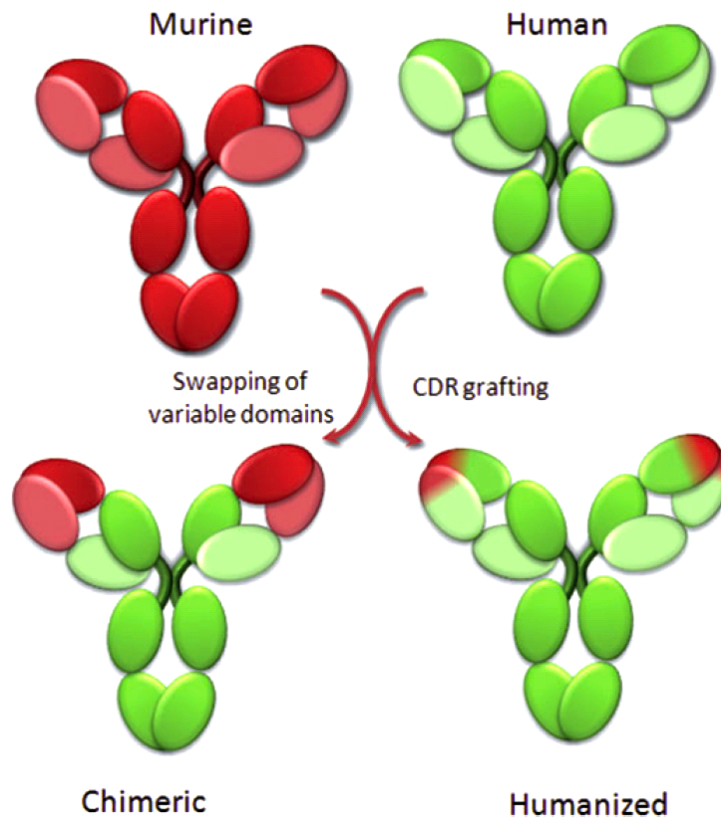


**Figure 1.1: Chimeric and humanized antibodies.** Murine sequences are shown in red and human sequences in green. Light chains are depicted in light colors and heavy chains in dark colours. *(Figure adapted from Chames et al, 2009)*

The binding activity of IgG molecules is generated by the variable domains of heavy and light chains. The fact that antibodies were highly conserved during evolution allowed the generation of chimeric antibodies by fusing murine variable domains (thus retaining the binding specificity) with human constant domains (Neuberger et al, 1985) **[Figure 1.1]**. These chimeric antibodies are 70% human and their Fc portion is fully human. Therefore, they are less immunogenic in humans and are able to interact efficiently with components of the human immune system.

An important accomplishment in the field of antibody engineering was the “antibody humanization”, obtained replacing the hypervariable loops of a fully human antibody with the hypervariable loops of the murine antibody. Humanization results in a further reduction of the murine components in mAbs. The technique is also referred to complementary-determining region grafting (Jones et al, 1986). These humanized antibodies are 80-90% human in sequence and are less immunogenic compared to the chimeric antibodies **[Figure 1.1 and Table 1.1]**.

Besides creation of chimeric or humanized antibodies, antibody engineering has been used to produce various antibody fragments that retain the binding activity of the full length IgG

**[Figure 1.2].** These new formats can be advantageous for certain applications (Hollinger and Hudson, 2005).

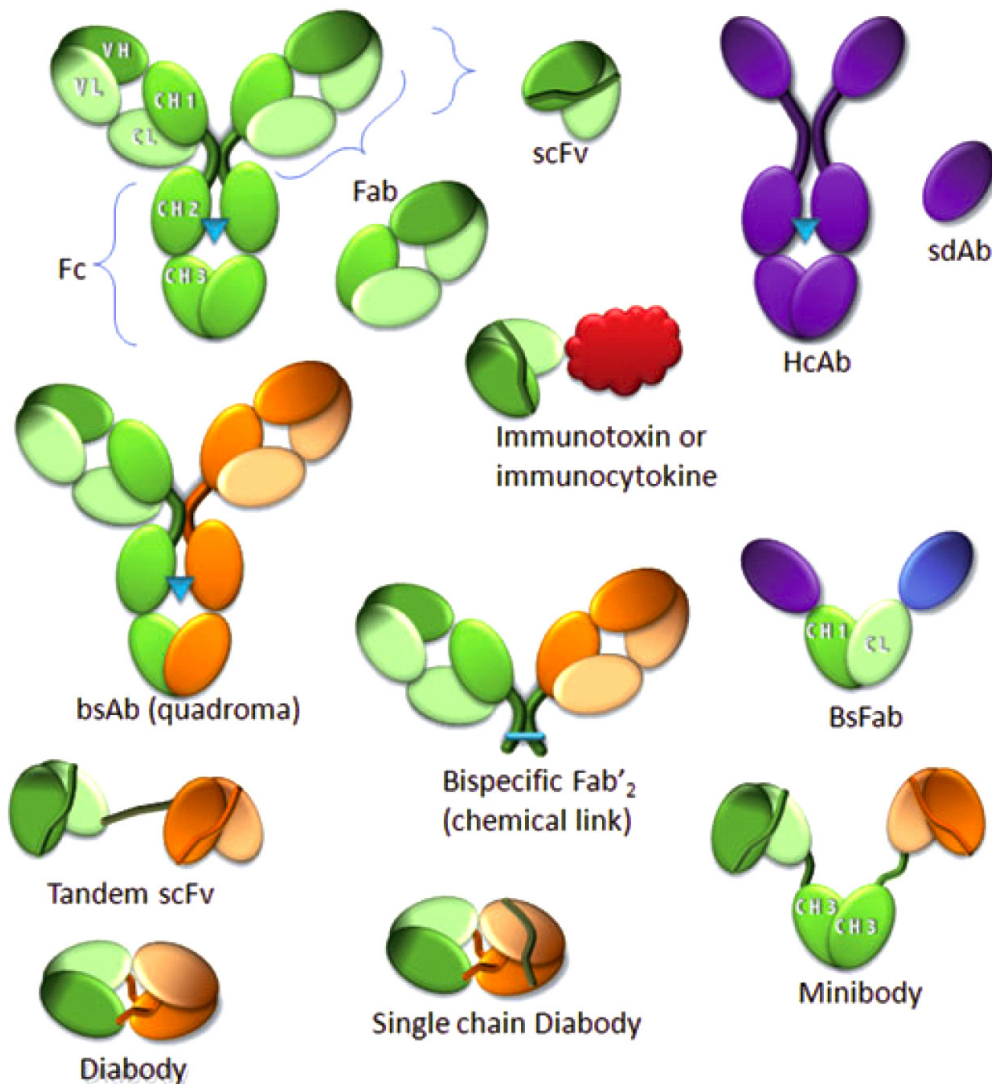


**Figure 1.2: Antibody fragments with therapeutical potential.** A conventional antibody is shown in green (light for the light chain, dark for the heavy chain, blue triangle indicating the glycosylation site) and the derived fragments (shaded areas represent the binding sites). The orange colour symbolizes a different specificity . HcAb from camelids and their fragments (sdAbs for single domain antibodies) are depicted in blue. The red molecule is depicting a cytokine or a toxin. bsAb, bispecific antibodies; bsFab, bispecific Fab fragment; HcAb, heavy chain only antibodies. *(Figure adapted from Chames et al, 2009)*

Full IgGs are limited in tumor penetration due to their large size, and their long serum half-life is not suitable for certain applications as radioimmunotherapy or imaging, since it would lead to irradiation of healthy tissue and high background. Antibody fragments such as single chain variable fragment (scFv), have no effector function, and represent attractive alternatives for certain applications, as they are monovalent and are rapidly eliminated by renal clearance **[Figure 1.2].**

### ScFv fragments

The scFv fragments consist of the variable domains of the heavy and the light chain linked by a flexible peptide linker **[Figure 1.2]**. They were described very early as small fragments retaining the binding activity of the full IgG molecule in a monovalent fashion (Bird et al, 1988). Due to its very short half life, the scFv format is not often used for *in vivo* therapeutic applications, although it has been extensively used as a binding moiety to be incorporated in more complex molecules. Recently, a scFv fragment binding to TNF- $\alpha$  (ESBA105) formulated as eye drops has entered phase I clinical trials for the topical administration in uveitis (Furrer et al, 2009). We anticipate a growing use of scFv fragments for locoregional applications, or for *in vivo* neutralization strategies where fast clearance is desired.

### Diabody fragments

Diabodies are formed by reducing the length of the linker between heavy and light chain of a scFv, thus inducing the formation of non-covalent homodimers (Hollinger et al, 1993) **[Figure 1.2]**. They are compact, medium-size (60 kDa) molecules and are a suitable choice for imaging applications. Besides increasing the molecular size, the dimerization provides bivalence, which leads to a higher avidity which is often desired and usually results in higher tumor retention. Thus, diabodies offer further advantages as rapid tissue penetration, high target retention and a rapid blood clearance.

### Single domain antibodies and heavy chain antibodies

More recently, several groups have shown that high affinities could be obtained using a single variable antibody domain **[Figure 1.2]**. The group of Greg Winter reported the use of mouse variable domains as binding units (Ward et al, 1989), but this approach was not further investigated because the majority of these domains tended to aggregate spontaneously. Later it was found that camelids and sharks express a type of antibody without light chains **[Figure 1.2]**, called heavy chain antibodies (HcAbs) (Hamer-Casterman et al, 1993). These antibodies have a single variable domain, which generates high affinities towards a large spectrum of antibodies. These small domains (13 kDa), termed single domain antibodies (sdAbs) or nanobodies, can easily be produced in bacteria or yeast. Nowadays, several studies have been demonstrated the possibility to develop human variable domains into stable sdAbs (Holliger and Hudson, 2005). These fragments exhibit several advantageous characteristics as high binding affinity and specificity, ease of production, and potentially, administration via alternative routes other than intravenous injection. Furthermore, sdAbs can be very efficiently engineered as targeting moiety of more complex molecular constructs.

### Miniantibody or small immuno proteins (SIPs)

The miniantibody format is created by fusing the scFv at the NH<sub>2</sub>-terminus of a human εCH4 domain of the secretory isoform S2 of human IgE (Borsi et al, 2002). Other groups have used the CH3 domain of IgG for homodimerization purposes (Wu and Yazaki, 2000). This domain promotes the formation of homodimers that are further stabilized by disulfide bonds between the COOH-terminal cysteine residues, resulting in a 75 kDa bivalent miniantibody. This format is superior to IgG and to scFv in achieving high tumor-to-organ ratios (Borsi et al, 2002) and for radioimmunotherapeutic applications (Berndorff et al, 2005) **[Figure 1.2]**.

The SIP format offers a good compromise between high tumor uptake and fast elimination from the blood and from organs (Hu et al, 1996; Wong et al, 2004). Furthermore, the bivalent nature of SIP-miniantibodies leads to improved functional affinity due to avidity effects compared with their monomeric scFv counterparts (Brack et al, 2006).

### Bispecific antibodies

Bispecific antibodies are able to bind two different antigens simultaneously, e.g. for the cross-linking of two receptors on a cell. The first method to produce bispecific antibodies was already described in 1983 (Milstein and Cuello, 1983) **[Figure 1.2]**. The so-called hybrid-hybridomas, or quadromas, comprises a fusion of two hybridoma cell lines. This procedure is complex, time-consuming and led often to inhomogenous protein preparations. As an alternative, the chemical or genetic coupling of Fab fragments was described in 1987 (Glennie et al, 1987). Furthermore, the inclusion of a CH3 domain into antibody fragments has been used as a dimerization domain, and a modified form of a CH3 domain has been used to direct hetero-dimerization (Carter, 2001). Perhaps the most effective way to generate bispecific antibody fragments is the expression of bispecific single-chain Fv fragment as diabodies **[Figure 1.3]** and as BiTE bispecifics. The latter ones are bispecific scFv fragments fused by peptidic linker and were commercialized by the biotechnology company Micromet. Micromet investigates currently several bispecific BiTe antibodies in Phase I and Phase II clinical trials, mainly for the treatment of cancer ([www.micromet.de](http://www.micromet.de)).

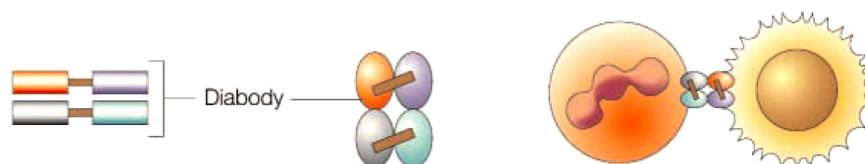


**Figure 1.3: Bispecific diabodies.** If a linker of a scFv fragment is about five amino acids long, the variable domains tend to dimerize. When equipped with variable domains exhibiting different specificities, such dimeric scFvs can make bispecific fragments called bispecific diabodies (*adapted from Brekke and Sandlie, 2003*).

## Immunocytokines and immunotoxins

Antibody fragments have also been used as the binding moiety in newly created molecules endowed with new effector functions. Various proteins have been fused to antibody fragments. For example, promising results have been obtained with immunocytokines consisting of a cytokine, e.g. IL-2, fused to the tumor targeting antibody fragment L19 (Borsi et al, 1998). These molecules have the potential to activate the immune system at the tumor site. Several antibody-cytokine fusions are currently tested in clinical trials (Schliemann et al, 2009).

### **1.1.3 Antibody alternatives**

#### **1.1.3.1 Scaffolds**

More recently, antibody-based efforts have been complemented by the development of alternative protein frameworks, termed “scaffolds”. Candidate domains for suitable scaffolds should have a structurally rigid core which allows either amino acid substitutions or inserts in loops or side chain replacements on a contiguous patch of the surface. In order to isolate new molecules with different functions and novel binding properties to a desired target protein, the scaffold protein should be suited for diversification and selection. The common approach is to use random mutagenesis of suitable amino acids of the scaffold to generate a synthetic library followed by selections of variants with desired binding activity. The scaffold protein should fulfill preferably certain properties as high protein solubility, thermodynamic and chemical stability, single polypeptide chain format, high bacterial expression for cheap production, functionality in absence of disulfide bonds and human origin (Friedmann and Stahl, 2009; Skerra, 2007; Nutall and Walsh, 2008).

Mutations introduced in the protein scaffold to produce diversity may compromise the three-dimensional structure, stability and solubility of the protein scaffold, thus making the isolation of protein binders based on other folding frameworks than the immunoglobulin fold difficult. Nevertheless, more than 50 scaffolds have been described for the generation of new protein binders (reviewed in Skerra, 2007). The vast majority of the described scaffolds have been used for research purposes only (e.g., probing the specificity determinants of WW-domains to their ligands (Dalby et al, 2000), elucidating target recognition rules of SH3 domains (Panni et al, 2002; Hiipakka et al, 1999), or identifying signal transduction pathways with the staphylococcal nuclease as scaffold (Norman et al, 1999). However, a few scaffolds are being pursued by small – and medium sized biotechnology companies (reviewed in Hey et al, 2005) for the development of drug candidates, the most advanced ones yielding first clinical data **[Figure 1.4]:**

- Adnectins (tenth type III domain of human fibronectin)
- Avimers (A-domains)
- DARPins (designed ankyrin repeat proteins)
- Kunitz type domains

The Adnectin called CT-322 is a VEGF-R2 antagonist that has recently completed phase I clinical trials in patients with advanced solid tumors and non-hodgkin's lymphoma (Adnexus homepage, now a Bristol Myers Squibb company). Notably, 31 out of 39 patients developed an immune response to the injected drug CT-322 (Beyond Antibodies Conference, 2009, San Diego). As the compound just entered phase II clinical trials, we will learn more in the near future about the suitability of Adnectins as therapeutic proteins.

Avimers are based on human A-domains (Huang et al, 1999; North et al, 1999), first commercialized by Avidia (now Amgen). The first drug candidate is an IL-6 inhibitor for the treatment of inflammatory diseases. However, after entering phase 1 clinical trials in 2006 in patients with Crohn's disease, no significant progress has been made with regards to the clinical development (Amgen homepage). Recent data in the public domain indicate that Amgen is further engineering Avimers for the neutralization of IL-6 mediated effects, before re-entering clinical trials in the near future (Beyond Antibodies Conference, 2009, San Diego).

The Zurich-based company Molecular Partners commercializes the DARPin technology, which is based on ankyrin repeat proteins (Binz et al, 2004). In January 2010, the first DARPin (MP0112) neutralizing VEGF entered phase I clinical trials for intravitreal injection in patients with diabetic macular edema. As the DARPins were newly designed and are not found in nature in this format, their immunogenic potential should be investigated in detail.

In December 2009, the first scaffold developed by Dyax Corp. called DX-88 was approved by FDA for the treatment of HAE (hereditary angioedema), a rare disorder with attacks of edema in the hands, face, feet, abdomen and/or throat. This condition is caused by a genetic deficiency of C1-esterase inhibitor. DX-88 is based on a Kunitz type domain and inhibits plasma kallikrein with an affinity of 40 pM, thereby preventing acute attacks of edema in these patients.

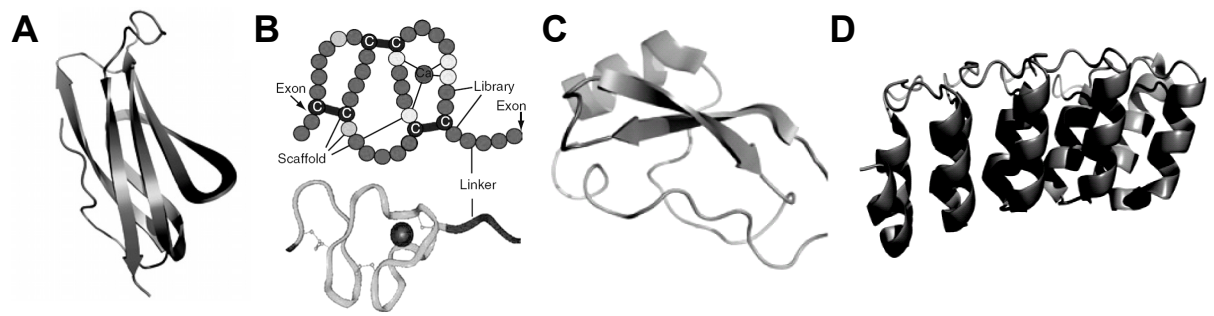


**Figure 1.4: Cartoon illustrating examples of scaffolds. A** Adnectins, **B** Avimers, **C** Kunitz type domains and **D** DARPins (*Figure adapted from Friedman and Stahl, 2009; Silverman et al, 2005*)

## **1.2 Generation of antibodies *in vitro***

### **1.2.1 Selection methodologies**

The isolation of proteins with desired binding properties from large repertoires of mutants can be a challenging task. As antibody libraries are very large (typically, billions of different clones in one single pot library) individual members of the repertoire cannot be assayed one by one due to practical reasons and time limitations. Therefore, a number of ingenious techniques have been developed which mimic the natural process of evolution in the laboratory. A common property of all selection technologies is the linkage of the genetic information (genotype) with the encoded polypeptide (phenotype). This allows the amplification of the genetic information of the isolated protein mutants, leading to the survival genotypes which code for favorable polypeptides. By repeating the two steps of generating genetic diversity followed by selection for a desired protein activity, proteins can be evolved *in vitro* (Hoogenboom, 2005). The next sections introduce the most established selection methodologies.

### **1.2.2 Phage display**

Phage display is a powerful methodology that allows the selection of a particular phenotype (e.g. a ligand specific to a desired antigen) from repertoires of polypeptides displayed on phage. In 1985 Smith reported the use of non-lytic filamentous bacteriophage fd for the display of specific binding peptides on the phage coat (Smith, 1985). Furthermore, besides the demonstration of peptides on phage, the groups of Winter (McCafferty et al, 1990) and Wells (Lowman et al, 1991) demonstrated the display of functional folded proteins as antibody fragments or hormones on the phage surface **[Figure 1.5]**. The technology is based on the fact that a polypeptide (capable of performing a function, typically the specific binding to an antigen of interest) can be displayed on the phage surface by inserting the gene coding for the polypeptide into the phage genome. Thus, the phage particle links phenotype and genotype.



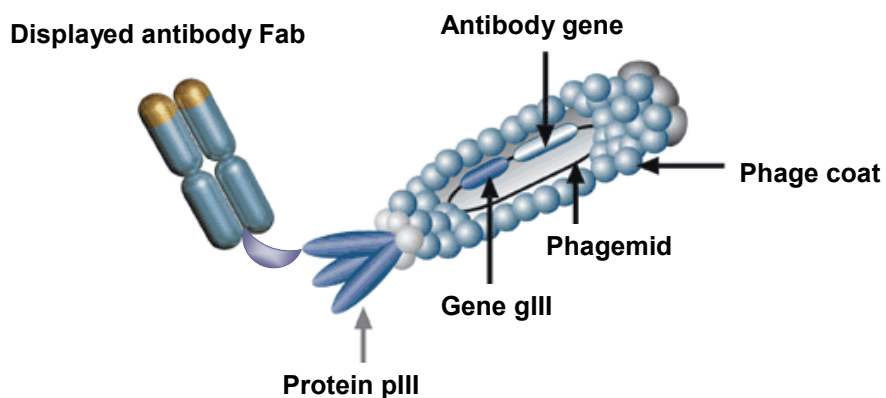


**Figure 1.5: Phage displaying a binding protein (in this case a Fab fragment) as fusion protein with the pIII protein of the phage.**

It is possible to create repertoires of phage (phage display libraries) in which the proteins displayed on each phage represent a population of different molecules with different properties. If a phage particle is isolated due to its phenotype displayed on the surface (e.g. binding specificity), the genetic information coding for the protein is co-isolated. As an example, one can consider the selection of a binding specificity from a displayed scFv fragment library. The library on phage is panned against an antigen of interest; unbound phage are washed away, whereas specifically binding phage are enriched and amplified in bacteria. Several rounds of selection can be performed (typically 2-4 rounds) **[Figure 1.6]**. As a result, even very rare phenotypes present in large repertoires can be selected and amplified from a background of phage carrying undesired phenotypes.

Phage particles are very stable and they are still infective when treated with acids, bases denaturants or proteases. Therefore, various elution protocols can be performed and have been used for other applications than for the isolation of binding proteins, e.g. for the selection of proteins with altered thermal stability (Bothmann and Pluckthun, 1998; Kristensen and Winter, 1998), the isolation of catalytically active enzymes (Pedersen et al, 1998; Demartis et al, 1999; Heinis et al, 2001), or to select aggregation resistant domain antibodies on phage by heat denaturation (Jespersen et al, 2004).

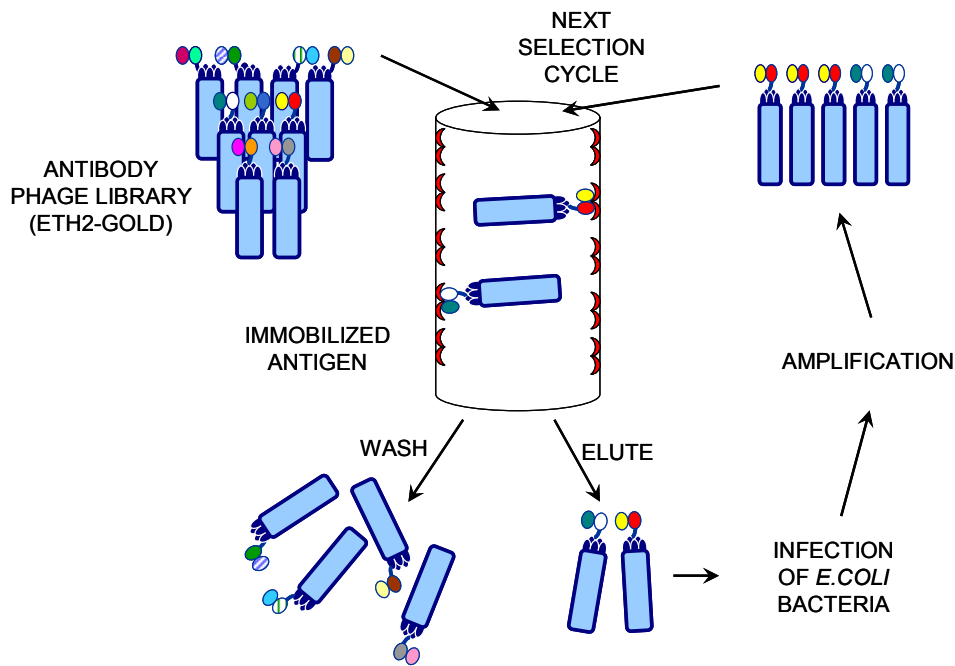


**Figure 1.6: Selection of binders from a phage display library.** A library of proteins displayed on the phage surface is used for performing the selections. Phage displaying a binding protein is captured on the immobilized antigen. Unbound phage can be discarded, whereas bound phage can be eluted and used for *E. coli* infection and can then be amplified. The eluted and amplified phage population can be used for further rounds of panning.

Filamentous phage particles covered by thousands of copies of a small major coat protein (pVIII) are around 6 nm in diameter and 900 nm in length. Few copies of the minor coat proteins pIII and pVI are displayed at one extremity of the phage particle, whereas pVII and pIX are present at the other extremity. The minor coat protein pIII, the product of gene III, is displayed in 3 to 5 copies and is responsible for the adsorption of the phage to the bacterial pilus. Peptides and proteins have been displayed on phage as fusions with different minor and major coat proteins (Silacci, 2006; Greenwood et al, 1991; Gao et al, 1999; Gao et al, 2001).

The first peptides and proteins were displayed on phage using phage vectors, essentially the phage genome with suitable cloning sites for pVIII or pIII fusions and an antibiotic resistance gene. Phage vectors carry all the genetic information necessary for the phage life cycle. Using phage vectors, most peptides and folded proteins can be displayed as pIII fusions, while only short peptides of 6 to 7 residues without cysteine give rise to functional phage when displayed as pVIII fusions (Iannolo, 1995).

Phagemids are more popular vectors for phage display. They are plasmid vectors that contain only the gene III with appropriate cloning sites and a packaging signal as phage-derived sequences. For the production of functional phage particles, phagemid containing bacteria need a superinfection with helper phage particles containing the complete phage

genome. Phagemid vectors encoding the polypeptide-pIII fusion are preferentially packaged into the phage particles, due to the fact that helper phage used for superinfection (such as M13K07 or VCS-M13) have a defective origin of replication, which also serves as packaging signal. The resulting phage particles may incorporate either pIII derived from the helper phage or the polypeptide-pIII fusion, encoded by the phagemid. Depending on the type of phagemid, growth conditions used and the nature of the polypeptide fused to pIII, ratios of (polypeptide-pIII): pIII ranging between 1:5 and 1:10000 have been reported in literature (Kristensen and Winter, 1998; Silacci et al, 2005). Furthermore, it has been reported that phage particles obtained by using a phage vector, are polyvalent (i.e. 3-5 identical polypeptides displayed on one phage particle), whereas the use of phagemids typically yields monovalent phage binders. This property may be useful for the isolation of high-affinity binders from a library, by reducing avidity effects.

Besides antibody fragments, mutants of globular proteins and enzymes have been successfully displayed and selected on phage, as for example domain antibodies (Jespers et al, 2004), lipocalins (Skerra, 2000), A-domains (Silverman et al, 2005), fibronectin type III domains (Koide et al, 1998), Kunitz type domains (Ley et al, 1996), SH3 domains (Panni et al, 2002; Hiipakka et al, 1999; Grabulovski et al, 2007), biotin ligase and trypsin (Heinis et al, 2001).

Not every protein can be displayed on phage as fusion with pIII, because proteins that fold well in bacteria are often displayed poorly on filamentous phage. The inefficient display of proteins are caused by several reasons such as proteolytic cleavage of the pIII fusions or poor incorporation of the pIII fusion protein into the phage coat, e.g. via competition with the pIII from helper phage. In order to obtain a sufficient number of phage particles displaying the fusion protein, high titers of phage are needed, thus limiting the diversity of protein mutants that can be accessed for selection.

An additional limitation of phage display is the need for transformation of bacterial cell by electroporation, which is laborious and time consuming. Typically, the size of phage display libraries are in the range of  $10^9$ - $10^{11}$  individual library members (Rauchenberger et al, 2003).

#### **1.2.2.1 ETH-2 Gold antibody library**

The ETH-2 Gold library is a synthetic human antibody phage library displaying antibody fragments in the scFv format. The scFv antibody format exhibits various advantageous properties as superior expression and stability compared to Fab fragments. The library has been cloned into a phagemid vector encoding scFv-pIII fusion proteins.

The ETH-2 Gold library contains three billions individual antibody clones and was produced by appending short variable complementary determining region 3 (CDR3) onto three antibody

germline segments (DP47, DPK22 and DPL16) [Figure 1.7]. These germlines dominate the functional repertoire in human beings and represents 12%, 25% and 16% respectively of the antibody repertoire in humans (Kirkhman et al, 1992; Griffiths et al, 1994). The use of the DP47 VH germline segment offers various advantages as a higher thermostability (Ewert et al, 2003) and the possibility of using protein A for antibody purification and detection (Hoogenboom and Winter, 1992). Variability was confined to the V $\kappa$  positions 91, 92, 93, 94 and 96 and to the V $\lambda$  positions 91 to 96 for VL CDR3 and to four to six residues at positions 95 to 100 in the VH CDR3 [Figure 1.7], in accordance with their role as common antigen contact regions and with the high variability of naturally occurring antibodies in these regions (Padlan, 1994).

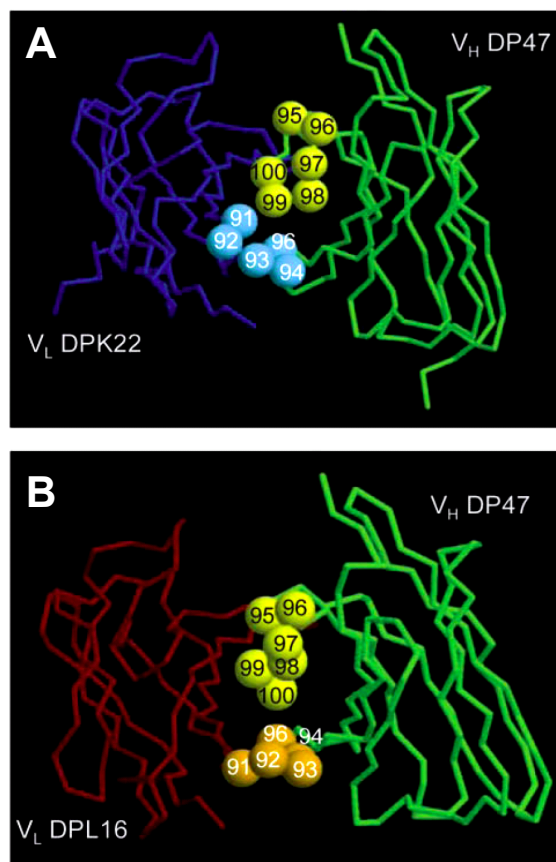


**Figure 1.7: Design of the ETH-2 Gold antibody phage library. Structures of the scFvs: A** The DPK22 (V $\kappa$ ) backbone is represented in blue and the DP47 (VH) in green. Residues subject to random mutation (spacefill representation) are DPK22 CDR3 positions 91, 92, 93, 94 and 96 (light blue) and DP47 CDR3 positions 95, 96, 97, 98, 99 and 100 (yellow) (**1igm** (Brookhaven database)).

**B** The DPL16 (V $\lambda$ ) backbone is represented in red and the DP47 (VH) in green. Residues subject to random mutation (spacefill representation) are DPL16 CDR3 positions 91, 92, 93, 94 and 96 (orange) and DP47 CDR3 positions 95, 96, 97, 98, 99, and 100 (yellow) (**8FAB** (Brookhaven Protein Data Bank)). (**Figure adapted from Silacci et al, 2005**)

### 1.2.2.2 *In vitro* affinity maturation by site-directed mutagenesis

A problem often associated with phage display is the relatively low affinity of antibodies isolated after selections from single pot libraries. However, phage display offers a solution to improve the low affinities of the isolated binders by so-called *in vitro* affinity maturation. *In vitro* affinity maturation procedures rely on the directed mutagenesis of antibody sequences to generate secondary libraries, thus mimicking *in vivo* affinity maturation [see Figure 1.8] (Carnemolla et al, 1996; Borsi et al, 2002; Pini et al, 1998; Schmitz et al, 1999).

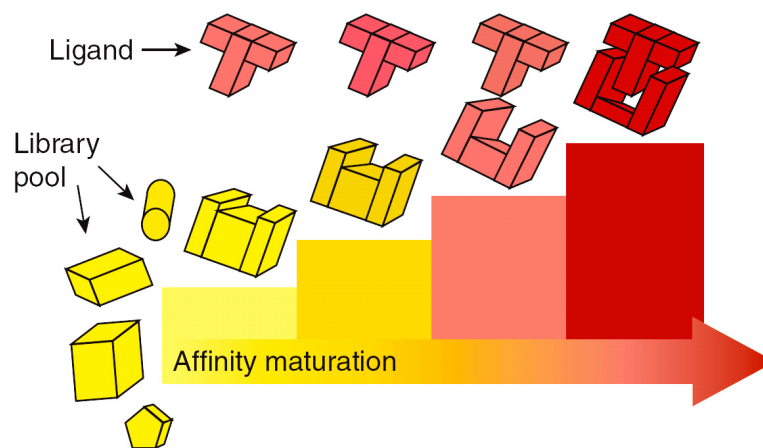
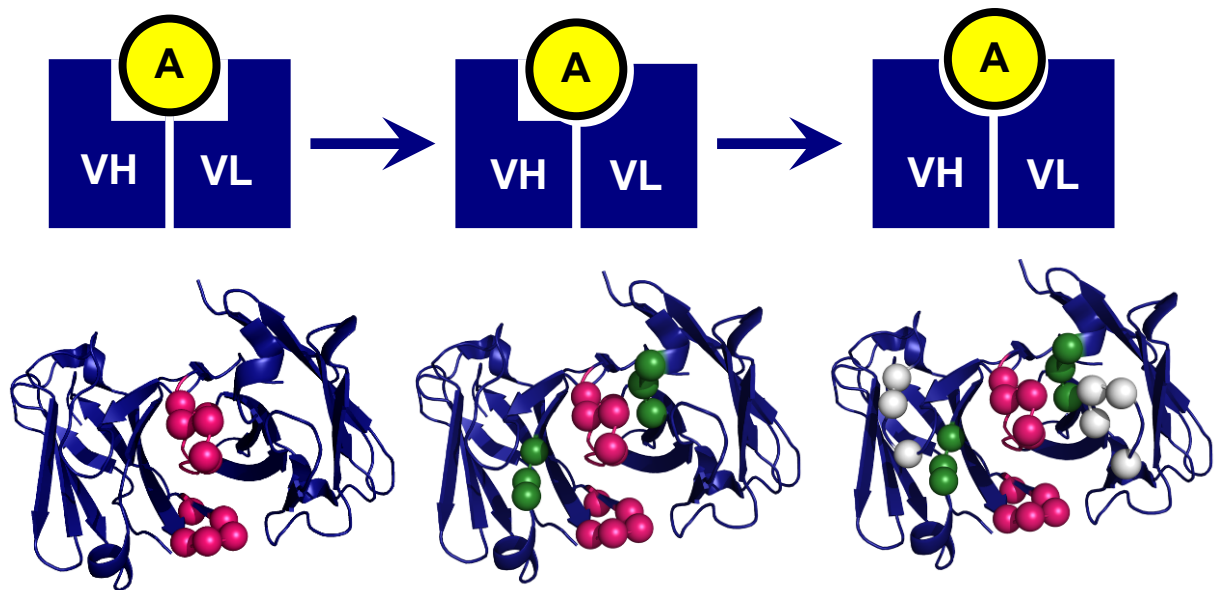


Figure 1.8: Concept of the affinity maturation. (Figure adapted from Rothe et al, 2006)

Antibodies are ideal candidates for targeted sequence diversification because of their high degree of sequence similarity and their conserved and well-studied protein fold. Many *in vitro* affinity maturation efforts using combinatorial libraries in combination with display technologies have targeted the complementary determining regions (CDRs) containing the antigen-binding site. Normally, amino acid residues are fully randomized with degenerate oligonucleotides. If applied to all positions in a given CDR, combinatorial mutagenesis would create more variants than can be displayed on phage. In addition, the indiscriminate mutation of too many residues creates many variants that no longer bind the antigen, thus reducing the functional library size. Therefore, some scientists restrict the number of mutations to only few residues per library (Thom et al, 2006). Furthermore, mutagenesis has also been focused on natural hotspots of hypermutation (Ho et al, 2005), or the residues to be targeted were chosen based on mutational or structural analyses as well as molecular modeling (Osborn et al, 1996; Yelton et al, 1995; Chen et al, 1999).

Further affinity improvements have been achieved by recombining mutations within the same or different CDRs of improved variants (Rajpal et al, 2005; Yelton et al, 1995; Chen et al, 1999).



**Figure 1.9: Schematic representation of an example for *in vitro* affinity maturation by mutation of CDR loops of an antibody from the ETH-2 Gold library.** An antibody selected from the ETH-2 Gold library (primary library with CDR3 of VH and VL in pink spacefill) is used as template for the construction of a secondary library with mutated residues in CDR1 of VH and VL (in green spacefill). The best performing clone from the secondary library is used as template for the the construction of a third library with mutations in CDR2 of VH and VL (in white spacefill). This procedure can be extended to more residues until the desired affinity is obtained (PDB entry: **8FAB**).

In animals, the diversity introduced by somatic hypermutation in the maturation process is mainly located at the periphery of the antigen-binding site, i.e. in CDR1 and CDR2 loops. Therefore, CDR1 and CDR2 of heavy and light chain are ideal target regions for *in vitro* affinity maturation procedures and are very well applicable for libraries based on single scaffolds such as the ETH-2 Gold library. Its modular design allows simple affinity maturation of antibodies of interest by introducing diversity in CDR1 and CDR2 using standard primers identical for each clone (Pini et al, 1998) **[Figure 1.9]**.

### 1.2.3 Iterative colony filter screening

Filter screening techniques could in principle represent an alternative to phage display. Clones (typically  $<10^6$ ) are simultaneously assayed for their ability to generate the binding specificity of interest, thereby preventing the loss of binders that may occur during biopanning. Gherardi *et al.* (Gherardi et al, 1990) described a filter screening methodology for the identification of the clones secreting an antibody specific to a given antigen, out of several thousands hybridoma clones. This methodology was improved by Skerra *et al.* (Skerra et al, 1991; Dreher et al, 1991) who developed a two-membrane system for detection of antigen binding antibodies by antibody Fab fragments secreted by bacterial colonies.

A modified version of this methodology was used for the isolation of antibodies from a large library with millions of different clones. The naïve ETH-2 antibody library was used (Viti et al, 2000), in form of a pool of antibody secreting bacteria, to isolate monoclonal antibodies specific for the extra-domain-B (EDB) of fibronectin (Giovannoni et al, 2001) [Figure 1.10].

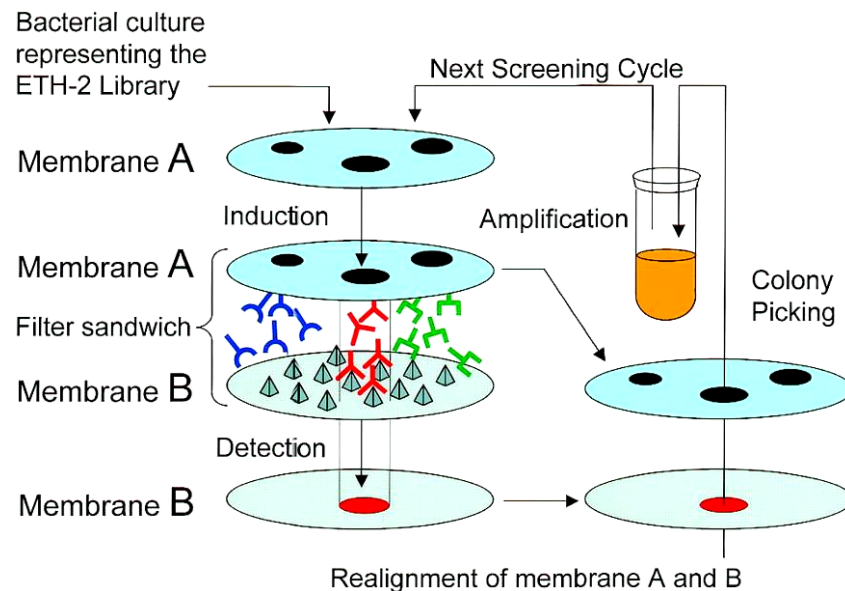


**Figure 1.10: Schematic representation of the iterative colony screening method.** Bacteria expressing potentially different antibody fragments were spread on a Durapore filter membrane (A). On the filter placed on a solid medium repressing expression of the antibody fragments, colonies were visible after 8 hours incubation at 37°C (three different colonies were depicted schematically). A second filter membrane (B) was coated with the antigen of interest (depicted as pyramids), placed on a solid medium able to induce the expression of scFvs, and in contact with membrane A. Antibody fragments were captured on membrane B, and could be determined by an enzymatic colourimetric reaction. The corresponding colonies could be identified on membrane A, could be regrown and the procedure was repeated until single positive colonies producing monoclonal antibodies were identified. (Figure adapted from Giovannoni et al, 2001)

## 1.2.4 Yeast surface display

Yeast cell surface display systems have been found to be effective for the display of scFv fragments and the development of antibodies with enhanced stability and affinity (Boder and Wittrup, 1997; Boder and Wittrup, 2000; Feldhaus et al, 2003). In the studies cited, functional scFv antibody fragments were successfully expressed on the yeast cell surface by fusion to the C-terminus of Aga2p. The Aga2p-scFv fusion protein was linked to Aga1p by two disulfide bonds [Figure 1.11]. Boder and Wittrup reported, that the scFv fragments of the antiferescein antibody displayed on the cell surface was able to bind fluorescein-conjugated dextran, demonstrating that the antibody-binding site is accessible to very large macromolecules (Boder and Wittrup, 1997). Yeast cell-surface display systems also offer many advantages for screening of large combinatorial scFv libraries, and together with

fluorescence activated cell sorting (FACS) allow the rapid isolation of rare clones with desired characteristics (Boder and Wittrup, 1997; Boder et al, 2000, Feldhaus et al, 2003). In addition, solid phase capturing methods, such as magnetic separation, are efficient tools to isolate target cells from large cell-surface libraries without using expensive equipment (Furakawa et al, 2003). Several successful cases of isolation of scFv with high affinity to a certain antigen have been reported (Boder and Wittrup, 2007; Boder and Wittrup, 2000; Feldhaus et al, 2003).

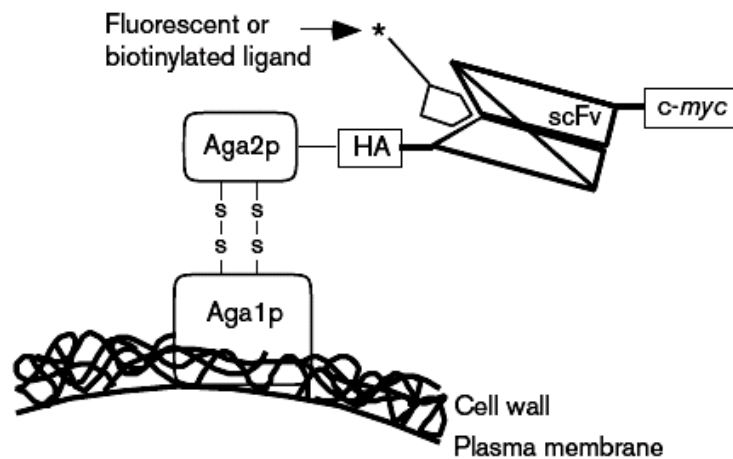


**Figure 1.11: Illustration of yeast surface display.** An epitope from the hemagglutinin antigen HA is fused to the carboxyl terminus of the Aga2 protein subunit of  $\alpha$ -agglutinin, followed by an antifluorescein scFv sequence, which in turn is fused to a c-myc epitope tag. The HA and c-myc epitope tags allow a quantification of the number of fusion proteins per cell and determination of the accessibility of the different domains of the fusion protein to the antibody detection. (*Figure adapted from Cereghino and Cregg, 1999*).

### 1.2.5 Ribosome display

In ribosome display (Mattheakis et al, 1994), the link between the antibody and encoding RNA is made by the ribosome, which is at the end of RNA translation made to stop without releasing the polypeptide. The ternary complex as a whole is then used for selections. (Hoogenboom, 2005) **[Figure 1.12]**.



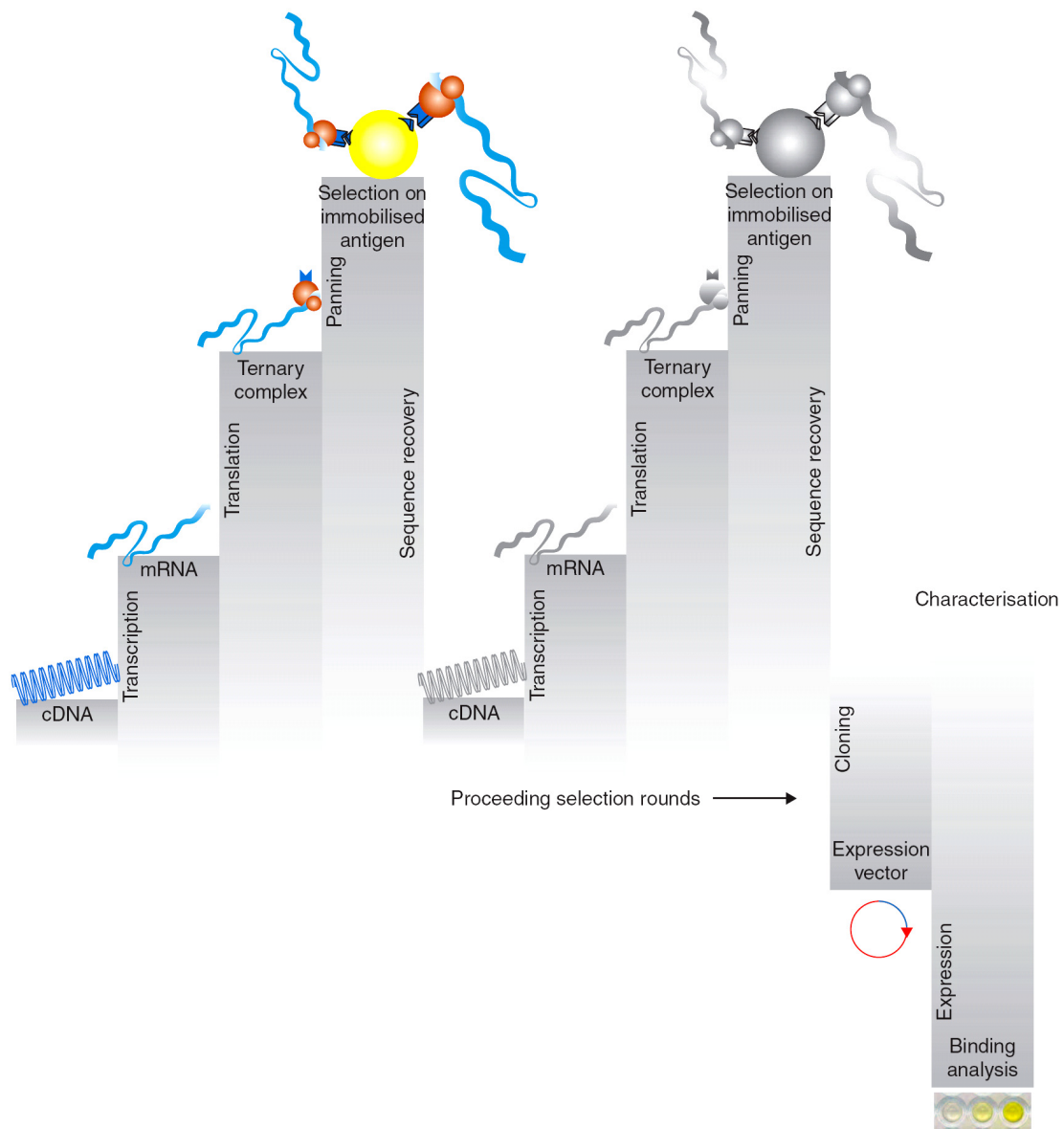


**Figure 1.12: Stepwise progression of *in vitro* ribosome display and panning on immobilized antigen.** The cDNA represents the gene repertoire, which has to be PCR-amplified to add a promoter for the RNase polymerase, usually the T7-promoter, a ribosome-binding site and translation initiation codon (AUG) to the 3'-end. Transcription and translation in a cell-free environment lead to the generation of ternary complexes containing the mRNA, the protein and the ribosome. These are then panned on immobilized antigen and sequence covered by RT-PCR. As the selection round proceed in repeated cycles, enriched binders can be cloned into an expression vector and then further characterized through functional binding analysis. **(Figure adapted from Rothe et al, 2006)**

This display method is carried out entirely *in vitro*, thereby eliminating the need of bacterial transformation. The other advantage of the method lies in the mutagenesis steps inherently associated with the library amplification (e.g. non-proof-reading polymerases) (Hoogenboom, 2005).

Antibodies with nanomolar and picomolar affinities have been selected with this *in vitro* method following rapid affinity maturation cycles (Hannes et al, 2000; Binz et al, 2004; Irving et al, 2001).

One disadvantage of this fully *in vitro* system is its sensitivity to RNase activity, which may lead to degradation of the mRNA, causing the ribosome complex causing to fall apart. Therefore, a ribonuclease-free environment is essential (Rothe et al, 2006). Furthermore, ribosome display implicitly depends on a large fraction of the ribosomes translating the protein to the end in order for it to fold properly. However, *in vitro*, such full-length translation rarely happens on all ribosomes. Therefore, a certain fraction of molecules displayed are not full-length. This in turn may limit the enrichment factor, as the incomplete synthesis products would be more likely not to fold, and, consequently bind non-specifically (Lipovsek et al, 2004).

## 1.3 Tumor targeting

### 1.3.1 The concept

The cancer chemotherapy relies on the expectation that the anti-cancer drugs will preferentially kill rapidly proliferating tumor cells rather than normal cells (Chari, 1998). Large doses of drug are needed to kill a large portion of tumor cells in order to maintain complete remission. Toxicity towards proliferating non-malignant cells and severe systemic side effects are the result of such high drug doses.



**Figure 1.13: The concept of tumor targeting.** Research in tumor targeting aims at achieving selective localisation of agents at the tumor site (typically administered by intravenous injection), for diagnostic or therapeutic applications. (*Figure adapted from Nilsson et al, 2001*)

Therefore, the most important goal of modern anti-cancer research is the development of more selective medicaments which are able to discriminate between healthy and diseased tissue and therefore achieve better therapeutic ratios.

One avenue to improve the selectivity of therapeutic molecules would be to target them on the tumor side while sparing normal tissue [Figure 1.13]. With the development of hybridoma technology for the production of murine antibodies of defined specificity the concept of therapeutic magic bullets, formulated by Ehrlich at the end of the last century gained again substantial interest.

Besides antibodies, various molecules (e.g. peptides, scaffolds, etc.) could be used as vehicles when having a certain affinity to tumor cells or when localizing at the tumor site by another mechanism. Tumor targeting could therefore be defined as the area of scientific research that aims at achieving selective localization of active compounds at the tumor sites (Nilsson et al, 2001).

## 1.4 Matrix metalloproteinases (MMPs)

### 1.4.1 The MMP family

Matrix metalloproteinases (MMPs) are a group of more than 20 zinc-containing extracellular proteinases that are capable of degrading multiple components of the extracellular matrix (ECM). Historically, the MMPs were divided into 4 different classes termed collagenases, gelatinases, stromelysins and matrilysins on the basis of their specificity for components of the ECM. The common names of the MMPs reflect this classification [Table 1.2]. Nowadays, as the list of MMP substrates has grown, a sequential numbering system has been adapted, and the MMPs are now grouped according to their structure. Seven different structural classes of MMPs are distinguished: four structural MMP classes are secreted and three are membrane-type MMPs (MT-MMP) (Egeblad and Werb, 2002) [Figure 1.14 and Table 1.2].

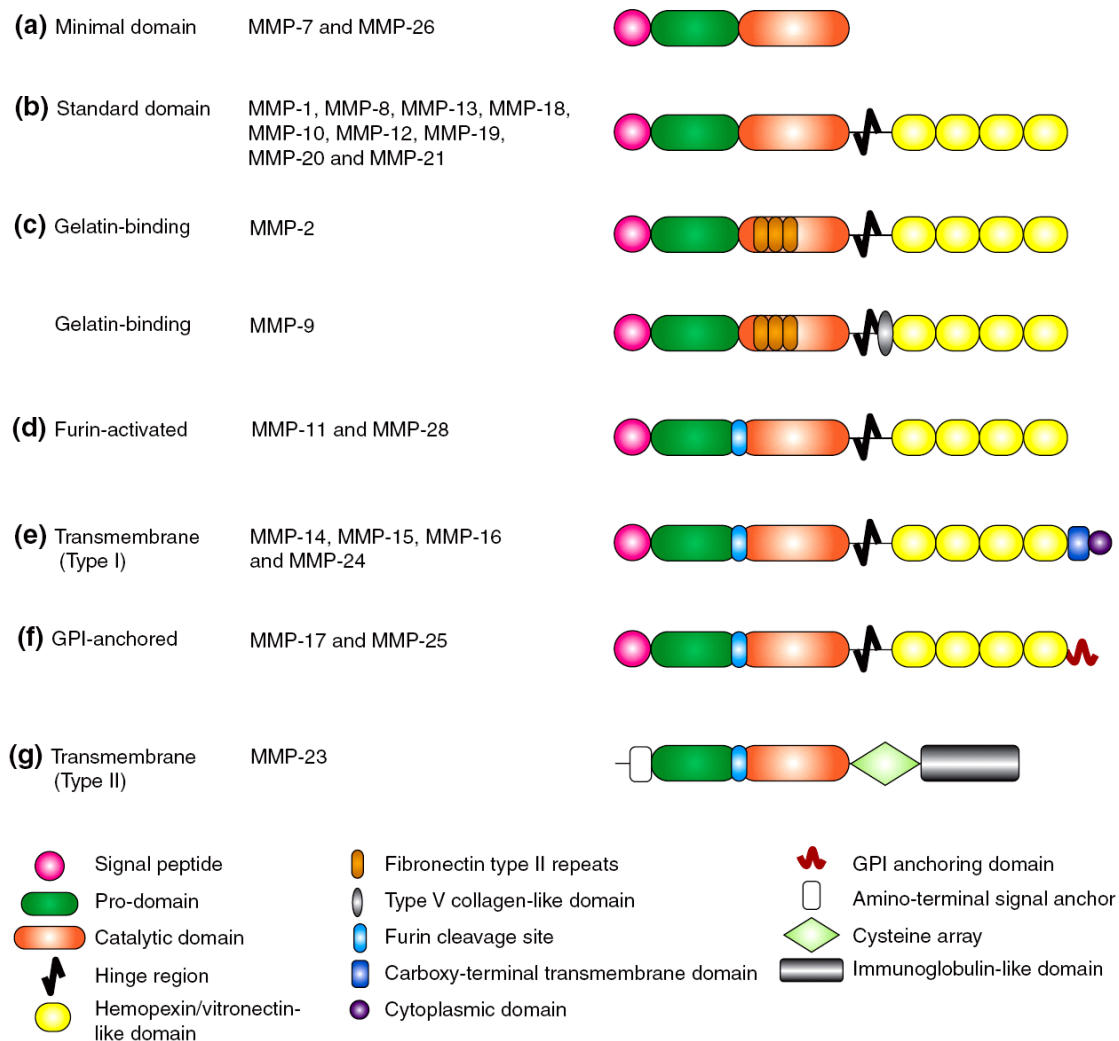


**Figure 1.14: The domain composition and important structural features of the various subtypes of MMPs.** (Figure adapted from Somerville et al, 2003)

Many of the extracellular signalling events in which MMPs are involved and that regulate cell behaviour occur near or at the cell membrane. The MT-MMPs are covalently linked to the cell-membrane, whereas the secreted MMPs were localized to the cell surface by binding to integrins (Werb, 1997) or to CD44 (Yu and Stamenkovic, 1999; Yu et al, 2002), or through interaction with cell-surface associated heparan sulphate proteoglycans, collagen type IV or the extracellular matrix metalloproteinase inducer (EMMPRIN) (Sternlicht and Werb, 2001).

**Table 1.2: Human and murine matrix metalloproteinases (adapted from Egeblad and Werb, 2002)**

Mouse gene	Human gene	Protein names (common)	Structural Class
Mcola	MMP-1	Collagenase 1, interstitial collagenase, fibroblast collagenase, tissue collagenase	Standard domain
Mcolb	Not present	Collagenase-like B	Standard domain
Mmp2	MMP-2	Gelatinase A, 72-kDa gelatinase, 72-kDa type IV collagenase, neutrophil gelatinase	Gelatin-binding
Mmp3	MMP-3	Stromelysin 1, transin-1, proteoglycanase, procollagenase-activating protein	Standard domain
Mmp7	MMP-7	Matrilysin, matrin, PUMP1, small uterine metalloproteinase	Minimal domain
Mmp8	MMP-8	Collagenase 2, neutrophil collagenase, PMN collagenase, granulocyte collagenase	Standard domain
Mmp9	MMP-9	Gelatinase B, 92-kDa gelatinase, 92-kDa type IV collagenase, granulocyte collagenase	Gelatin-binding
Mmp10	MMP-10	Stromelysin 2, transin-2	Standard domain
Mmp11	MMP-11	Stromelysin 3	Furin-activated
Mmp12	MMP-12	Metalloelastase, macrophage elastase, macrophage metalloelastase	Standard domain
Mmp13	MMP-13	Collagenase 3	Standard domain
Mmp14	MMP-14	MT1-MMP, MT-MMP1	Transmembrane (Typl)
Mmp15	MMP-15	MT2-MMP, MT-MMP2	Transmembrane (Typl)
Mmp16	MMP-16	MT3-MMP, MT-MMP3	Transmembrane (Typl)
Mmp17	MMP-17	MT4-MMP, MT-MMP4	GPI-anchored
Mmp19	MMP-19	RASI 1	Standard domain
Mmp20	MMP-20	Enamelysin	Simple hemopexin domain
Mmp21	MMP-21	XMMP, Homologue of Xenopus XMMP	Standard domain

	MMP-22	Simple hemopexin domain	(chicken; no human homologue known)
Mmp23	MMP-23A	Cystein array MMP (CA-MMP), femalysin, MIRF; MMP-21/MMP-22	Type II membrane
Not present	MMP-23B	CA-MMP	Type II membrane
Mmp24	MMP-24	MT5-MMP, MT-MMP5	Transmembrane (Typ I)
Mmp25	MMP-25	MT6-MMP, leukolysin, MT-MMP6	GPI-anchored
Not present	MMP-26	Matrilysin 2, endometase	Minimal domain
Mmp27	MMP-27	CMMP	Simple hemopexin domain
Mmp28	MMP-28	Epilysin	Furin-activated

#### 1.4.1.1 MMP-1

Matrix metalloproteinase 1 (MMP-1) belongs to the structural class of the standard domain MMPs [Figure 1.14 and Table 1.2]. It comprises a signal peptide, a propeptide, a catalytic domain, a hinge region and a hemopexin-like domain. Figure 1.15 shows the structure of the catalytic domain of human MMP-1. Stable knockdown of MMP-1 expression in cancer cells implanted in mice confirmed the important role of MMP-1 in tumorigenesis and metastasis (Overall and Kleifeld, 2006). Furthermore, it was recently shown that upregulation of MMP-1 in cancer patients is associated with a poor prognosis (Murray et al, 1996). In inflammatory diseases, the proinflammatory cytokine IL-17 induces MMP-1 production (Cortez et al, 2007). This finding is in keeping with earlier studies, which showed a correlation between MMP-1 expression and the development of arthritis (Vincenti and Brinckerhoff, 2002).



**Figure 1.15: Ribbon diagram of the catalytic domain of human MMP-1.** Using the program PyMOL, the structures were modulated from the protein data base file 1CQR of Brookhaven Protein Data Bank.

#### 1.4.1.2 MMP-2

Matrix metalloproteinase 2 (MMP-2) belongs historically to the subgroup of the gelatinases [Figure 1.14 and Table 1.2] and to the structural group of the gelatin-binding MMPs. It comprises additionally three fibronectin type II domains inserted into the catalytic domain (Nagase and Woessner, 1999; McCawley et al, 2004) [Figure 1.16]. MMP-2 has been proposed as a therapeutic drug target for over 20 years, because of its high expression in many human tumors and its association with highly invasive cells (Liotta et al, 1980; Stetler-Stevenson et al, 1994). Levels of MMP-2 expression were correlated with tumor aggressiveness (Davies et al, 1993). In experimental models, MMP-2 knockout mice showed reduced angiogenesis induction, melanoma growth and lung carcinoma metastasis (Itoh et al, 1998). In arthritic joints, MMP-2 expression is highly increased compared to the low expression levels in normal joint tissue (Kontinen et al, 1999; Yoshihara et al, 2000).

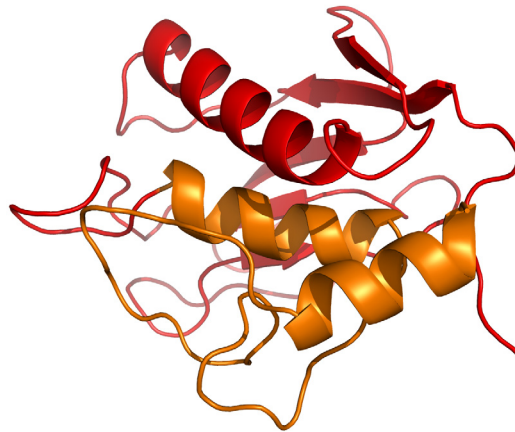


**Figure 1.16: Ribbon diagram of the catalytic domain of murine MMP-2 (lacking the three fibronectin type 2 domains).** Using the program PyMOL, the structures were modulated from the protein data base file **1QIB** of Brookhaven Protein Data Bank.

#### 1.4.1.3 MMP-3

Matrix metalloproteinase 3 (MMP-3) belongs historically to the stromelysins and to the structural group of the standard domain MMPs. It comprises, as MMP-1, a signal peptide and a propeptide, a catalytic domain and a hemopexin-like domain, but exhibits different substrate specificity [Figure 1.14 and Figure 1.17] (Overall and Kleifeld, 2006; Cawley et al, 2004). Its expression is associated with tumorigenesis in mouse models (Fingleton, 2003). However, contradictory *in vivo* data were published about the role of MMP-3 in cancer development. McCawley and coworkers described recently the protective role of MMP-3 in squamous cell carcinoma (McCawley et al, 2008), whereas several studies demonstrated that MMP-3 expression in tumors is associated with increased aggressiveness (Kerkela and

Saarialho-Kere, 2003; Shima et al, 1992; Kusakawa et al, 1995; Airolo et al, 1997). In inflammatory diseases, MMP-3 contributes directly to the degradation of articular cartilage matrix components during naturally occurring and experimentally induced arthritis (Mudgett et al. 1998; Hasty et al, 1990; Brinckerhoff, 1991; Martel-Pelletier et al, 1994).

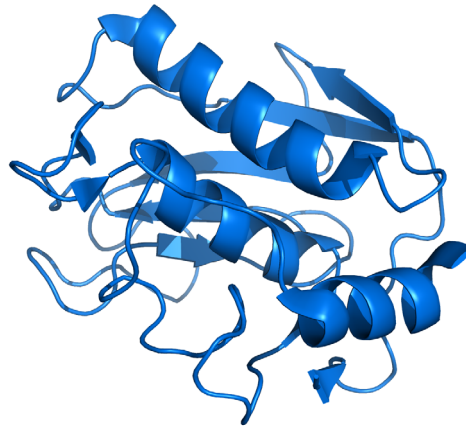


**Figure 1.17: Ribbon diagram of the catalytic domain of the murine MMP-3.** Using the program PyMOL, the structures were modulated from the protein data base file **966C** of Brookhaven Protein Data Bank.

#### **1.4.2 Regulation of MMP activity**

The MMPs are synthesized as inactive zymogens (proMMPs). They are kept inactive by an interaction between a cysteine-thiol group in the propeptide domain and the zinc ion bound to the catalytic domain: activation requires proteolytic removal of the propeptide prodomain (Sternlicht and Werb, 2001) **[Figure 1.18]**. Most of the MMPs are activated outside the cell by other activated MMPs or serine proteases. However, MMP-11, MMP-28 and MT-MMPs can also be activated by intracellular furin-like serine proteases before they reach the cell surface (Sternlicht and Werb, 2001).



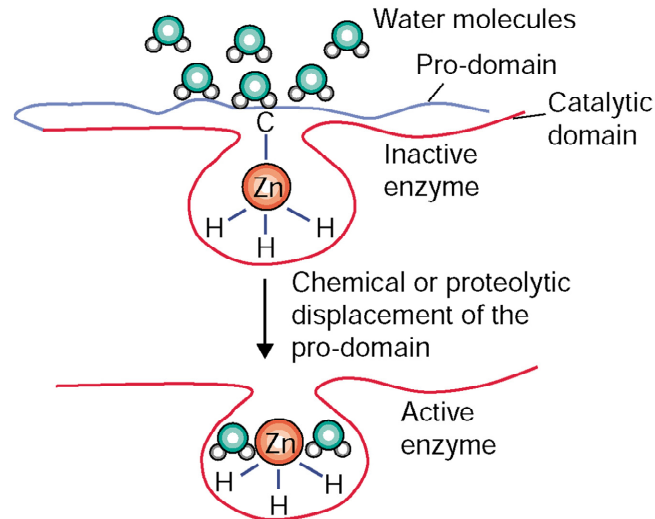


**Figure 1.18: The 'cysteine-switch' mechanism regulating the MMP zymogen.** The thiol group of a conserved cysteine (C) at the carboxyl terminus of the pro-domain acts as a fourth inactivating ligand for the catalytic zinc atom in the active site; this results in the exclusion of water and keeps the enzyme latent. Displacement of the pro-domain by conformational change or proteolysis disrupts this cysteine-zinc pairing and the thiol group is replaced by water. The enzyme can then cleave the peptide bonds of its substrates. *(Figure adapted from Somerville et al, 2003)*

Furthermore, the MMP activity is tightly controlled by endogenous inhibitors. Alpha-macroglobulin, an abundant plasma protein (Sottrup-Jensen and Birkedal-Hansen, 1989) is the main inhibitor of MMPs in tissue fluids. Alpha-macroglobulin binds to MMPs and this complex then binds to a scavenger receptor and is irreversibly cleared by endocytosis. Similarly, thrombospondin-2 forms a complex with MMP-2 and allows the scavenger-receptor-mediated endocytosis and clearance (Yang et al, 2001). Whereas, thrombospondin-1 binds to pro-MMP-2 and 9 and directly inhibits their activation (Bein and Simons, 2000). The best studied endogenous MMP-inhibitors are the tissue inhibitors of MMPs (TIMPs) -1, -2, -3 and -4, which reversibly inhibit MMPs in an one to one stoichiometric fashion (reviewed in Edwards, 2001). MMP inhibitors containing a subdomain with a structural similarity to TIMPs also exist, e.g. the carboxyterminal fragment of the procollagen C-terminal proteinase enhancer protein (Mott et al, 2000) or the NC1 domain of collagen type IV (Netzer et al, 1998).

### 1.4.3 MMPs and Tissue Inhibitors of MMPs (TIMPs) in human cancer

Enzymes that degrade the ECM have long been viewed as essential for tumor progression. In the early view of MMP action in cancer, MMPs were prime candidates for these activities. Then MMP family members can virtually degrade all structures of the extracellular matrix and

were present in almost all tumor cell lines [Figure 1.19]. Several studies reported that changes in MMP levels can markedly affect the invasive behaviour of tumor cells and their ability to metastasize in experimental animal models (Coussens et al, 2002).

Further evidence supporting the hypothesis that MMPs promote tumor progression came from studies of their endogenous tissue inhibitors (TIMPs). Several groups demonstrated that overexpression of TIMPs reduced experimental metastasis (DeClerck and Imren, 1994; Montgomery et al, 1993; Koop, 1994; Khokha et al, 1994). Other studies exploited transgenic technology to reveal TIMP/MMP function; for example, mouse 3T3 cells became more tumorigenic after antisense depletion of TIMP-1, and TIMP-1 overproduction slowed chemical carcinogenesis in skin (Buck et al, 1999).

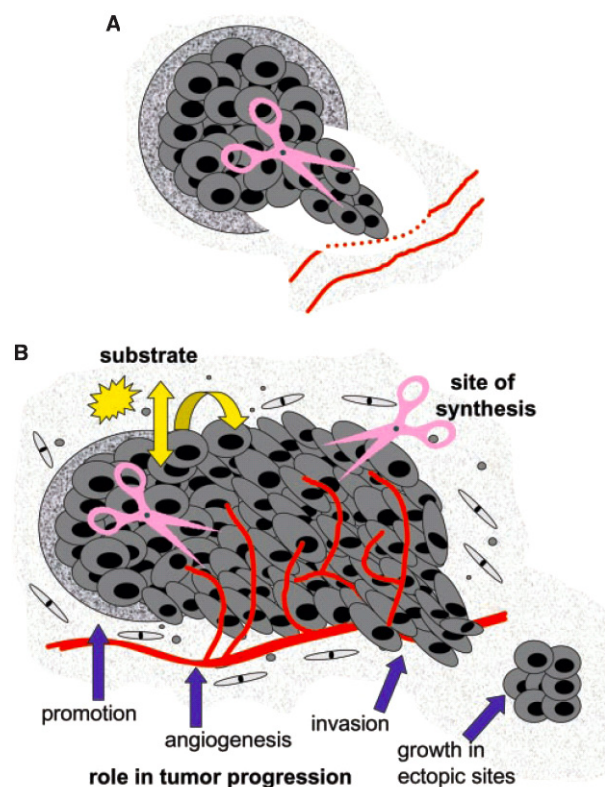


**Figure 1.19: Early and current view of the role of MMPs in cancer.** **A** Early view of MMP action in cancer. MMPs (represented as scissors) were classically viewed as enzymes responsible degrading basement membrane and extracellular matrix components, thereby facilitating tumor cell invasion and metastasis. **B** Current view of MMP action in cancer. MMPs are now known to contribute to multiple steps of tumor progression in addition to invasion, including tumor promotion, angiogenesis, and the establishment and growth of metastatic lesions in distant organ sites. Although creating gaps in matrix barriers remains a role of MMP activity, MMPs are also known to solubilise cell surface and matrix-bound factors that can then act in an autocrine or paracrine manner to influence cellular properties such as growth, death and migration. (*Figure adapted from Coussens et al, 2003*)

Additionally, clinical data strongly support a role for MMPs in the progression of human cancer (Egeblad and Werb, 2002). A negative association between MMPs and prognosis is shown in most reports. However, there are few studies known in which increased expression of specific MMPs reflects a favourable prognosis. In colon cancer for example, MMP-12 expression by carcinoma cells is associated with an increased survival (Yang et al, 2001) and MMP-9 expression by infiltrating macrophage is associated with reduced metastasis (Takeha et al, 1997).

In several clinical studies, high levels of TIMP-1 and TIMP-2 also correlate with poor prognosis. This might reflect the fact that the balance between expression of MMPs and TIMPs, although still favouring the MMPs, is at a higher overall level during the increased matrix remodelling that occurs in tumor progression. High TIMP levels are therefore associated with bad prognosis and tumor progression, but they do not cause it (Egeblad and Werb, 2002).

However, it seems that in some experimental settings TIMPs may contribute to cancer progression. For example, TIMPs can upregulate vascular endothelial growth factor (VEGF) secretion and thereby influence tumor angiogenesis (Yoshiji et al, 1998). Furthermore, animal experiments show that TIMP-2, despite its name, is an important activator of MMP-2 (Egeblad and Werb, 2002).

In human tumors, cancer cells are not the only source of MMPs. Whereas some MMPs are synthesized by cancer cells (for example MMP-7), many other MMPs are predominantly produced by stromal cells (e.g. MMP-2 and MMP-9). Tumoral stromal cells might be stimulated by cancer cells to produce MMPs in a paracrine manner through secretion of interleukins, interferons, emmprin and growth factors (Sternlicht and Werb, 2001). MMPs secreted by stromal cells can still be recruited to the cancer-cell membrane. For example, in human breast tumors MMP-2 mRNA is expressed by stromal cells, whereas MMP-2 protein is found on both stromal and cancer cell membrane (Polette et al, 1994) **[Figure 1.20]**.

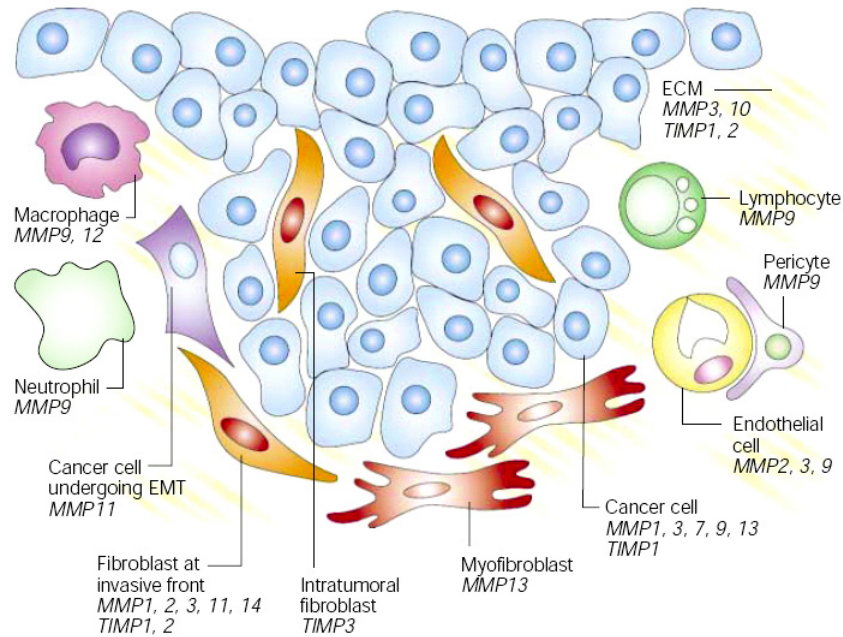


**Figure 1.20: Expression of MMPs and TIMPs in breast tumors.** In addition to cancer cells, tumors consist of stromal cells (including fibroblasts, myofibroblasts, endothelial cells, pericytes, macrophage, neutrophils and lymphocytes). Besides cancer cells different MMPs and TIMPs are produced by stromal cells. *(Figure adapted from Egeblad and Werb, 2002)*

Unlike classical oncogenes, MMPs are not upregulated by gene amplification or activating mutations in cancer cells. However, certain polymorphisms in MMP promoters can affect gene transcription and influence cancer susceptibility. For example, a single nucleotide polymorphism in the MMP-1 promoter contains either one or two guanines. The presence of two guanines leads to an enhanced transcription, so MMP-1 protein expression is higher in tumors from patients who carry two guanines compared to patients with one guanine in the promoter region of the MMP-1 gene (Kanamori et al, 1999). Additionally, it was reported that two homozygotes are more likely to develop invasive tumors (Ye et al, 2001; Zhu et al, 2001). Another promoter polymorphism that is also linked with cancer is the one in the promoter of the MMP-3 gene, which contains either five or six adenosines (A). The frequency of the 6A allele which has half of the transcriptional activity of the 5A allele (Ye et al, 2000) is lower in cancer patients than in the control population (Biondi et al, 2000). These increased levels of MMPs over a lifetime might foster increased susceptibility of tumorigenesis, these resembles the observations in transgenic mice overexpressing MMPs.

## 1.4.4 MMPs in inflammatory and vascular diseases

### 1.4.4.1 Arthritis

After the observation that rheumatoid synovial tissue is able to degrade tissue, arthritis was the first disease which was linked with MMPs (Harris and Krane, 1972). Studies over the past 40 years have confirmed that MMPs and TIMPs play an important role in connective tissue destruction in rheumatoid arthritis and osteoarthritis (Martel-Pelletier et al, 2001, Celiker et al, 2002; Mengshol et al, 2002; Burrage et al, 2006).

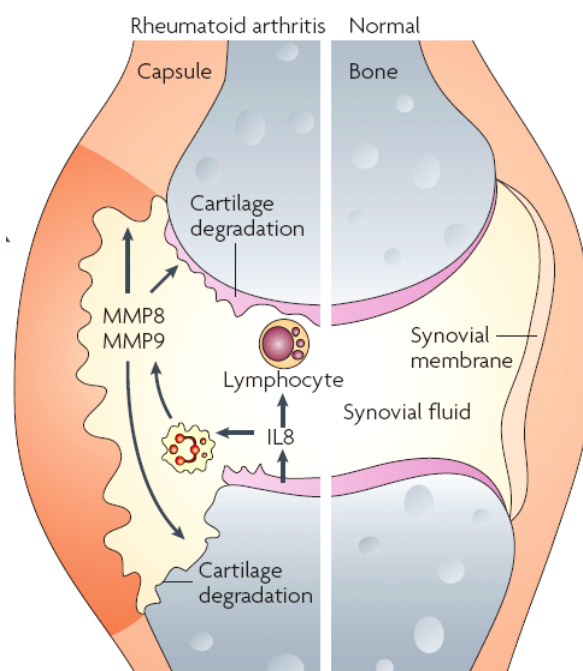


**Figure 1.21: Rheumatoid arthritis.** Pathogenic MMPs and key substrates are indicated. (Figure adapted from Hu et al, 2007)

Collagenases (MMP-1, MMP-8 and MMP-13) are responsible for the first cleavage of collagen II, an important structural component of cartilage. In addition, MMPs are one of the main factors which are responsible for the migration of inflammatory leucocytes. The treatment with MMP inhibitors led to a good outcome in different animal models of arthritis (DiMartino et al, 1997; Hu et al. 2007) [Figure 1.21].

Single nucleotide polymorphisms (SNPs) in MMP-2 are known to be related to the development of rheumatoid arthritis, whereas SNPs in MMP-1, MMP-3, MMP-7, MMP-9 and MMP-13 are not correlated with arthritis development (Rodriguez-Lopez et al, 2006). However all these MMPs are upregulated in arthritis (Vartak and Gemeinhart, 2007).

#### **1.4.4.2 Cardiovascular and vascular diseases**

MMPs play an important role in cardiovascular diseases as clearly demonstrated by several studies with genetically modified mice (transgenic or knock-out mice) (Janssens and Lijnen, 2006; Newby et al, 2006).

MMP-2 overexpression and activity has been shown to induce lower contractility in cardiac tissue (Wang et al, 2006). Increased MMP levels have been demonstrated to cause adverse left ventricular remodeling after myocardial infarction. During infarction MMP production is induced by inflammatory processes. In the myocardial interstitium various signaling pathways interact and lead to the induction and activation of several MMPs. Therefore, it has been proposed that pharmacological intervention at the level of these signaling molecules may provide potential therapeutic strategies for the adverse ventricular remodeling associated with the progression of heart failure (Janicki et al, 2004; Tsuruda et al, 2004; Ahmed et al, 2006).

Vascular remodeling plays a central role in (re-) stenosis, plaque rupture and aneurysm formation, and is dependent on the action of several MMPs. Restenosis can occur after interventions for treatment of arterothrombosis and is caused by proliferation and migration of vascular smooth muscle cells. Plaque rupture can cause the obstruction of the blood vessels, whereas loss of elasticity in the blood-vessel wall can lead to aneurysm formation.

**[Figure 1.22].**

Selective disruption of MMP-3 results in larger arteriosclerotic lesions. Furthermore MMP-3 has a disadvantageous role by enhancing the infiltration of macrophage in the lesions resulting in enhanced plaque instability (Silence et al, 2001). In addition, macrophage infiltration and collagen disposition are similarly promoted by MMP-9 (Luttun et al, 2004) and MMP-3, MMP-9 and MMP-12 have important roles in the degradation of elastic lamina and aneurysm formation. All together, these studies indicate paradoxical roles of different MMPs in different pathologic processes in vascular diseases (Hu et al, 2007).

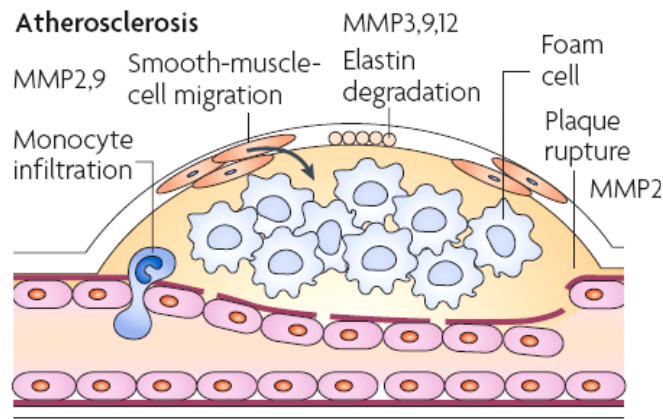


**Figure 1.22: Artherosclerosis.** Pathogenic MMPs and key substrates are indicated. *(Figure adapted from Hu et al, 2007).*

Nevertheless, a number of broad-spectrum MMP inhibitors showed some positive effects in animal models, exhibiting that MMP inhibition might be therapeutically useful. Therefore, the development and use of more specific inhibitors is needed and might lead to effective therapies in the treatment of these vascular diseases (Hu et al, 2007).

#### 1.4.4.3 Oral diseases

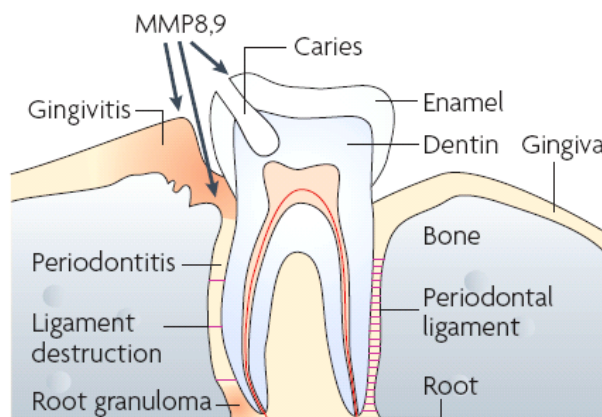


**Figure 1.23: Periodontitis and caries.** Pathogenic MMPs and key substrates are indicated. *(Figure adapted from Hu et al, 2007)*

The best example of MMP as a drug target is its role in oral diseases. ECM and dentin degradation are important processes in the pathogenesis of periodontitis and in the formation of caries lesions [Figure 1.23]. Originally, bacterial proteases were thought to be responsible, but increasing evidence indicates that the presence and activity of collagenases, mainly MMP-8, cause substantial connective tissue destruction, which leads to periodontitis

(Sorsa et al, 2004) **[Figure 1.23]**. The general MMP inhibitor doxycycline was approved by the FDA for the treatment of periodontitis (Ingmann et al, 1996). It is the only case where inhibition of MMPs has yielded clinical acceptance.

The list of pathologies given above where MMPs play a crucial role is by no means complete, but the listing is intended to exemplify the wide impact of various MMPs in several pathologies (Hu et al, 2007; Vartak and Gemeinhart, 2007).

### **1.4.5 MMPs and potential pharmaceutical interventions**

Abnormal expression of MMPs contributes to a variety of pathologic conditions. In the tumor environment, for example, host and tumor derived MMPs are often upregulated, while being expressed at low levels in normal organs (Overall and Kleinfeld, 2006; Pfaffen et al, 2010). The fact that MMPs are overexpressed under pathologic conditions could be important for different types of pharmaceutical intervention.

#### **1.4.5.1 Inhibition of MMPs**

As MMPs seemed to be attractive cancer targets drug development programmes were initiated 20 years ago by many companies to therapeutically block the extracellular matrix-degrading activities of MMPs in metastasis and angiogenesis. Initially, TIMP-1 and TIMP-2 were considered as potential therapeutics for cancer, but technical difficulties avoided their development into useful drugs. Therefore, MMPs became an attractive target for small organic molecule inhibitors, and a lot of energy was invested into the investigation of substrate specificity and structure of these enzymes (Whittaker et al, 1999) **[Figure 1.24]**. Small molecules containing both hydroxamate and non-hydroxamate zinc-binding sites, as well as natural products (tetracyclines and their derivatives), were developed as MMP inhibitors (MMPIs) (Coussens et al, 2002) **[Table 1.3]**.

However, the clinical development of MMPIs had to overcome different unforeseen problems:

- 1) Early phase clinical trials (dose escalation studies designed to evaluate safety) showed that prolonged treatment with MMPIs caused musculoskeletal pain and inflammation, complications not seen in preclinical models. Fortunately, the side effects were reversible and patients could continue after a short drug holiday, but the unexpected complications limited MMPI dosages in subsequent trials. In an attempt to minimize these side effects Agouron and Bayer developed “deep-pocket” MMPIs (prinomastat and tanomastat), which were more selective inhibitors for MMP-2 and



MMP-9 than for the other MMPs; however prinomastat still produced similar side effects (Whittaker et al, 2002).

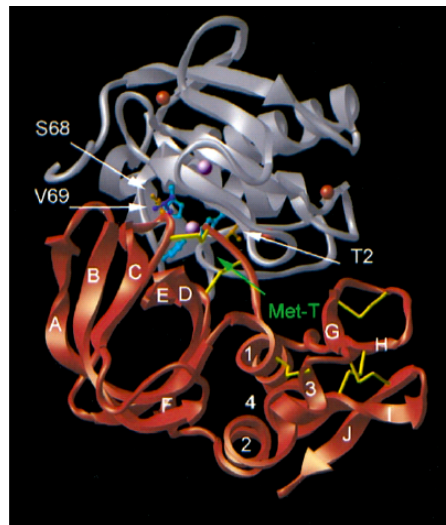


**Figure 1.24: Ribbon diagram of the complex of TIMP-1 and the catalytic domain of MMP-3.** MMP-3 is shown in *silver* and TIMP-1 in *red* (Brookhaven Protein Data Bank Entry 1UEA). The catalytic and structural zinc ions are shown as purple spheres. (*Figure adapted from Nagase and Woessner, 1999*)

- 2) Phase II clinical trials (designed to examine efficacy) turned out to be problematic as well. Because MMPi are cytostatic (cells are growth arrested but viable) rather than cytotoxic (cells are killed), therefore common measures to determine drug efficacy as reduction of tumor size could not be used to monitor drug activity. The reduction of tumor markers in serum was used as a measure for efficacy (Nemunaitis et al, 1998), but this was highly criticized.
- 3) Phase III clinical trials (large – scale studies that evaluate efficacy in comparison to standard treatment) were initiated in the mid-1990s. The first trials examined the efficacy of the MMPI alone versus that of cytotoxic drugs. In later clinical trials the effect of an MMPI, either in combination with or after treatment with cytotoxic drugs was compared with the effect of the cytotoxic drugs alone. In summary, the results of clinical phase III trials have been largely disappointing (Overall and Kleifeld, 2006). The failure of many MMPi in late-stage cancer clinical trials could be explained by the fact that MMPs are also involved in the early stage of cancer. Another reason for the lack of efficacy of most MMPi tested in cancer clinical trials could be their poor selectivity. Most MMPi target several MMPs – even those that prevent tumor progression and can enhance tumor vascularization by decreasing the production of angiogenesis inhibitors that are generated by MMP proteolysis of larger molecules.

**Table 1.3: Matrix metalloproteinases inhibitor drugs in clinical trials (Overall and Kleifeld, 2006)**

Inhibitor	Company	Structure	Specificity
Batimastat (BB-94)	British Biotech	Peptidomimetic	Broad spectrum
Ilomastat (GM-6001)	Glycomed	Peptidomimetic	Broad spectrum
Marimastat (BB-2516)	British Biotech, Schering-Plough	Peptidomimetic	Broad spectrum
Tanomastat (BAY-12-9566)	Bayer	Small molecule	Higher specificity towards MMP-2, MMP-3 and MMP-9
Prinomastat (AG-3340)	Agouron, Pfizer	Small molecule	Broad spectrum
Metastat (COL-3)	Collagenex	Low-dose tetracycline derivative	Broad spectrum; higher specificity towards MMP-2 and MMP-9
Neovastat (AE-941)	AEterna	Shark cartilage extract	Broad spectrum
BMS-275291	Bristol-Meyers Squibb, Celltech	Small molecule	Broad spectrum
MMI-270B (CGS-270B)	Novartis	Small molecule	Broad spectrum
Trocade (Ro-32-3555)	Roche	Peptidomimetic	MMP-1, MMP-8 and MMP-13
MMI-166	Shionogi	Small molecule	Broad spectrum

To overcome this problem, inhibitory antibodies could be developed that bind to a specific MMP while sparing all the other MMPs and related proteases (Overall and Lopez-Otin, 2002). In contrast to inhibitory antibodies, small organic MMP inhibitors usually bind to the zinc-binding site (similar in all MMPs). It is therefore hardly possible to develop such a small organic inhibitor specific for one single member of the MMP family.

Recently, it was reported on the blocking of matrix metalloproteinase-14 by DX-2400, a highly selective fully human inhibitory antibody discovered using phage display technology. This inhibitory  $\alpha$ -MMP-14 antibody blocked proMMP-2 processing on tumor and endothelial cells and inhibited angiogenesis *in vitro*. Furthermore, it was shown that DX-2400 affected tumor growth of MDA-MB 231 and BT-474 tumors when used as single agent or in combination. In contrast, this antibody did not alter the growth of MCF-7 (MMP-14 negative tumors) derived tumors, showing MMP-14 dependency for DX-2400. This reagent combines potency, selectivity and robust *in vivo* activity and shows the potential of a selective MMP-14 inhibitor for the treatment of solid tumors (Devy et al, 2009).

Until recently, few studies could provide the definitive evidence required to determine, if an MMP is a target for inhibition or if it is an anti-target for inhibition in cancer therapy.

A target for inhibition is a molecule that contributes to disease initiation or progression. The normal state of cell and tissue is restored, when its activity is downmodulated. In cancer, drugs downmodulating the reactivity of this target should slow down disease progression or might specifically kill tumor cells.

An anti-target for inhibition is a molecule with essential roles in normal cell and tissue function, and unacceptable side effects may result from its downmodulation. This results in shorter onset time of the disease, increased disease burden, poorer patient outcome or decreased survival time.

According to a review of Overall and Kleinfeld (Overall and Kleinfeld, 2006) only 3 out of 23 MMPs [Table 1.2] have been validated as targets (MMP-1, MMP-2 and MMP-7) for inhibitory tumor therapy, whereas other MMPs have been clearly validated as anti-targets as MMP-3, MMP-8 or MMP-9.

#### **1.4.5.2 Imaging of MMPs**

Early detection of primary tumors and metastatic lesions remain a major task in the diagnosis. The recognition of the role of MMPs in both the growth and metastasis of tumors has guided the development not only of therapeutic strategies utilizing MMPis, but also of catalyzed methods to detect and image tumors *in vivo*. These approaches include the use of radiolabeled MMP inhibitors as targeting agents or fluorogenic MMP-specific substrates combined with optical imaging modalities or contrast agents linked to MMPis.

The advantages using MMPs as a molecular target for an imaging agent are several-fold:

- 1) These enzymes are secreted and activated in the extracellular environment, avoiding their need to transfer the probe to the intracellular compartments.
- 2) They are active at physiological pH.
- 3) Their activity is catalytic and thus providing an opportunity for signal amplification not found with targets that bind in a one to one fashion.

Imaging of MMPs includes optical imaging (OIM), positron emissions tomography (PET), single photon emission computed tomography (SPECT), and magnetic resonance imaging (MRI). A number of new probes and techniques are under development for the molecular

imaging of MMPs that can be applied to give both temporal and spatial resolution to characterize not only the progression of the disease, but have also the potential to assess response to therapy (Scherer et al, 2008).

#### Optical imaging (OIM):

The main objective of OIM is to accumulate fluorophores at a targeted region that upon excitation emit photons. Several fluorescent agents have been developed so far that either target receptors, visualize the enzyme biodistribution or elucidate protein function and gene regulation (Weissleder and Ntziachristos, 2003).

The *in vivo* optical detection and imaging of protease activity was first demonstrated less than a decade ago by Weissleder *et al.* (Weissleder et al, 1999). The optical contrast agents developed utilized near-infrared fluorophores as optical sensors attached to a linear polylysine-polyethyleneglycol copolymer. The location of the fluorophores on the polymer quenched the fluorescent signal. After proteolytic cleavage of the peptide linker, fluorescent signal was enhanced producing an optically detectable near infrared fluorescence (NIRF) signal associated with the tumor.

#### MRI contrast agents:

Magnetic resonance imaging (MRI) has become widely available in hospitals and clinical centers and is a common used technique for imaging cancer. Conventional contrast agents are mainly Gadolinium (Gd) -based and they often lack molecular targeting moieties and therefore do not provide functional imaging capabilities to assess biological properties of tumors (Scherer et al, 2008).

Recently, Lepage et al. postulated that cleavage of MRI contrast agents by extracellular proteinases could be used to detect the expression of these enzymes in the microenvironment of tumors or metastatic lesions (Lepage et al, 2007). The authors presented a new contrast agent designed to display less solubility after cleavage by MMP-7.

#### PET and SPECT:

Positron emission tomography (PET) is a highly sensitive and quantitative molecular imaging modality. Radiolabeled tracer molecules are used in clinical and experimental medicine as imaging agents. The radioactive isotope has a short half-life and emits a positron by decaying. Whenever the positron interacts with a close-by electron, positron annihilation occurs and two 511 keV photons are emitted. As the emitted photons travel in a straight line

coincident to another one, a scintillation detector is used to localize the source of the annihilation (Scherer et al, 2008).

Single photon emissions computed tomography (SPECT) utilizes radiolabeled tracers containing isotopes with gamma radiation. A simple gamma camera is capable to measure the biodistribution of biomolecules in small concentrations *in vivo*. SPECT offers also the possibility of 3D-reconstruction (Scherer et al, 2008).

Since MMPi recognizes the active site of MMPs and inhibit catalysis, they can serve as tools for the identification of the active site of MMPs and are therefore able to discriminate between active MMPs and ProMMPs and MMPs inhibited by TIMPs.

Several attempts at radiolabeled MMPs revealed disappointing results *in vivo*. For example Zheng et al. tested a potent radiolabeled MMPi and observed high levels of unspecific binding in mouse models of breast cancer (Zheng et al, 2002), whereas *in vitro* the same inhibitor exhibited blocking effectiveness for several MMPs (Fei et al, 2003).

In principle, radiolabeled monoclonal antibodies could be considered as an alternative to the MMPi for *in vivo* tumor targeting applications. As advantages they would offer specificity to an individual MMP and more suitable pharmacokinetic properties than the small organic molecules.

#### **1.4.5.3 Targeting of MMPs for pharmacodelivery applications**

The treatment of solid tumors with most chemotherapeutic drugs relies on the expectation that the drugs will preferentially kill rapidly dividing tumor cells, rather than normal cells. But, the lack of selectivity towards tumor cells leads to toxicities in normal tissues with enhanced proliferation rates, such as the bone marrow, gastrointestinal tract and hair follicles. One avenue to develop more efficacious and better tolerated anti-cancer drugs relies on the targeted delivery of therapeutic agents to the tumor environment, thus sparing normal tissues. Monoclonal antibodies are increasingly being used for the selective delivery of bioactive molecules (e.g. radionuclides, drugs, cytokines) to the site of disease, thus sparing normal organs (Carter, 2006). Although mainly antibodies specific to membrane antigens on cancer cells have been used so far for tumor targeting applications, there is a growing interest in the use of stromal antigens and of markers of angiogenesis as antibody targets (Neri and Bicknell, 2005), with the potential to offer broad tumor coverage and low expression in normal tissues. In the tumor environment, for example, host and tumor derived MMPs are often upregulated, while being expressed at low levels in normal organs (Overall and Kleifeld, 2006; Pfaffen et al, 2010). Such antigens, expressed in wide range of different

tumors and virtually absent in normal tissues could serve as potential targets for pharmacodelivery applications.

#### 1.4.5.4 MMP-specific prodrug design or MMP-activated drug delivery

Besides the use of MMPs as target proteins either for inhibition or for pharmacodelivery applications, MMPs can also be utilized for the specific cleavage of a prodrug, which results in a release of the active drug at the site where MMPs are overexpressed. Drug activation would lead to increased local concentration of the active drug at the disease site compared to the surrounding tissue and other parts of the body where MMP activity is low.

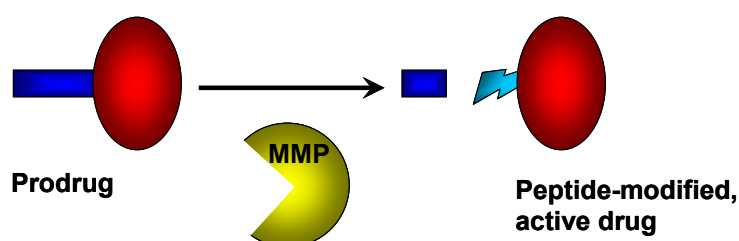


**Figure 1.25: Scheme of MMP-activation of a peptide prodrug.** To utilize MMP targeting, an active peptide is attached to a drug. When MMP is present, the MMP cleaves the peptide releasing an inactive peptide and a peptide-modified active drug. The peptide-fragment that is retained as part of the chemotherapeutic agent must be appropriate that the agent is active after MMP-cleavage. *(Figure adapted from Vartak and Gemeinhart, 2007)*

In the late 1990s, first attempts were made to exploit MMP activity for targeting purposes in respect of prodrug design. Some examples of approaches are listed below:

##### MMP activated peptide prodrugs:

In prodrug approach, therapeutic drugs were simply attached to a MMP substrate peptide. When the peptide is cleaved the drug becomes available. Several prodrugs have been designed in such a way for various anti-cancer agents (Glazier, 1997; Firestone and Telan, 2005) [Figure 1.25]. For example MMP specific conjugates of doxorubicin were shown to preferentially release leucine-modified doxorubicin and doxorubicin in a targeted fashion in MMP-expressing xenografts. These conjugates also showed much higher therapeutic index compared to the given doxorubicin alone (Albright et al, 2005).

### MMP activated carrier-peptide drug conjugate:

The drawbacks of peptide prodrug conjugates are their fast clearance and their non-specific accumulation in non-target tissues. Therefore, carrier-peptide drug conjugates were developed which protect the drug from clearance, from non-specific activation and from increased accumulation in the diseased tissue [Figure 1.26].

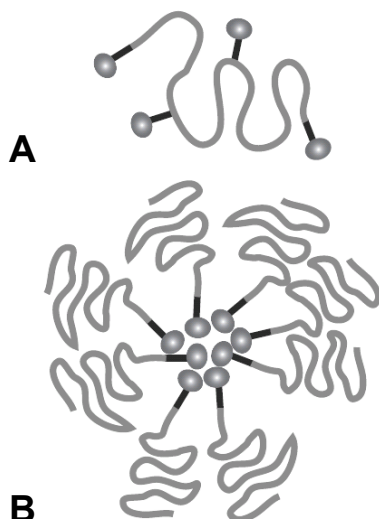


**Figure 1.26: Schematic depiction of MMP-activation of carrier peptide prodrugs. A** A macromolecule is modified to bear one or more peptide-prodrugs on the macromolecule chain. **B** Macromolecular carriers may be randomly placed into higher ordered structures such as micelles. (*Figure adapted from Vartak and Gemeinhart, 2007*)

To allow biological acceptance, the carrier molecule can be of natural origin, such as albumin, the most abundant protein in circulation.

A maleimide doxorubicin derivative incorporating a MMP-2 specific peptide sequence was synthesized. The conjugate binds rapidly and selectively to cysteines of albumine. When injected in A375 melanoma xenograft bearing mice, equivalent amounts of the conjugate and the doxorubicin did not show any difference in efficacy, but the maximal tolerated dose of the conjugate was higher than the one of doxorubicin alone (Kratz et al, 2001; Mansour et al, 2003).

### MMP activated peptide and protein delivery:

Besides the conjugation of small organic molecules to MMP-cleavable peptides, biomacromolecules can also be attached to carrier molecules for MMP activation. As an example Decay accelerating factor (DAF), an anti-complement protein, is highly effective in reducing the activity of the complement system in inflammatory diseases as arthritis, but

leads to severe systemic effect, when not administered as prodrug. DAF was in this approach fused to a human IgG in order to increase circulation half life, and was armed with a MMP sensitive polypeptide sequence to assure targeted delivery. Initial *in vivo* studies demonstrating distribution of prodrug and efficacy in reducing inflammation are warranted (Harris and Krane, 2003).

In addition to these three prodrug approaches, MMPs have also been used for the targeted delivery of viral vectors for gene delivery applications and for improving the targeting ability of galactosylated liposomes to hepatocellular carcinoma (HCC) (reviewed in Vartak and Gemeinhart, 2007).



## 1.5 Aim of the thesis

The aim of this thesis was the isolation of human monoclonal antibodies specifically binding to matrix metalloproteinases, particularly to murine MMP-1A, MMP-2 and MMP-3. A special interest of this work was the investigation of their *in vivo* tumor targeting properties.

Matrix metalloproteinases (MMPs) are a group of more than 20 zinc-containing extracellular proteinases that are capable of degrading multiple components of the extracellular matrix. Abnormal expression of MMPs contributes to a variety of pathologic conditions. In the tumor environment, for example, host and tumor derived MMPs are often upregulated, while being expressed at low levels in normal organs. Several studies on the use of MMPs as targets for imaging purposes have been reported so far. These approaches include the use of radiolabeled MMP inhibitors as targeting agents, or the use of fluorogenic MMP-specific substrates combined with optical imaging modalities. Since attempts at using radiolabeled MMP inhibitors for *in vivo* tumor targeting applications have often proved unsuccessful either for a lack of specificity or for unsuitable pharmacokinetic properties, radiolabeled monoclonal antibodies could in principle be considered as an alternative (Overall, et al, 2006; Scherer et al, 2006).

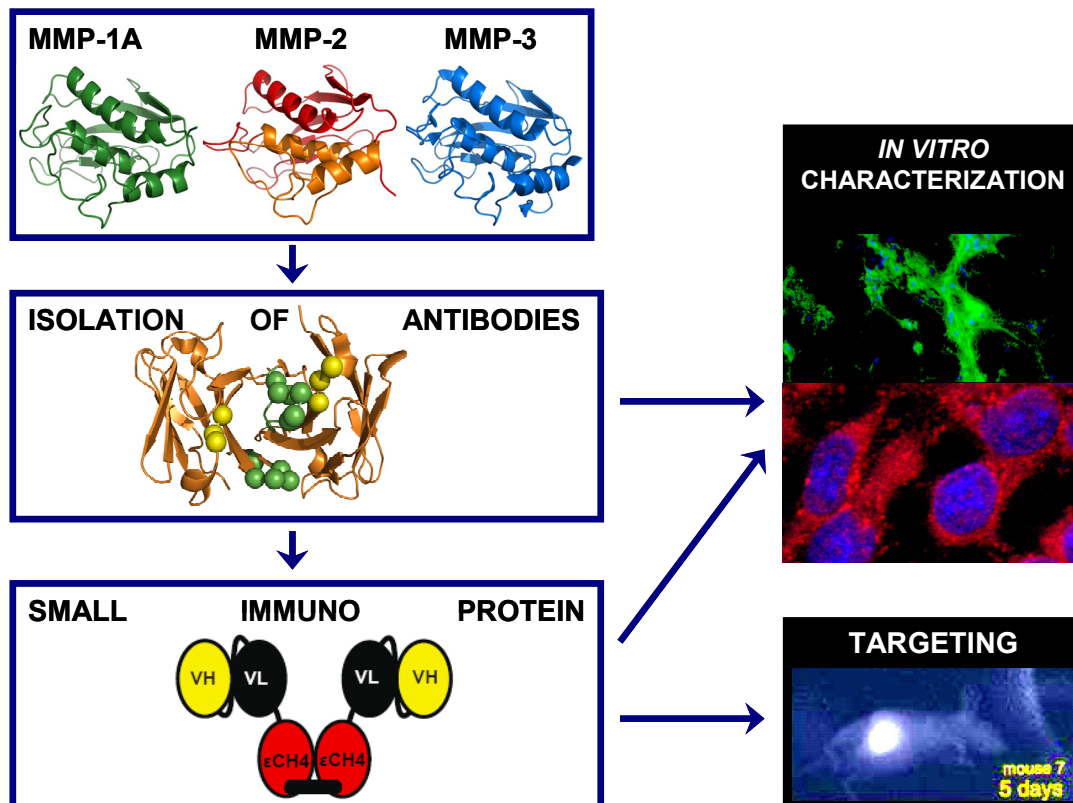


**Figure 1.27: Workflow of the antibody generation and their further analysis.** First step: production of active catalytic domains of MMP-1A, MMP-2 and MMP-3. Second step: Isolation of high-affinity antibodies by phage

display and their *in vitro* characterization. Third step: Cloning and production of the isolated scFvs in the small immuno protein antibody format and their testing *in vitro* and *in vivo*.

High affinity human monoclonal antibodies specific to the catalytic domains of MMP-1A, MMP-2 and MMP-3 were isolated by phage display technology. The performance of these novel reagents was tested in a comprehensive immunofluorescence analysis to assess the MMP expression patterns in healthy, cancerous and arthritic murine tissues.

Furthermore, these antibodies were cloned in the SIP (small immuno protein) mini-antibody format, produced and characterized using biochemical and immunochemical methods. Biodistribution analyses were performed to examine their tumor targeting properties at different time points in mice bearing subcutaneous F9 tumors using radioiodinated protein preparations.

## 2 RESULTS

### 2.1 Production and characterization of MMP-1A, MMP-2 and MMP-3

#### 2.1.1 Cloning, expression, purification and activity measurements of recombinant catalytic domains of MMP-1A, MMP-2 and MMP-3

The catalytic domain of murine MMP-1A (residues 95-280) was cloned and expressed in *E.coli* and purified from inclusion bodies by refolding on Ni-NTA-resin. The recombinant protein ran at 22 kDa in SDS-PAGE analysis and revealed a potent catalytic activity on the OmniMMP substrate (Knight et al, 1992), with a  $k_{\text{cat}} / K_{\text{M}}$  value of  $2 \times 10^2 \text{ s}^{-1}\text{M}^{-1}$  [Figure 2.1]. Similarly, the catalytic domain of murine MMP-3 was cloned and expressed as soluble protein from the cytosolic fraction of *E.coli*, with a  $k_{\text{cat}} / K_{\text{M}}$  value of  $1.44 \times 10^4 \text{ s}^{-1}\text{M}^{-1}$  [Figure 2.1]. By contrast, the two subunits of the catalytic domain of MMP-2 (residues 112-219 and 393-445) were fused sequentially for bacterial expression of the corresponding polypeptide, which was purified to homogeneity and displayed a  $k_{\text{cat}} / K_{\text{M}}$  value of  $7.4 \times 10^3 \text{ s}^{-1}\text{M}^{-1}$  [Figure 2.1].

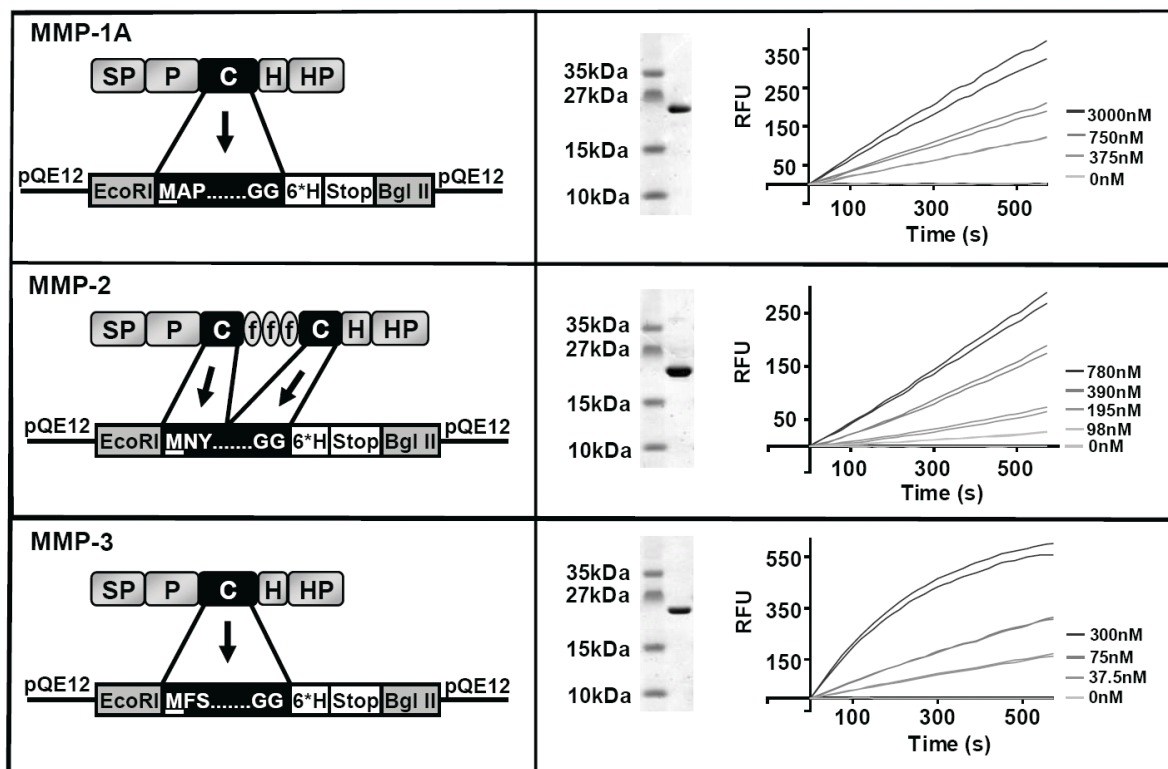


**Figure 2.1: Cloning, purification and quality control of recombinant catalytic domains of MMP-1A, MMP-2 and MMP-3.** Left panel: **Schematic representation of MMP-1A, MMP-2 and MMP-3.** The three MMPs consist of a signal peptide (SP), a propeptide (P), a catalytic domain (C), a hinge region (H) and a hemopexin-like domain (HP). MMP-2 contains additionally three fibronectin type II domains (f) inserted into the catalytic domain. **Cloning strategy.** The catalytic domains of MMP-1A (residues 95-280), MMP-2 (residues 112-219 and 393-445) and MMP-3 (residues 100- 273) containing a 6 x His-Tag (6\*H) were cloned with the restriction enzymes *EcoRI* and *BglII* into the pQE12 expression vector.

Right panel: **Measurement of the enzymatic activity.** The catalytic activity of the three purified recombinant proteins was measured at different concentrations by a fluorescent quenching peptide (OmniMMP substrate) at 8.3  $\mu\text{M}$  final concentration by recording the change of fluorescence signal ( $\lambda_{\text{ex}}$  328 nm;  $\lambda_{\text{em}}$  393 nm) over 10 min.

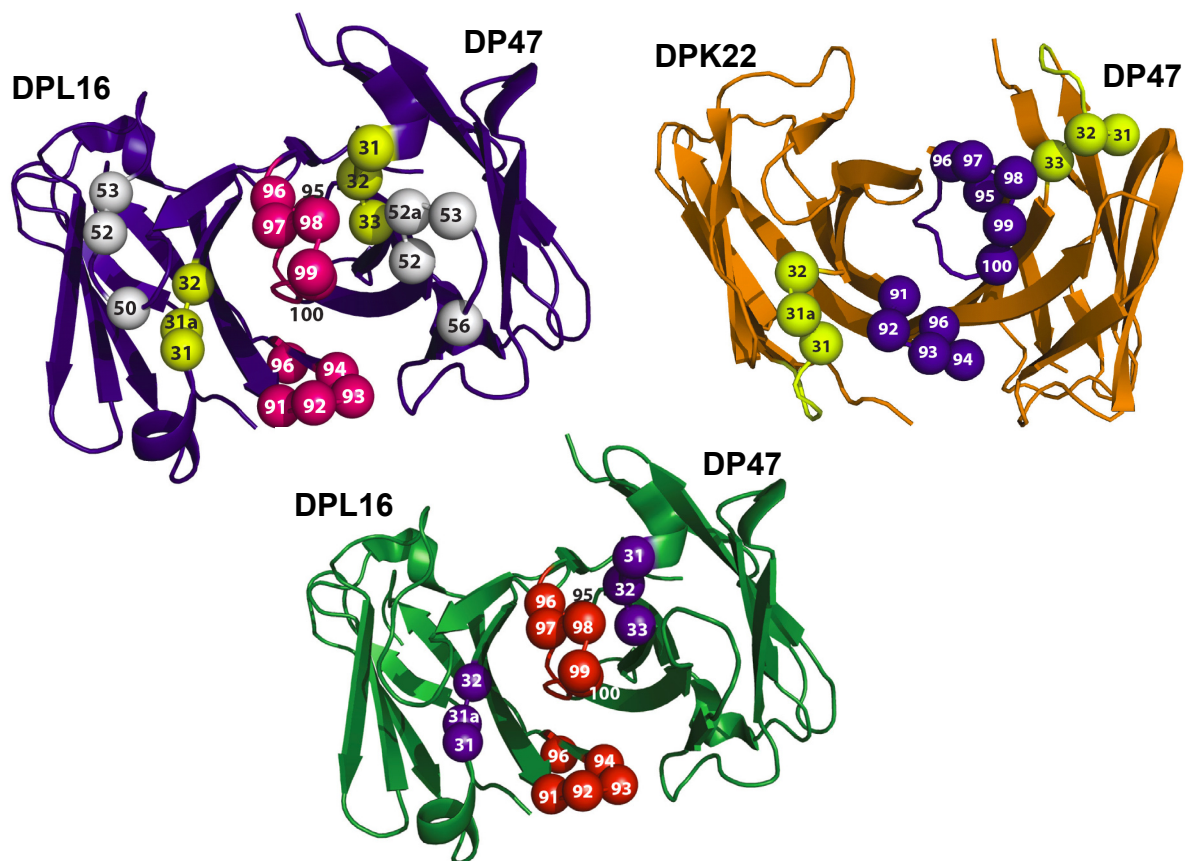
## **2.2 Generation and characterization of scFv antibody fragments specific to MMP-1A, MMP-2 and MMP-3**

### **2.2.1 Antibody phage display selections**

#### **2.2.1.1 An overview**

The recombinant catalytic domains were used for the isolation of human monoclonal antibodies from the ETH-2-Gold phage antibody library (Silacci et al, 2005). Clones from this library feature diversity on CDR3 loops of VH and VL domains. They contain a single VH germline gene (DP47, which confers binding to Protein A; (Hoogenboom and Winter, 1992)), while the VL domain is based either on a V $\kappa$  DPK22 scaffold (Tomlinson et al, 1992) or on a V $\lambda$  DPL16 scaffold (Tomlinson et al, 1992) **[Figure 2.2]**. Monoclonal antibodies in scFv format were isolated from the library by biopanning on immobilized antigen (Silacci et al, 2005) and showed specific binding in ELISA, plasmon surface resonance analysis (Villa et al, 2008) and immunohistochemical staining in tumor tissues (*data not shown*). The isolated antibodies were affinity matured by combinatorial mutagenesis of residues in CDR1 loops of VH and VL domains according to a procedure recently developed in our group (Villa et al, 2008; Silacci et al, 2006). This methodology yielded the human monoclonal antibody SP2, specific to MMP-2, and the antibodies SP3 and 9H, specific to murine MMP-3.

The antibody clone 1A specific to MMP-1A was initially isolated from the ETH-2 Gold library and affinity matured by randomization of the CDR1 loops leading to 11D. This clone was affinity-matured by mutagenesis of CDR2 loops (Pini et al, 1998), leading to the isolation of the antibody clone 5E. A further mutagenesis of CDR1 loops, followed by phage selections under stringent conditions, led to the isolation of daughter clone SP1 **[Figure 2.2]**. The amino acid sequence of relevant portions of CDR loops, which had been subjected to combinatorial mutagenesis, are shown in **Figure 2.2**, for the antibodies specific to MMP-1A, MMP-2 and MMP-3.



	VH			VL		
	31-33 <sup>a</sup>	52-56 <sup>a</sup>	95-100 <sup>a</sup>	31-32 <sup>a</sup>	50-53 <sup>a</sup>	91-96 <sup>a</sup>
<u>5E</u>	<u>RRP</u>	<u>TAAGGR</u>	<u>HPSVT</u>	<u>GWY</u>	<u>GKAG</u>	<u>FPFAPF</u>
<u>SP1</u>	<u>RQH</u>	<u>TAAGGR</u>	<u>HPSVT</u>	<u>RYY</u>	<u>GKAG</u>	<u>FPFAPF</u>
<u>SP2</u>	<u>RGA</u>	<u>SGSGGS</u>	<u>HGSSRN</u>	<u>PRL</u>	<u>GKNN</u>	<u>TLSRPS</u>
<u>9H</u>	<u>WMA</u>	<u>SGSGGS</u>	<u>ISSFH</u>	<u>NSG</u>	<u>GASS</u>	<u>PRGAPT</u>
<u>SP3</u>	<u>GYA</u>	<u>SGSGGS</u>	<u>ISSFH</u>	<u>GRR</u>	<u>GASS</u>	<u>PRGAPT</u>

**Figure 2.2: ScFv antibody fragment structures and sequences.** The DP47 and DPK22 backbones (orange) and DP47 and DPL16 backbones (blue and green) of antibodies in the ETH-2-Gold library are depicted in blue, orange and green respectively. All randomized residues of the CDR loops are shown in spacefill representation. Certain CDR3 residues (pink, blue or red) were randomized in the parental library, while certain residues in CDR1 loops (yellow or blue) and/or CDR2 loops (white) were combinatorially mutated for affinity maturation procedures. Using the program PyMOL, the structures of the scFvs were modulated from the protein data base file 1igm (DPK22), respectively 8FAB (DPL16) (Brookhaven Protein Data Bank). <sup>a</sup> Numbering according to Tomlinson *et al.* (Tomlinson *et al.*, 1992)

### 2.2.1.2 Affinity maturation libraries

In antibody phage display selections, two to three rounds of panning were performed. After the second or the third round, monoclonal bacterial supernatants of selected antibody clones were produced in a 96 well microtiter plates and screened by ELISA and by plasmon surface

measurements for binding to their cognate antigen. Several clones positive in ELISA were purified and further characterized in immunohistochemistry analysis, surface plasmon resonance and in specificity ELISA.

Like most clones isolated from naïve synthetic antibody libraries, the clones 1A (specific to MMP-1A), 4G and 5H (specific to MMP-2) and 7G (specific to MMP-3) [Table 2.1] exhibited an affinity good enough for most *in vitro* applications like ELISA or immunohistochemistry. However, for *in vivo* applications as tumor targeting, higher affinity antibodies would be preferable.

**Table 2.1: Overview on the different affinity maturation libraries constructed.**

Antigen	Parental antibody	VL	Affinity maturation library (CDR1)	Best clones	Affinity maturation library (CDR2)	Best clone	Affinity maturation library (CDR1)	Best clone
<b>MMP-1A</b>	1A	DPL16	$3.0 \times 10^7$	11D	$1.2 \times 10^8$	<u>5E</u>	$7.5 \times 10^7$	<u>SP1</u>
<b>MMP-2</b>	4G	DPL16	$2.0 \times 10^8$	<u>SP2</u>				
	5H	DPL16	$5.6 \times 10^7$					
<b>MMP-3</b>	7G	DPK22	$1.2 \times 10^8$	<u>9H</u> <u>SP3</u>				

We attempted to improve the affinity of all parental clones mentioned above in an approach similar to the one employed by Pini *et al.* for the generation of L19 (Pini *et al.*, 1998), an antibody specific to the extra-domain B of fibronectin, which is currently evaluated in clinical trials.

In brief, a subset of residues within the CDR1 and CDR2 of VH and of DPL16 or DPK22 was randomized, allowing all 20 amino acids at the chosen positions. From the resulting library, the clones with the highest affinity were selected by phage display.

**Table 2.1** gives an overview on the constructed affinity maturation libraries. The best clones in respect of their affinity assessed by surface plasmon resonance analysis are mentioned in **Table 2.1**. Clones underlined were not only characterized *in vitro*, but also in mouse models of cancer.

### 2.2.1.3 Generation of high affinity antibodies specific to MMP-1A

#### The 1A affinity maturation library: randomization of CDR1 loops

The residues 31, 32 and 33 of the CDR1 of the heavy chain and the residues 31, 31a and 32 of the light chain were chosen for construction of the 1A affinity maturation library and were randomized by PCR using partially degenerated primers (Silacci et al, 2006; Villa et al, 2008) [Figure 2.3].

Insert and vector were ligated and electroporated into freshly prepared electrocompetent TG-1 bacteria. The obtained library size was  $3.0 \times 10^7$  [Table 2.1]. The library was characterized by PCR screening to assess the percentage of clones with the correct insert and by sequencing a number of randomly picked clones to check for randomization of the chosen CDR1 residues.

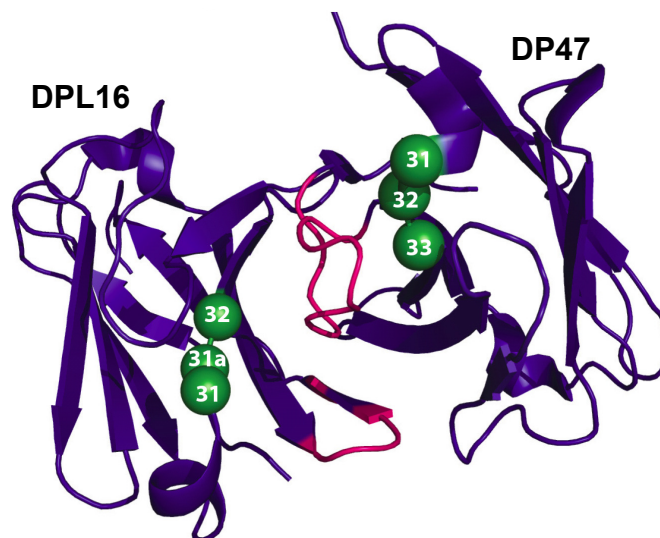


**Figure 2.3: Design of the 1A affinity maturation library.** DP47 and DPL16 backbones of antibodies in the 1A affinity maturation library are depicted in blue. All residues of the CDR1 loops randomized in this affinity maturation library are shown in spacefill representation. The CDR3 residues combinatorially mutated in the parental library are shown in pink. Using the program PyMOL, the structure of the scFv was modulated from the PDB file 8FAB (Brookhaven Protein Data Bank). Numbering according to Tomlinson *et al.* (Tomlinson *et al.*, 1992)

The 1A affinity maturation library was subjected to two rounds of phage panning using the antigen immobilized on an immunotube [Table 2.2]. The phage selections were performed under stringent conditions meaning increased number of washing steps before eluting the bound phage. This led to the isolation of daughter clone 11D [Figure 2.6 and Table 2.2] revealing a dissociation constant  $K_D$  of 250 nM.

A further round of mutagenesis was performed to further improve the affinity of clone 11D.



**Table 2.2: Selections performed with the affinity maturation library 1A.**

	Unbiotinylated catalytic domain of MMP-1A (Maxisorb)	
<i>Round of panning</i>	<i>1st</i>	<i>2nd</i>
Mode of selection	washing: 20 x PBS, 20 x PBS-Tween	washing: 20 x PBS, 20 x PBS-Tween
Titers	$3.0 \times 10^5$	$1.0 \times 10^7$
Number of positives in ELISA	9 / 94	100 / 188
<b>Isolated clone</b>		<b>11D (<math>K_D = 250\text{nM}</math>)</b>

### The 11D affinity maturation library: randomization of the CDR2 loops

The clone 11D was used as template for the construction of the second affinity maturation library. Mutagenesis of CDR2 loops of heavy and light chain was applied as previously reported (Pini et al, 1998). The residues of the CDR2 loops randomized are depicted in **Figure 2.4**. The resulting library exhibited a size of  $1.2 \times 10^8$ . Quality controls were performed as described above.

The library was submitted to phage display selections under various, more stringent conditions:

- 1) The antigen was either immobilized on an immunotube or biotinylated and captured on streptavidin coated wells to perform the selections [**Table 2.3**].
- 2) In addition to the increased number of washing steps before eluting the bound phage, the soluble antigen was added as competitor in molar excess to favor clones with a slow  $k_{\text{off}}$  rate.
- 3) To select only the good binding clones a stepwise elution of the bound phage was performed either at pH 10 or pH 14.

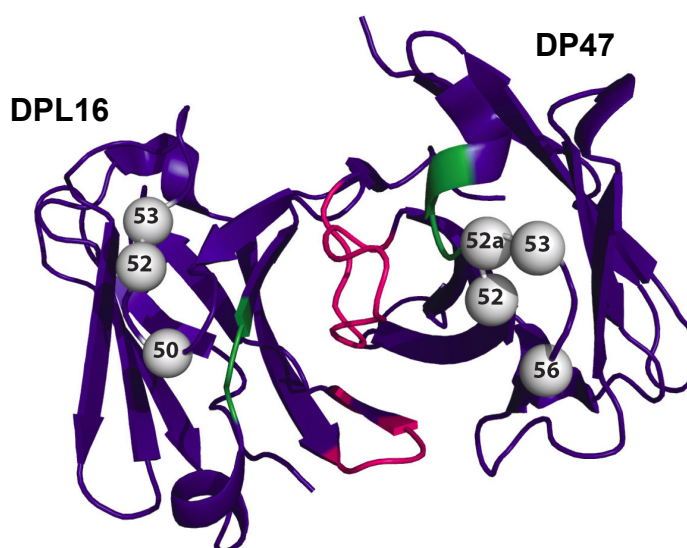


**Figure 2.4 Design of the 11D affinity maturation library.** DP47 and DPL16 backbones of antibodies in the 11D affinity maturation library are shown in blue. All residues of the CDR2 loops randomized in this affinity maturation library are shown in spacefill representation (white). The CDR1 loops randomized in the 1A affinity maturation

library are shown in green, whereas the CDR3 residues combinatorially mutated in the parental library are depicted in pink. Using the program PyMOL, the structure of the scFv was modulated from the PDB file 8FAB (Brookhaven Protein Data Bank). Numbering according to Tomlinson *et al.* (Tomlinson *et al.*, 1992)

The selection using the antigen as competitor before elution of the phage yielded to the isolation of the antibody clone 5E [Figure 2.6]. ScFv(5E) exhibited a  $K_D$  of 20 nM meaning a 12.5 fold enhancement of the affinity compared to clone scFv(11D). Clone 5E was reformatted into SIP format and was submitted to *in vivo* targeting experiments (see chapter 2.3.2 Quantitative biodistribution studies).

Selections with the antigen coated on immunotube did not lead to clones with better binding properties compared to the parental clone 11D.

**Table 2.3: Selections under various conditions performed with the affinity maturation library 11D.**

	Unbiotinylated catalytic domain of MMP-1A (Maxisorb)		Biotinylated catalytic domain of MMP-1A		
Round of panning	1st	2nd	1st		
Mode of selection	washing: 20 x PBS, 20 x PBS-Tween	washing: 20 x PBS, 20 x PBS-Tween	washing: 20 x PBS, 20 x PBS-Tween	competition with the soluble MMP-1A	stepwise elution at different pHs
Titers	$4.0 \times 10^5$	$1.0 \times 10^7$	$1.6 \times 10^7$	$1.2 \times 10^7$	pH 10: $2 \times 10^6$ pH 14: $1.6 \times 10^7$
Number of positives in ELISA	23 / 94	25 / 94	7 / 94	11 / 94	4 / 94
<b>Isolated clone</b>				<b>5E (<math>K_D = 20\text{nM}</math>)</b>	

#### The 5E affinity maturation library: randomization of the CDR1 loops

To further improve the affinity of clone 5E a third affinity maturation library was constructed. Within this library certain residues of the CDR1 loops of heavy and light chain were combinatorially mutated (Pini *et al.*, 1998). The randomized residues are depicted in **Figure 2.5**.

The affinity maturation library 5E exhibited a size of  $7.5 \times 10^7$  [Table 2.1]. As quality controls PCR screening and sequencing of several randomly picked clones were performed.

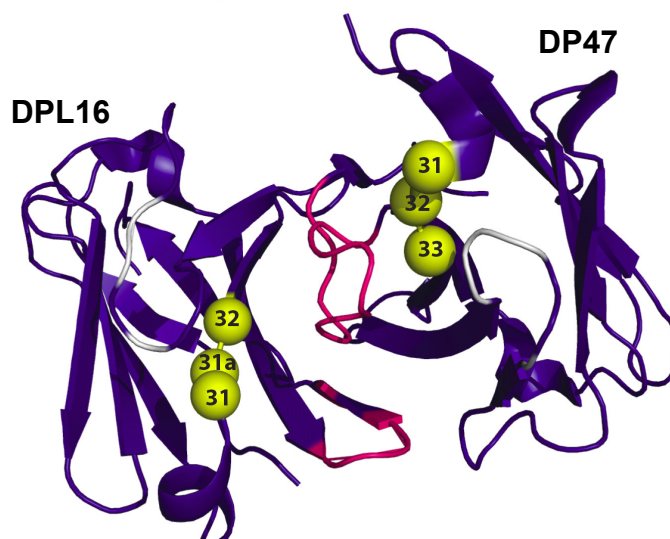


**Figure 2.5: Design of the 5E affinity maturation library.** DP47 and DPL16 backbones of antibodies in the 5E affinity maturation library are shown in blue. All residues of the CDR1 loops randomized in this affinity maturation library are shown in spacefill representation (yellow). The CDR2 loops randomized in the 11D affinity maturation library are shown in white, whereas the CDR3 residues of the parental library are depicted in pink. Using the program PyMOL, the structure of the scFv was modulated from the PDB file 8FAB (Brookhaven Protein Data Bank). Numbering according to Tomlinson *et al.* (Tomlinson *et al.*, 1992)

Phage display selections were performed with the constructed 5E affinity maturation library [Table 2.4]. As before the antigen was biotinylated prior to the selections and immobilized on streptavidin coated wells.

Next to the use of soluble antigen as competitor, the clone 5E with an affinity in the nanomolar range was applied as competing agent before elution of the bound phage in order to favor clones with good binding properties.

**Table 2.4: Selections under various conditions performed with the affinity maturation library 5E.**

Biotinylated catalytic domain of MMP-1A			
Round of panning	1st		
Mode of selection	washing: PBS 20x, PBS-Tween 20x	addition of soluble MMP-1A as competitor	addition of soluble 5E as competitor
Titers	$3.0 \times 10^6$	$2.0 \times 10^6$	$1.0 \times 10^6$
Number of positives in ELISA	97 / 188	21 / 94	48 / 94
<b>Isolated clone</b>	<b>SP1 (<math>K_D = 6nM</math>)</b>		

The selections using the soluble MMP-1A in molar excess as competitor yielded to the isolation of the antibody clone SP1 [Figure 2.6] exhibiting the best binding properties compared to the other clones selected.

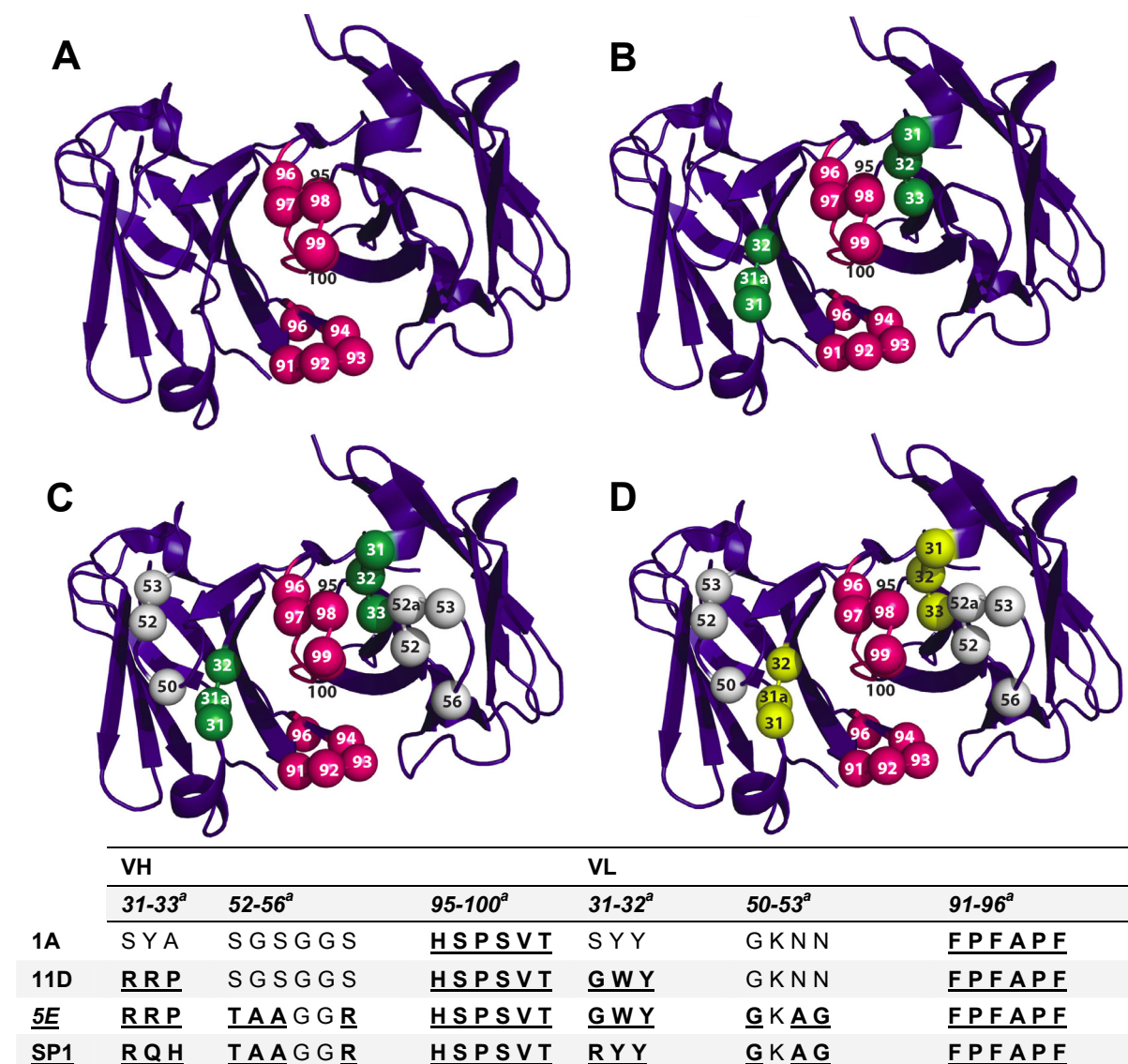


**Figure 2.6 Structures and sequences of the scFv antibody fragments specific to MMP-1A.** The DP47 and DPL16 backbones of antibodies in the ETH-2-Gold library are depicted in blue. All randomized residues of the CDR loops are shown in spacefill representation. **A Structure of the parental scFv(1A).** Certain CDR3 residues (pink) were randomized in the ETH-2 Gold library. **B Structure of the affinity matured scFv(11D).** The randomized CDR3 residues are shown in pink, while certain residues in the CDR1 loops (yellow), mutated in the affinity maturation procedure are depicted in green. **C Structure of the affinity matured scFv(5E).** Residues mutated in the ETH-2 Gold library are depicted in pink, whereas residues randomized during further affinity maturation procedures are shown in green (CDR1) and in white (CDR2). **D Structure of the affinity matured scFv(SP1).** Certain residues of the CDR3 loops mutated in the parental library are depicted in pink, whereas residues randomized during further affinity maturation procedures are shown in yellow (CDR1) and in white (CDR2). Using the program PyMOL, the structures of the scFvs were modulated from the protein data base file 8FAB (DPL16) (Brookhaven Protein Data Bank). <sup>a</sup> Numbering according to Tomlinson *et al.* (Tomlinson *et al.*, 1992).

### 2.2.1.4 Generation of high-affinity antibodies specific to MMP-2

#### The 4G and the 5H affinity maturation library: randomization of the CDR1 loops

The parental clones 4G and 5H were used as template for the construction of these two affinity maturation libraries. Residues 31, 32 and 33 of the DP47 heavy chain and residues 31, 31a and 32 of the DPL16 light chain were chosen for combinatorial mutagenesis [Figure 2.7].

The size of the 4G affinity maturation library was  $2.0 \times 10^8$  and of the 5H affinity maturation library  $5.6 \times 10^7$  [Table 2.1]. As quality controls PCR screening and sequencing of several randomly picked clones were performed.

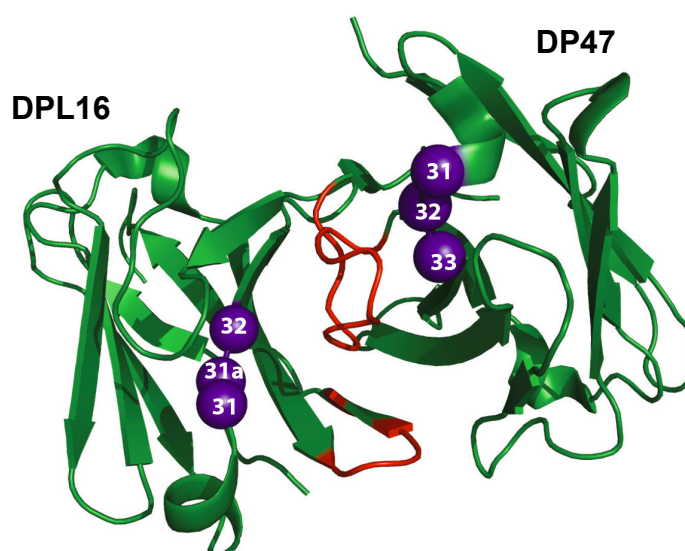


**Figure 2.7: Design of the 4G and the 5H affinity maturation library.** DP47 and DPL16 backbones of antibodies in the 4G affinity maturation library and in the 5H affinity maturation library respectively are depicted in green. All residues of the CDR1 loops randomized in this affinity maturation library are shown in spacefill representation (blue). The CDR3 residues randomized in the parental library are shown in pink. Using the program PyMOL, the structure of the scFv was modulated from the PDB file 8FAB (Brookhaven Protein Data Bank). Numbering according to Tomlinson *et al.* (Tomlinson *et al.*, 1992)

**Table 2.5: Selections performed with the affinity maturation libraries 4G and 5H.**

	Biotinylated catalytic domain of MMP-2	
<b>Round of panning</b>	<b>1st</b>	
Library	4G	5H
Mode of selection	washing: 20x with PBS, 20x with PBS-Tween	washing: 20x with PBS, 20x with PBS-Tween
Titers	$3.0 \times 10^6$	$2.0 \times 10^6$
Number of positives in ELISA	69 / 94	9 / 94
<b>Isolated clone</b>	<b>SP2 (<math>K_D = 24</math> nM)</b>	

Prior to selections with the two affinity maturation libraries the catalytic domain of MMP-2 was biotinylated. Selections with the 4G affinity maturation library led to the isolation of the scFv(SP2) exhibiting an affinity of 24 nM as assessed by BIAcore measurements [Figure 2.8]. A fifty fold affinity improvement was achieved since the affinities of the parental clones 4G and 5H were in the micromolar range.

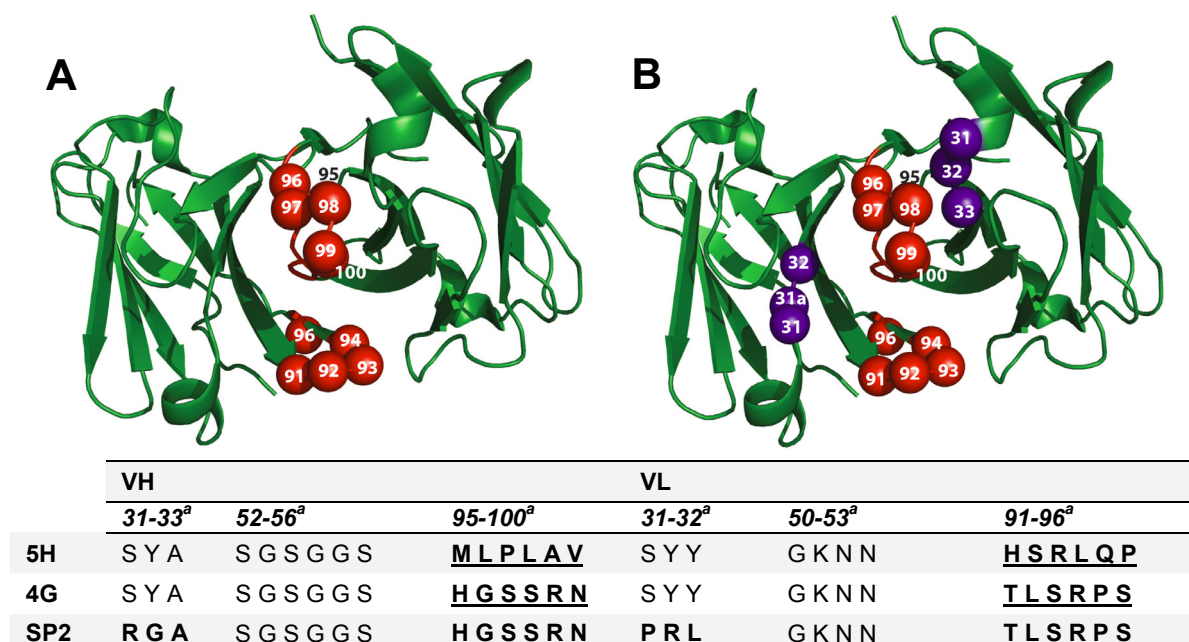


**Figure 2.8: Structures and sequences of the scFv antibody fragments specific to MMP-2.** The DP47 and DPL16 backbones of antibodies in the ETH-2-Gold library are depicted in green. All randomized residues of the CDR loops are shown in spacefill representation. **A Structure of the parental scFv(4G) and scFv(5G).** Certain CDR3 residues (red) were randomized in the ETH-2 Gold library. **B Structure of the affinity matured scFv(SP2).** The randomized CDR3 residues of the parental library are shown in red, while certain residues of the CDR1 loops mutated in the affinity maturation procedure are depicted in blue. Using the program PyMOL, the structures of the scFvs were modulated from the protein data base file 8FAB (DPL16) (Brookhaven Protein Data Bank). <sup>a</sup> Numbering according to Tomlinson *et al.* (Tomlinson *et al.*, 1992)

### 2.2.1.5 Generation of high-affinity antibodies specific to MMP-3

#### Generation of the 7G affinity maturation library: randomization of the CDR1 loop

The sequence of the parental clone 7G originally isolated from the ETH-2 Gold library was used as template for the construction of this affinity maturation library. As before mutagenesis of certain residues of the CDR1 loops of heavy and light chain was applied [Figure 2.9]. After ligation of vector and insert and electroporation into freshly prepared electrocompetent TG-1 bacteria, the 7G library exhibited a size of  $1.2 \times 10^8$ . Quality controls to evaluate the performance of the library were done as described above.

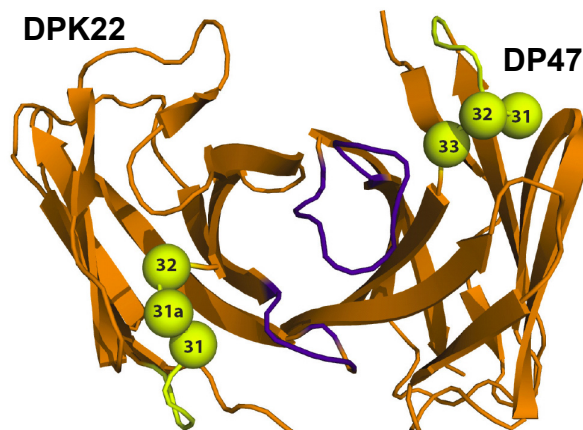


**Figure 2.9: Design of the 7G affinity maturation library.** DP47 and DPK22 backbones of antibodies in the 7G affinity maturation library are depicted in orange. All residues of the CDR1 loops randomized in this affinity maturation library are shown in spacefill representation (yellow). The CDR3 residues randomized in the parental library are shown in blue. Using the program PyMOL, the structure of the scFv was modulated from the PDB file 1igm (Brookhaven Protein Data Bank). Numbering according to Tomlinson *et al.* (Tomlinson *et al.*, 1992)

The affinity maturation library 7G was submitted to phage display selections under various, stringent conditions:

- 1) Immobilization of the catalytic domain of MMP-3 was either achieved by coating on an immunotube or by biotinylation prior to selections and capturing on streptavidin coated wells [Table 2.5].
- 2) In addition to the increased number of washing steps, soluble MMP-3 was added as competitor in molar excess before eluting the bound phage to favor clones with a slow  $k_{off}$  rate.
- 3) To select only clones with good binding properties a stepwise elution of the bound phage first at pH 10 followed by triethylamine 100mM at pH 14.

**Table 2.5: Selections performed under various conditions with the affinity maturation library 7G.**

Round of panning	Unbiotinylated catalytic domain of MMP-3 (Maxisorb)		Biotinylated catalytic domain of MMP-3			
	1st	2nd	1st			
Mode of selection	washing: 20x PBS, 20x PBS-Tween	washing: 20x PBS, 20x PBS-Tween	washing: 20x PBS, 20x PBS-Tween	competition with the soluble catalytic domain of MMP-3		stepwise elution at different pHs
Titers	$2.0 \times 10^5$	$9.0 \times 10^5$	$2 \times 10^6$	1 <sup>st</sup> round $1 \times 10^7$	2 <sup>nd</sup> round	pH10: $2 \times 10^6$ pH14: $4 \times 10^7$
Number of positives		108 / 188	1 / 94	4 / 94	13 / 188	1 / 94
<b>Isolated clones</b>				<b>9H (<math>K_D = 10</math> nM) (1<sup>st</sup>)</b> <b>SP3 (<math>K_D = 8</math> nM) (2<sup>nd</sup>)</b>		

Again, the selection using the soluble MMP-3 as competing agent led to the isolation of the antibody clones 9H and SP3 [Figure 2.10]. Both scFvs exhibited dissociation constants  $K_D$  in the nanomolar range which means a hundred fold affinity improvement compared to the micromolar affinity of the parental clone 7G.

Selections with the antigen coated on immunotube did not yield to clones with better binding properties compared to the parental clone 7G.

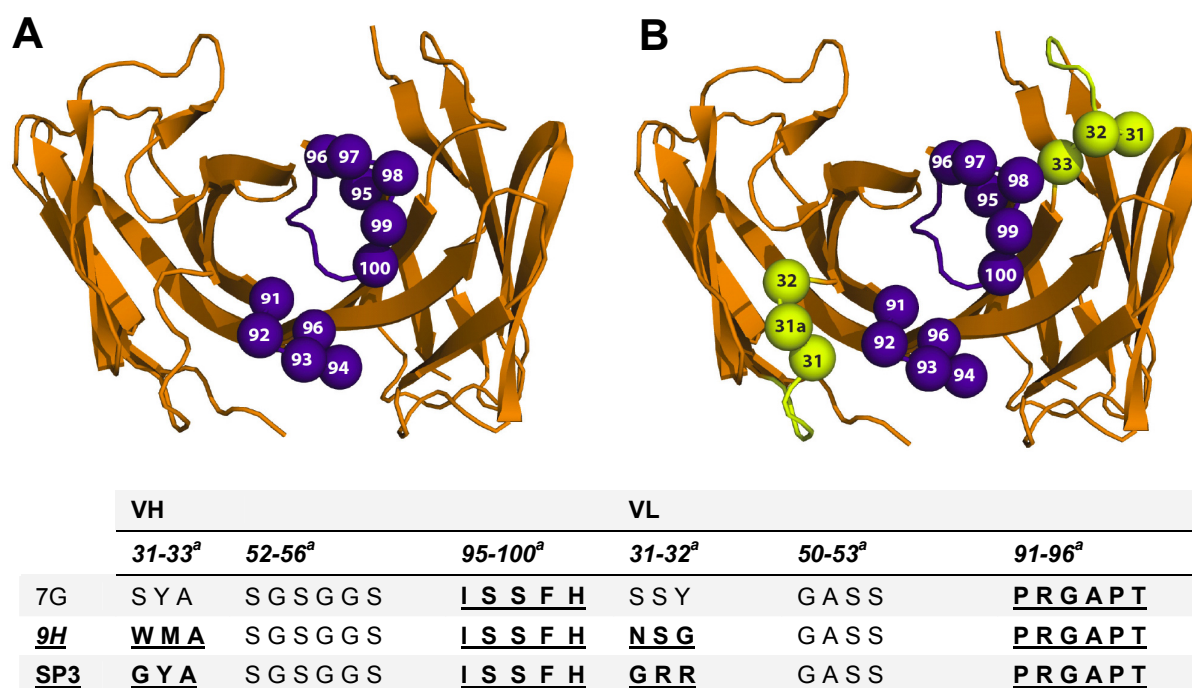


**Figure 2.10: Structures and sequences of the scFv antibodies specific to MMP-3.** The DP47 and DPK22 backbones of antibodies in the ETH-2-Gold library are depicted in orange. All randomized residues of the CDR loops are shown in spacefill representation. **A Structure of the parental scFv(7G).** Certain CDR3 residues (red) were randomized in the ETH-2 Gold library. **B Structure of the affinity matured scFv(9H) and scFv(SP3).** The mutated CDR3 residues of the parental library are shown in blue, while certain residues of the CDR1 loops mutated in the affinity maturation procedure are depicted in yellow. Using the program PyMOL, the structures of the scFvs were modulated from the protein data base file 1igm (Brookhaven Protein Data Bank). <sup>a</sup> Numbering according to Tomlinson *et al.* (Tomlinson *et al.*, 1992).



## 2.2.2 *In vitro* characterization of three scFv antibody fragments specific to MMP-1A, MMP-2 and MMP-3

### 2.2.2.1 Affinity measurements and specificity of scFv(SP1), scFv(SP2) and scFv(SP3)

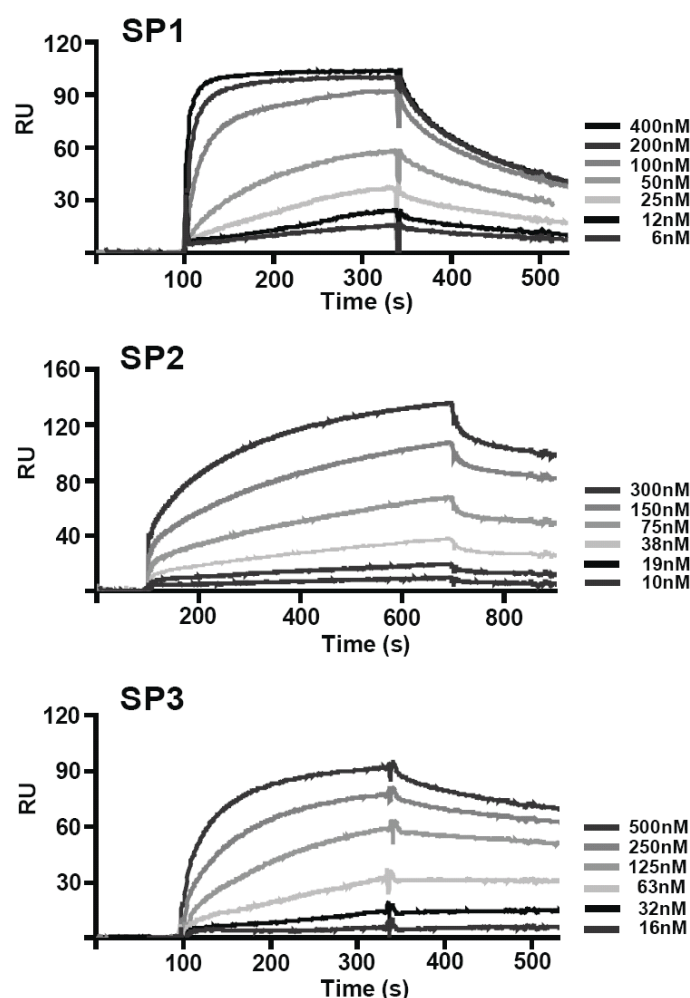


**Figure 2.11: BIAcore sensograms of the purified monomeric anti-MMP antibody preparations injected at different concentrations.** SP1 (specific to MMP-1A) revealed a dissociation constant ( $K_D$ ) of 6 nM [ $k_{on} = 1.6 \times 10^6 \text{ M}^{-1}\text{s}^{-1}$  and  $k_{off} = 9.7 \times 10^{-3} \text{ s}^{-1}$ ], SP2 (specific to MMP-2) had a  $K_D$  of 24 nM [ $k_{on} = 3.6 \times 10^4 \text{ M}^{-1}\text{s}^{-1}$  and  $k_{off} = 8.6 \times 10^{-4} \text{ s}^{-1}$ ] and SP3 (specific to MMP-3) revealed a  $K_D$  of 8 nM [ $k_{on} = 3.6 \times 10^4 \text{ M}^{-1}\text{s}^{-1}$  and  $k_{off} = 2.9 \times 10^{-4} \text{ s}^{-1}$ ]. Kinetic constants were calculated with the BIAevaluation 4.1 software.

The monomeric fractions of the SP1, SP2 and SP3 antibodies in scFv format were isolated by size-exclusion chromatography and analyzed by real-time interaction analysis on a BIAcore instrument, using an antigen-coated microsensor chip. **Figure 2.11** illustrates sensograms of the three antibodies, revealing a  $K_D$  dissociation constant of 6 nM [ $k_{on} = 1.6 \times 10^6 \text{ M}^{-1}\text{s}^{-1}$  and  $k_{off} = 9.7 \times 10^{-3} \text{ s}^{-1}$ ] for SP1 (specific to MMP-1A), 24 nM [ $k_{on} = 3.6 \times 10^4 \text{ M}^{-1}\text{s}^{-1}$

and  $k_{\text{off}} = 8.6 \times 10^{-4} \text{ s}^{-1}$ ] for SP2 (specific to MMP-2), and 8 nM [ $k_{\text{on}} = 3.6 \times 10^4 \text{ M}^{-1}\text{s}^{-1}$  and  $k_{\text{off}} = 2.9 \times 10^{-4} \text{ s}^{-1}$ ] for SP3 (specific to MMP-3).

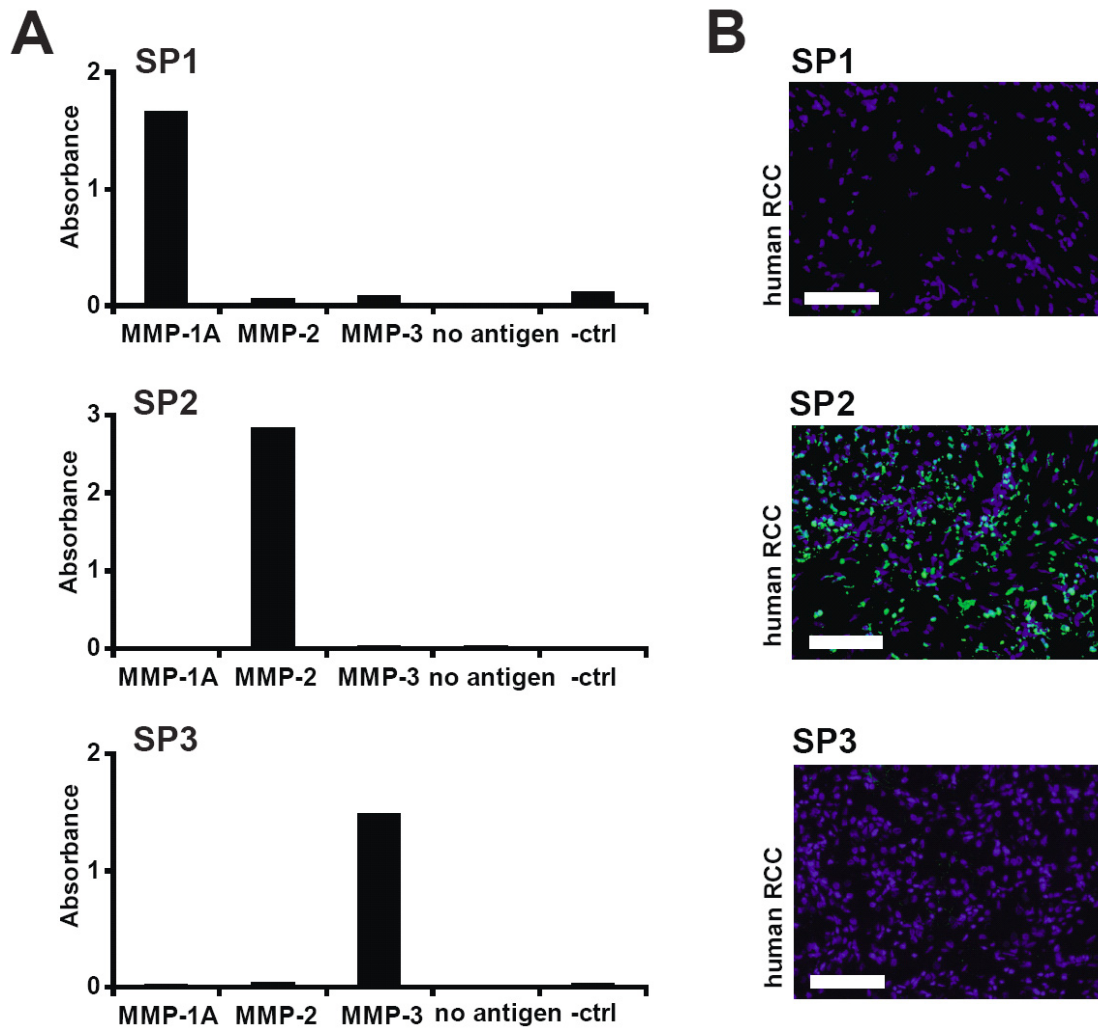


**Figure 2.12: Specificity of the MMP-binding antibodies.** **A** ELISA signals against catalytic domains of murine MMP-1A, MMP-2 and MMP-3 for the antibodies SP1, SP2 and SP3. No antigen, wells only blocked with PBS, milk. **B** Immunofluorescence analysis on cryosections of human renal cell carcinoma was performed to test the crossreactivity of SP1, SP2 and SP3 with the human catalytic domain of MMP-1, MMP-2 and MMP-3. MMPs were stained in green, whereas cell nuclei were stained in blue using DAPI. Scale bar = 100  $\mu\text{m}$ .

Importantly, the three antibodies SP1, SP2 and SP3 bound the corresponding MMP antigen in a highly specific manner and did not cross-react with any of the other two structurally related catalytic domains [Figure 2.12 A]. The ability of the antibodies SP1, SP2 and SP3 to recognize the human catalytic domain of MMP-1, MMP-2 or MMP-3 was tested by immunofluorescence analysis on cryosections of human renal cell carcinoma. Figure 2.12 B shows that only with SP2 a strong green staining could be observed, whereas the antibodies SP1 and SP3 did not cross-react with the human MMP-1, respectively with the human MMP-

3. The homology between the human and murine MMP catalytic domain is 61% for human MMP-1, 98% for human MMP-2, and 82% for human MMP-3.

#### **2.2.2.2 Immunofluorescence with SP1, SP2 and SP3 on cancer and arthritis sections**

The recombinant antibodies SP1, SP2 and SP3 were extensively characterized by immunofluorescence on cryosections of murine and human (xenograft) tumors, murine arthritis specimens and healthy tissues. In all tumors studied (human glioblastoma U87, human kidney clear cell carcinoma Caki-1, human ovarian carcinoma SKOV-3, human lung carcinoma H460, murine melanoma B16 and human renal cell carcinoma 786-O), a moderate to very strong staining could be observed with all three antibodies. Some differences in staining patterns could be observed for the three antibodies. SP1 (specific to MMP-1A) showed the strongest staining on murine melanoma B16 and on human renal cell carcinoma 786-O, whereas SP2 (specific to MMP-2) stained strongest human kidney clear cell carcinoma Caki-1. Clone SP3 (specific to MMP-3) exhibited the strongest staining on human ovarian carcinoma SKOV-3 **[Figure 2.13 and 2.14]**. The antibodies also showed a moderate (SP1) to a very strong (SP2 and SP3) staining in inflamed joint specimens of mice with collagen-induced arthritis **[Figure 2.13 and 2.14]**.

No MMP-1A expression was detectable in the normal organs tested, while MMP-2 was found expressed in brain and liver and a strong MMP-3 staining was detected in mouse liver **[Figure 2.13 and 2.14]**.

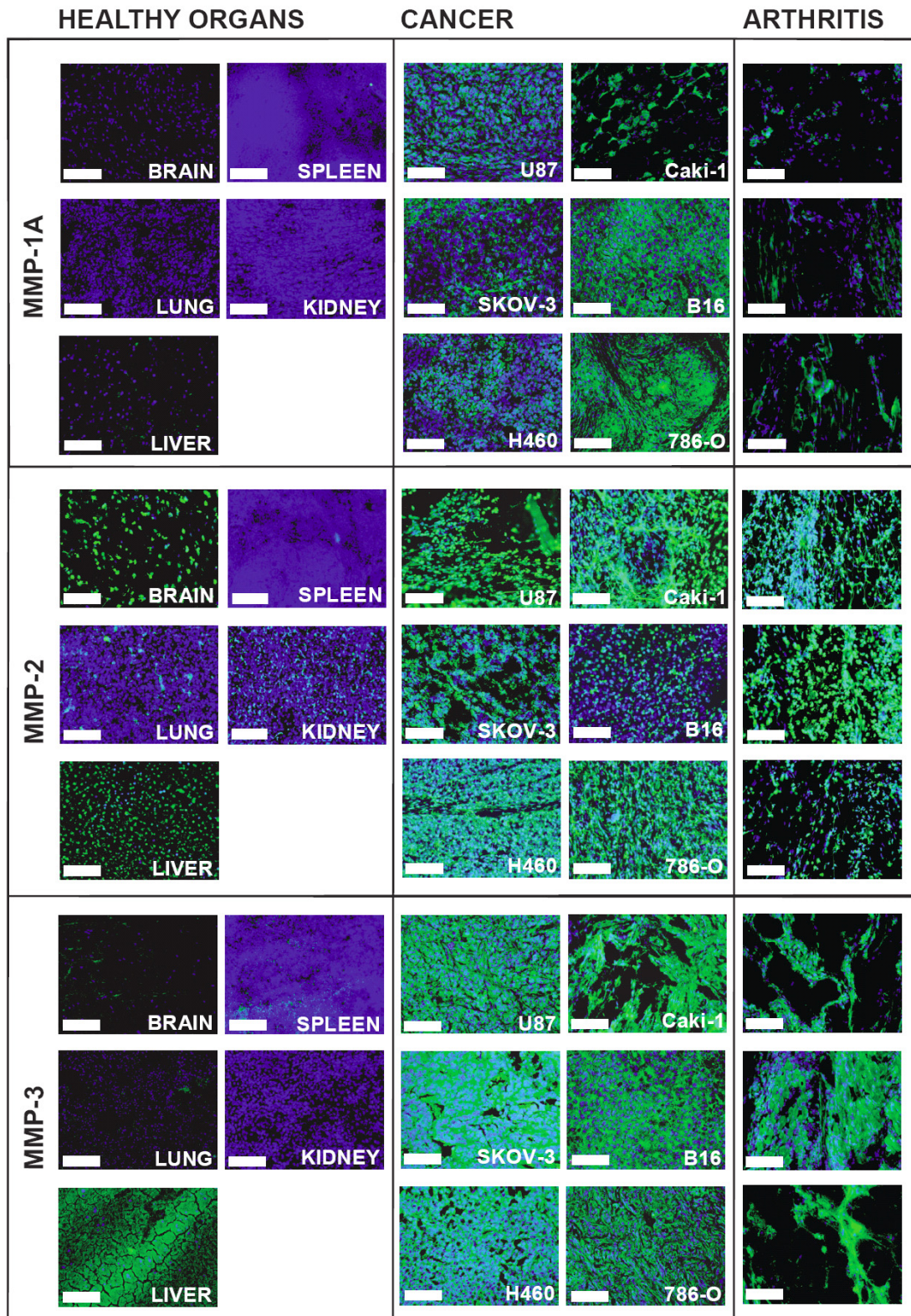


Figure 2.13: Immunofluorescence analysis performed on cryosections of murine and human (xenograft) tumors (U87 glioblastoma, B16 melanoma, Caki-1 renal clear cell carcinoma, SKOV-3 ovarian cancer, 786-O renal cell carcinoma, H460 lung carcinoma), murine arthritis tissue and healthy tissues (liver, spleen, kidney, brain, lung). MMP-1A, MMP-2 and MMP-3 were stained in green, whereas cell nuclei were stained in blue using DAPI. Scale bar = 100  $\mu$ m.

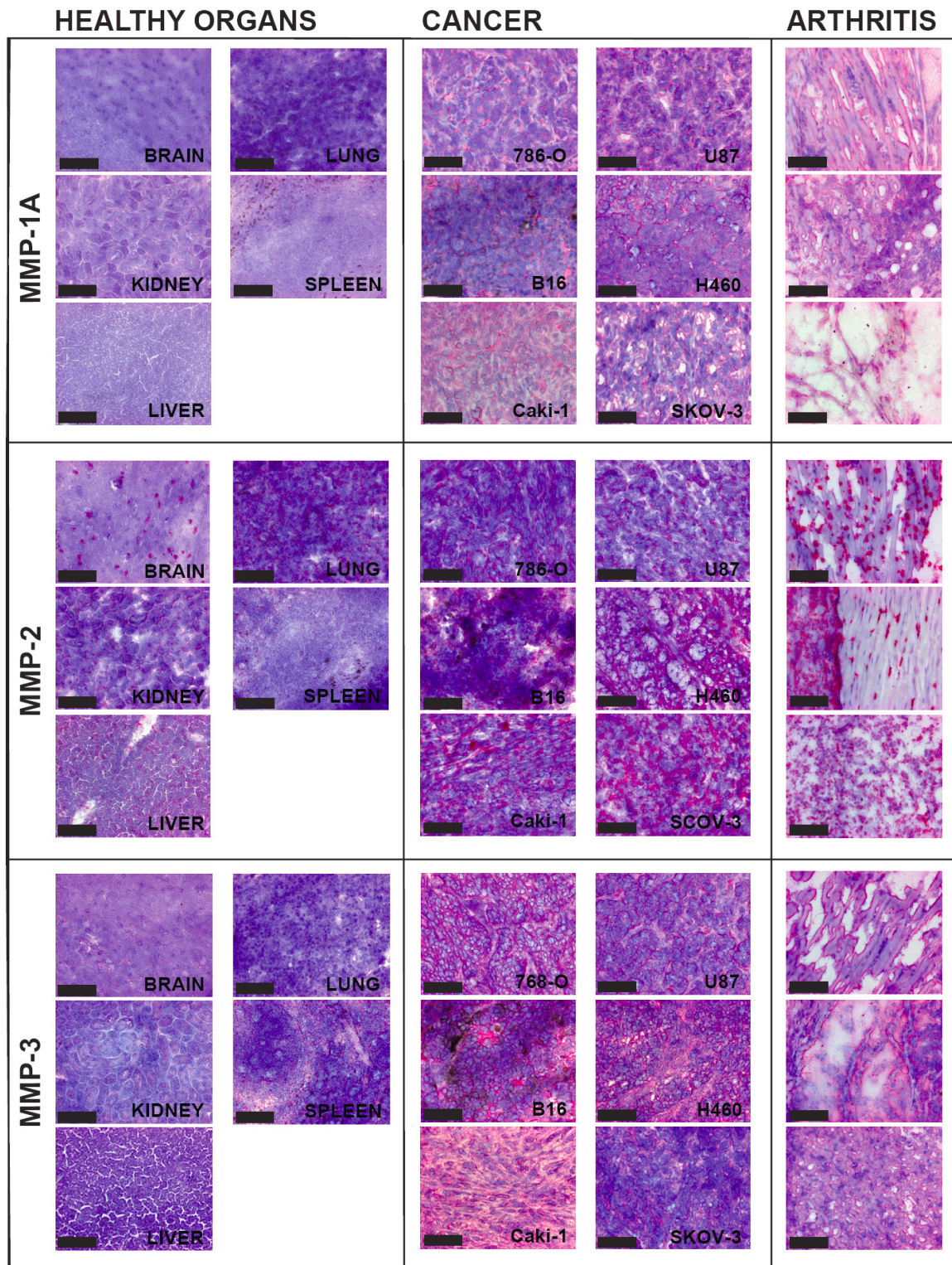
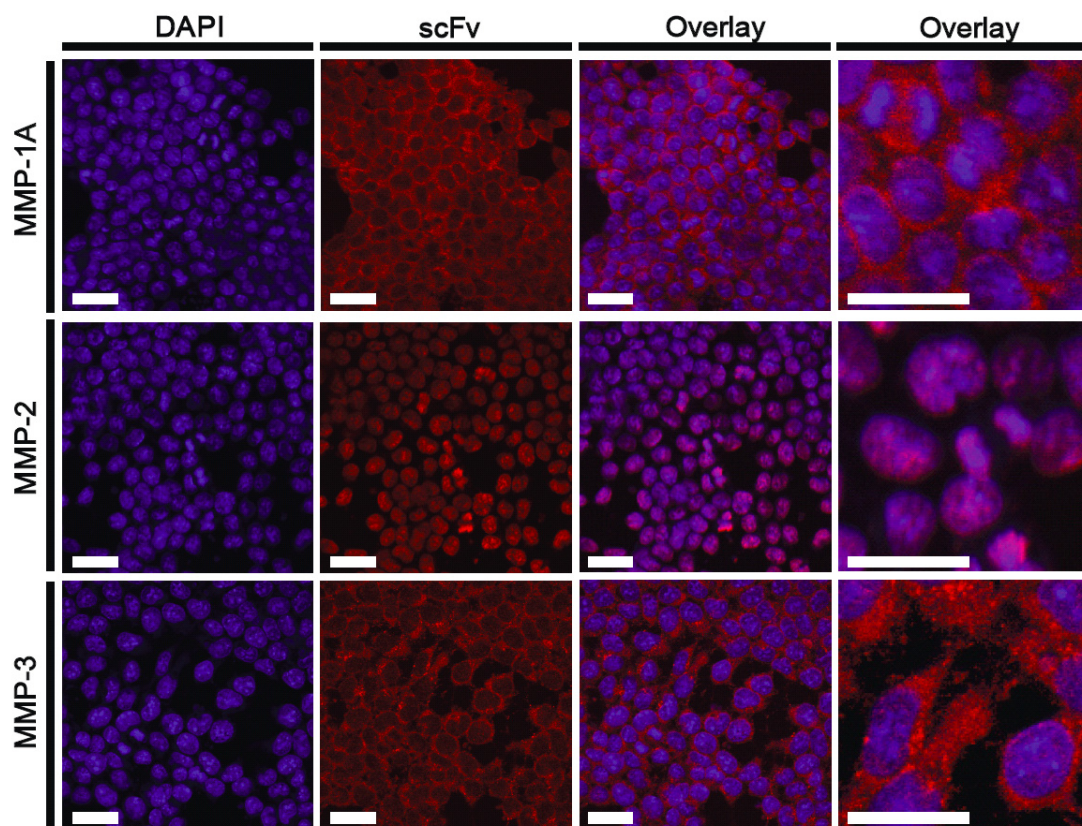


Figure 2.14: Immunohistochemical analysis performed on cryosections of murine and human (xenograft) tumors (U87 glioblastoma, B16 melanoma, Caki-1 renal clear cell carcinoma, SKOV-3 ovarian cancer, 786-O renal cell carcinoma, H460 lung carcinoma), murine arthritis tissue and healthy tissues (liver, spleen, kidney, brain, lung). MMP-1A, MMP-2 and MMP-3 were stained in red, whereas cell nuclei were stained in blue using hematoxyline. Scale bar = 100µm.

### 2.2.2.3 Confocal laser scanning microscopy studies with the scFv fragments SP1, SP2 and SP3

To examine if tumor cells, besides stromal cells, are able to express MMP-1A, MMP-2 and MMP-3, a confocal laser scanning microscopic analysis was performed using the antibodies SP1, SP2 and SP3.

**Figure 2.15** shows a two color fluorescence microscopic analysis of F9 cells, revealing expression of MMP-1A, MMP-2 and MMP-3 by the murine teratocarcinoma cells. SP1 and SP3 (specific to MMP-1A, MMP-3 respectively) showed a clear cytoplasmatic staining, whereas SP2 (specific to MMP-2) preferentially stained nuclear structures.



**Figure 2.15** Immunofluorescence analysis and confocal laser scanning microscopy were performed on murine F9 teratocarcinoma cells. MMP-1A, MMP-2 and MMP-3 were stained in red, whereas cell nuclei were stained in blue using DAPI. Scale bar = 25  $\mu$ m.

## **2.3 Generation and characterization of antibodies in the small immuno protein format (SIP)**

### **2.3.1 Production and *in vitro* characterization of SIP antibodies specific to MMP-1A, MMP-2 and MMP-3**

The human monoclonal antibody fragments scFv(SP1) and scFv(5E) specific to MMP-1A, scFv(SP2) specific to MMP-2 and scFv(SP3) and scFv(9H) specific to MMP-3 were cloned in SIP format by genetically fusing the scFv moiety at the N-terminal extremity of a human  $\epsilon$ CH4 domain of the secretory isoform S2 of human IgE (Borsi et al, 2002) [Figure 2.16a]. This domain promotes the formation of homodimers that are further stabilized by disulfide bonds between the COOH-terminal cysteine residues, resulting in a 75 kDa bivalent mini-antibody [Figure 2.16a]. This format has previously been shown to offer a good pharmacokinetic compromise between the rapidly cleared scFv antibody fragments and the antibodies in full IgG format, which display long circulatory half-lives *in vivo*. Tumor-targeting SIPs typically result in high tumor-to-organ ratios at 24 hours and at later time points after injection (Borsi et al, 2002).

SIP(SP1), SIP(5E), SIP(SP2), SIP(SP3) and SIP(9H) were expressed in Chinese Hamster Ovary Cells (CHO-S) from a pcDNA3.1 based expression vector and purified by Protein A affinity chromatography from cell culture supernatant. All five recombinant antibodies quantitatively formed cysteine-linked covalent homodimers, as shown by SDS-PAGE analysis in reducing and non-reducing conditions [Figure 2.16b and Figure 2.17a] and by size-exclusion chromatography [Figure 2.16c and Figure 2.17b]. The purified SIP(SP1), SIP(5E), SIP(SP2), SIP(9H) and SIP(SP3) antibodies were also analyzed by real-time interaction analysis on a BIAcore instrument on a low-density microsensor chip, confirming their high affinity to the cognate antigens [Figure 2.16d and Figure 2.17c]. The apparent  $K_D$  values were 1.8 nM for SIP(SP1), 5.0 nM for SIP(5E), 2.4 nM for SIP(SP2) and 1.9 nM for SIP(SP3) and 2.5 nM for SIP(9H).

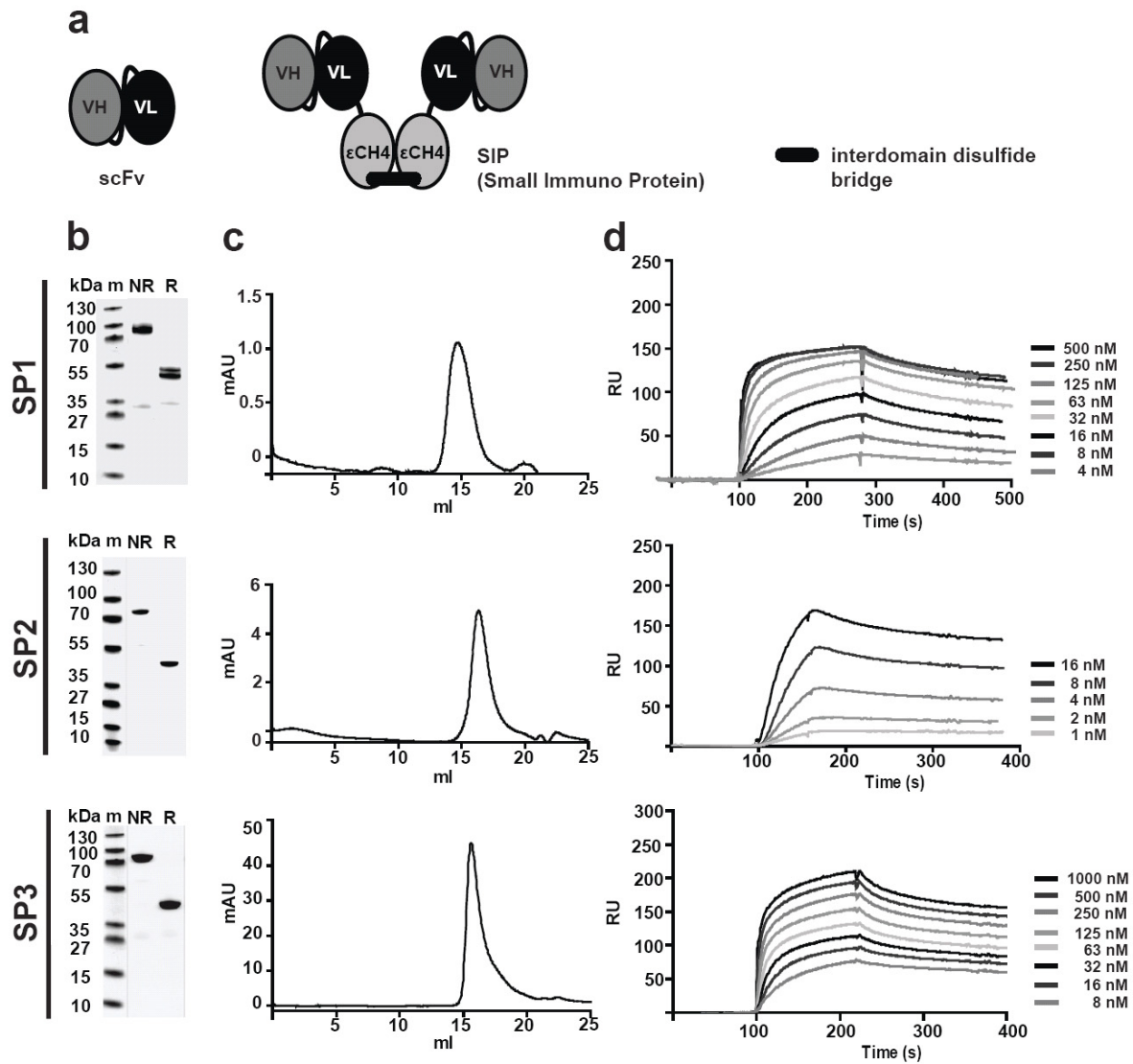


**Figure 2.16: Antibodies in SIP format against the catalytic domain of murine MMP-1A, MMP-2 and MMP-3.** **a** Schematic illustration of the scFv format consisting of a heavy chain (VH) and a light chain (VL) linked by a peptide linker and schematic illustration of the SIP format consisting of a disulfide linked homodimer. **b** SDS-PAGE analysis of affinity-purified anti-MMP-antibodies SIP(SP1), SIP(SP2) and SIP(SP3). M, molecular weight marker; R, SIP-antibodies under reducing conditions; NR, SIP-antibodies under non-reducing conditions. **c** Size exclusion chromatogram of SIP(SP1), SIP(SP2) and SIP(SP3) on a Superdex 200 HR10/300 column. The major peak eluting at ~15ml (for SIP(SP1)) and at ~16ml (for SIP(SP2) and SIP(SP3)) corresponds to the molecular weight of the covalent homodimer. **d** BIAcore sensograms of the antibodies SIP(SP1), SIP(SP2) and SIP(SP3). Kinetic constants were calculated with the BIA evaluation 4.1 software



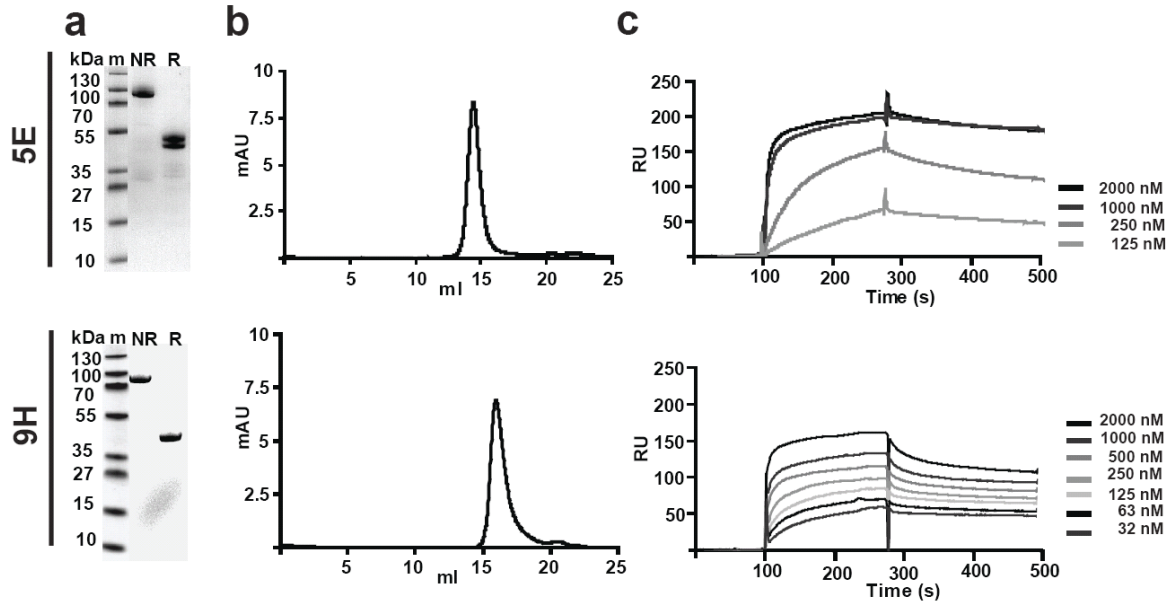


**Figure 2.17: Antibodies in SIP format against the catalytic domain of murine MMP-1A and MMP-3.** **a** SDS-PAGE analysis of affinity-purified antibodies SIP(5E) specific to the catalytic domain of MMP-1A and SIP(9H) specific to the catalytic domain of MMP-3. M, molecular weight marker; R, SIP-antibodies under reducing conditions; NR, SIP-antibodies under non-reducing conditions. **b** Size exclusion chromatogram of SIP(5E) and SIP(9H) on a Superdex 200 HR10/300 column. The major peak eluting at ~15ml (for SIP(5E)) and at ~16ml (for SIP(9H)) corresponds to the molecular weight of the covalent homodimer. **c** BIAcore sensograms of the antibodies SIP(5E) and SIP(9H). SIP(5E) reveals an apparent dissociation constant  $K_D$  of 5 nM, whereas SIP(9H) exhibits a  $K_D$  of 2.5nM. Kinetic constants were calculated with the BIA evaluation 4.1 software

The SIP(SP1) and the SIP(5E) ran as a double band in SDS-PAGE under reducing and non-reducing conditions due to an N-glycosylation of an asparagine in the scaffold region of the antibody as assessed by deglycosylation with PNGase [Figure 2.18].

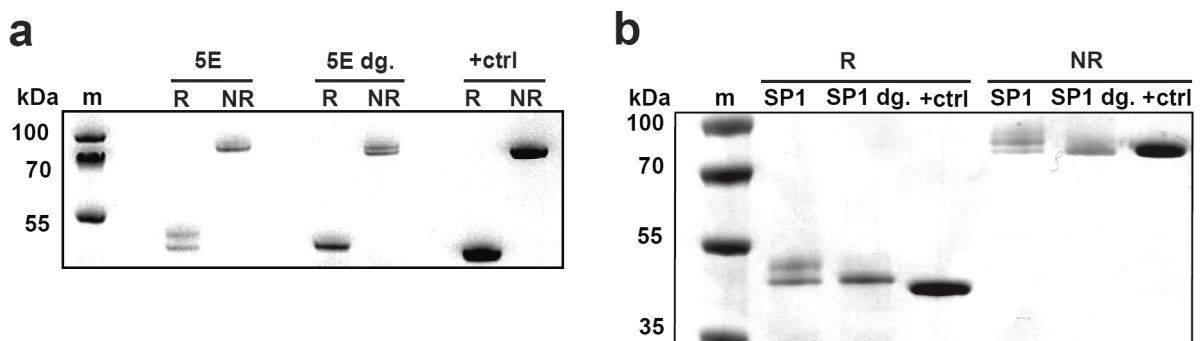


**Figure 2.18: Deglycosylation of antibodies SIP(5E) and SIP(SP1) specific to MMP-1A.** **a** SDS-PAGE analysis of SIP(5E) specific to the catalytic domain of MMP-1A before and after deglycosylation by PNGase. **b** SDS-PAGE analysis of SIP(SP1) specific to the catalytic domain of MMP-1A before and after deglycosylation by PNGase. **+ctrl**, an unglycosylated SIP antibody fragment; **m**, molecular weight marker; **R**, SIP-antibodies under reducing conditions; **NR**, SIP-antibodies under non-reducing conditions; **dg**, deglycosylated SIP-antibodies.

## 2.3.2 Quantitative biodistribution studies

### 2.3.2.1 Biodistribution studies with SIP(5E) specific to MMP-1A and SIP(9H) specific to MMP-3

**Figure 2.18a** depicts biodistribution results in tumor and normal organs for the syngeneic F9 tumor model, 24 hours after intravenous injection of  $^{125}\text{I}$ -labeled antibodies. As negative control the SIP(HyHEL-10) antibody, an antibody specific to the hen egg lysozyme was used. This negative control antibody was cleared very rapidly from the blood stream and from the normal organs and did not show any selective accumulation at the site of tumor [**Fig. 2.19a**]. By contrast, particularly SIP(9H), specific to MMP-3 preferentially accumulated at the tumor site with 5.0 % ID/g after 24 hours, but was rapidly cleared out from other organs (tumor to organ ratios up to 16 to 1) [**Fig. 2.19b**]. The accumulation of SIP(5E) in the tumor was lower compared to SIP(9H) and persistent levels of radioactivity were observed in the kidney. Microautoradiographic and immunofluorescence studies [**Fig. 2.19b and 2.19c**] confirmed the localization of the two antibodies SIP(5E) and SIP(9H) at the tumor site, while the negative control antibody SIP(HyHEL-10) antibody did not exhibit any detectable staining.

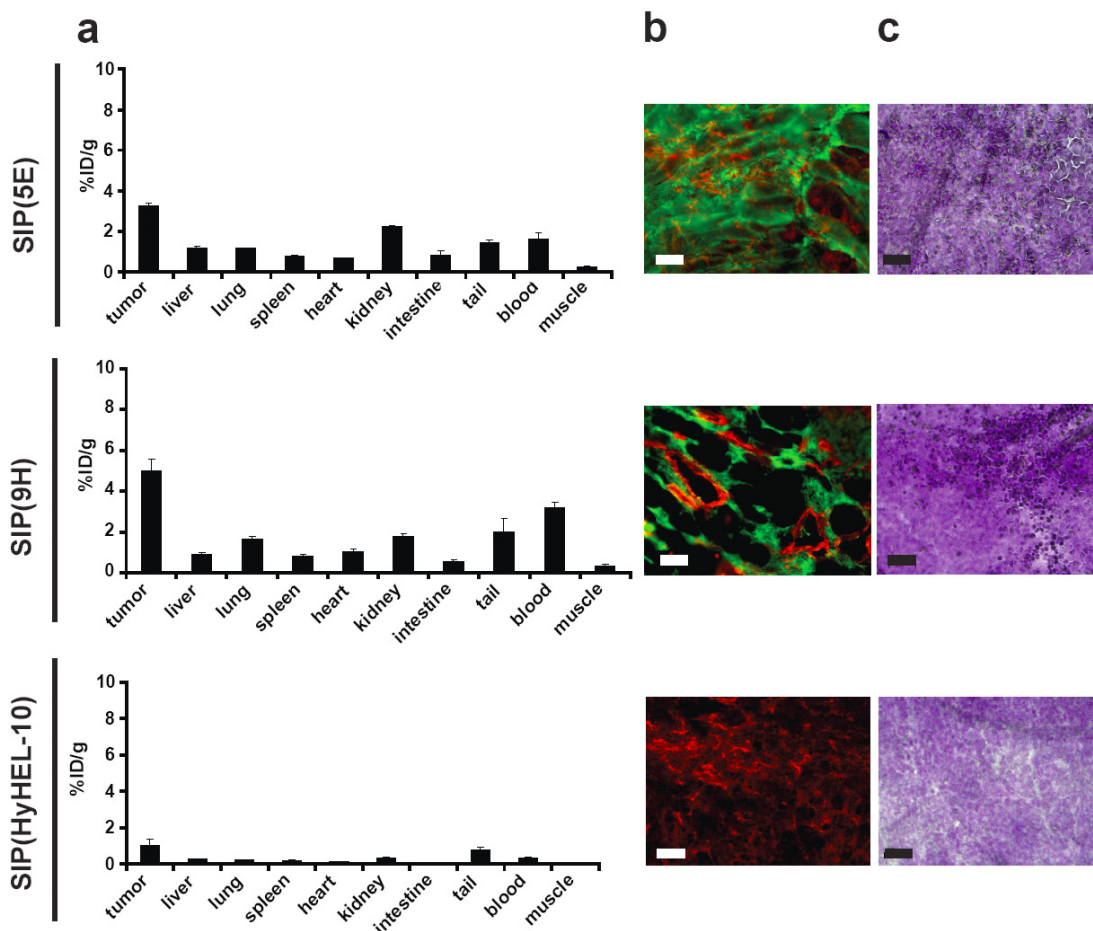


**Figure 2.19: Biodistribution in F9 tumor-bearing mice at 24 hours after i.v. injection.** a Biodistribution of  $^{125}\text{I}$ -labeled SIP(5E) specific to MMP-1A, SIP(9H) specific to MMP-3 and of one negative control antibody SIP(HyHEL-

10). Each time point corresponds to an average of 3 to 4 animals. Results are expressed as %ID/g tissue. **b and c** Microscopic analysis of antibody localization on tumor lesions. The panels present microautoradiograms of 20µm-thick sections, counterstained with hematoxylin. Sections from the same specimens were also processed by immunofluorescence analysis, CD31 as blood vessel marker (red) and for the *in vivo* localized monoclonal antibody (green). Scale bars = 50µm

### **2.3.2.2 Biodistribution studies of SIP(SP1), SIP(SP2) and SIP(SP3) in F9 tumor-bearing mice**

The *in vivo* targeting performance of radioiodinated SIP(SP1), SIP(SP2) and SIP(SP3) antibody preparations was evaluated by biodistribution studies in mice bearing F9 teratocarcinoma. <sup>125</sup>I-labeled SIP(L19), a clinical-stage recombinant antibody of proven tumor targeting performance (Neri and Bicknell, 2005; Borsi et al, 2002), was used as positive control. SIP(HyHEL-10) was used as negative control. All three anti-MMP antibodies, as well as L19, strongly stained F9 tumor sections as revealed by immunofluorescence analysis, while HyHEL-10 did not exhibit any detectable staining, as expected [**Figure 2.20a**]. A confocal laser microscopy analysis revealed that MMP-1A and MMP-3 were strongly expressed in the cytoplasm and on the membrane of the F9 tumor cells, while MMP-2 was predominantly found in intracellular structures [**Figure 2.21**]. The antibodies were injected intravenously. At different time points (3 hours, 24 hours, 48 hours), animals were sacrificed, organs were excised, weighed and radioactivity was counted. Biodistribution results were expressed as percent injected dose per gram of tissue or body fluid [**Table 2.6 and Fig. 2.20b**].

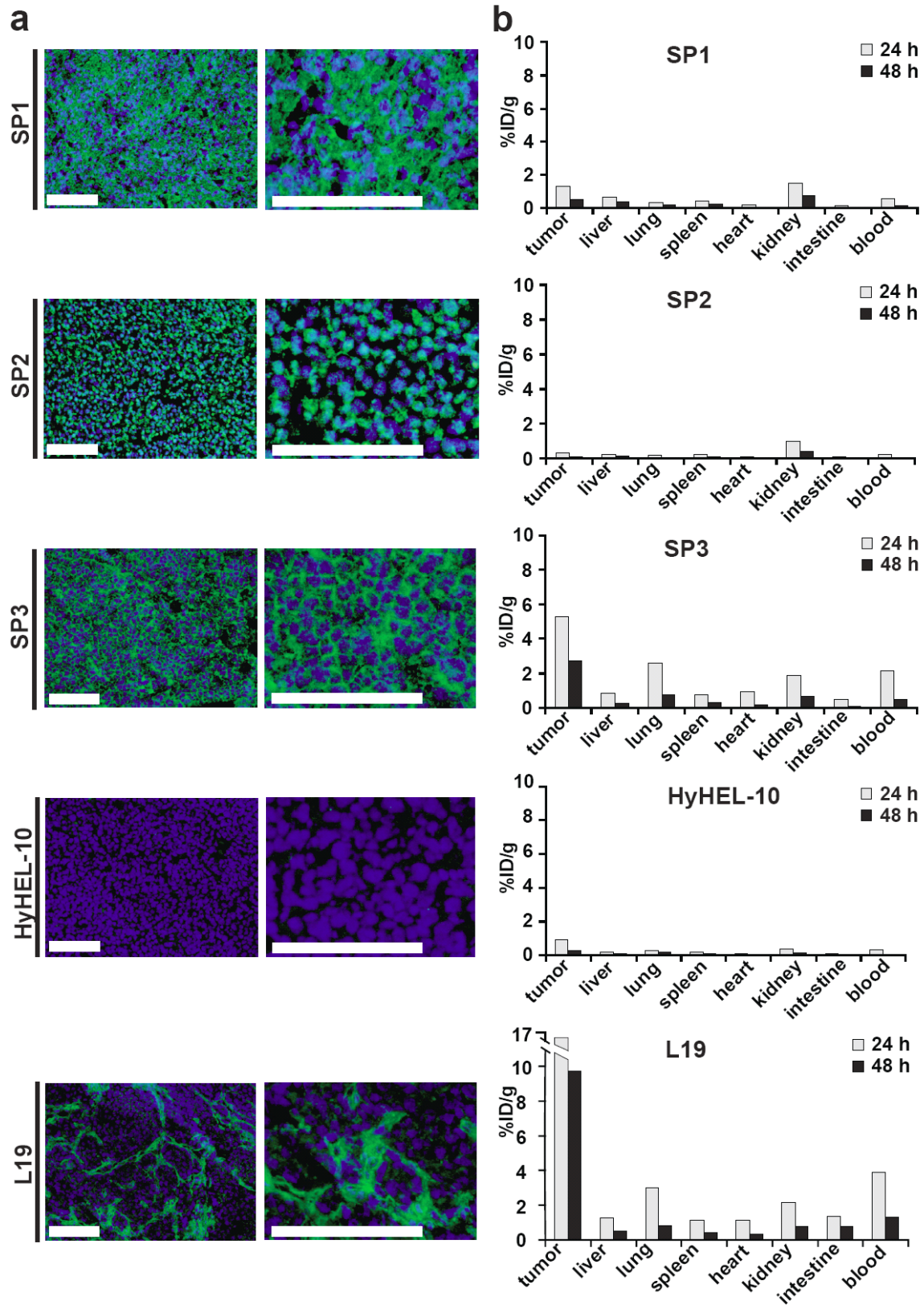


**Figure 2.20: Biodistribution in F9-bearing mice at 24 and 48 hours after i.v. injection and immunofluorescence analysis.** **a** Immunofluorescence analysis was performed on cryosections of murine F9 teratocarcinoma. MMP-1A, MMP-2, MMP-3 and extradomain B of fibronectin were stained in green, whereas cell nuclei were stained in blue using DAPI. Scale bar = 100  $\mu$ m **b** Biodistribution of  $^{125}$ I-labeled SIP (SP1), SIP (SP2),

SIP(SP3) and of two control antibodies SIP(L19) and SIP(HyHEL-10). Each time point corresponds to an average of 3 to 6 animals. Results are expressed as %ID/g tissue.

**Table 2.6: Biodistribution experiment with radioiodinated antibodies. The results are expressed as %ID/g  $\pm$  S.E.**

<b>3 hours</b>					
	<b>SIP(SP1)</b>	<b>SIP(SP2)</b>	<b>SIP(SP3)</b>	<b>SIP(HyHEL-10)</b>	<b>SIP(L19)</b>
<b>Tumor</b>	4.15 $\pm$ 0.60	2.19 $\pm$ 0.11	14.42 $\pm$ 0.74	5.54 $\pm$ 0.60	20.21 $\pm$ 1.21
<b>Liver</b>	4.72 $\pm$ 0.90	3.72 $\pm$ 0.21	12.72 $\pm$ 0.33	2.70 $\pm$ 0.29	4.81 $\pm$ 0.27
<b>Lung</b>	3.55 $\pm$ 0.35	1.68 $\pm$ 0.18	11.91 $\pm$ 0.41	3.93 $\pm$ 0.51	8.96 $\pm$ 0.85
<b>Spleen</b>	3.23 $\pm$ 0.48	2.22 $\pm$ 0.17	9.51 $\pm$ 0.69	2.42 $\pm$ 0.28	4.94 $\pm$ 0.43
<b>Heart</b>	2.49 $\pm$ 0.40	1.03 $\pm$ 0.04	10.11 $\pm$ 0.30	2.28 $\pm$ 0.22	6.32 $\pm$ 0.60
<b>Kidney</b>	7.39 $\pm$ 1.91	6.75 $\pm$ 0.30	19.31 $\pm$ 0.31	4.72 $\pm$ 0.52	10.73 $\pm$ 0.85
<b>Blood</b>	7.76 $\pm$ 1.25	2.78 $\pm$ 0.23	33.36 $\pm$ 1.39	7.89 $\pm$ 0.80	19.64 $\pm$ 1.38
<b>Intestine</b>	1.69 $\pm$ 0.32	0.98 $\pm$ 0.06	6.34 $\pm$ 1.09	2.02 $\pm$ 0.26	6.41 $\pm$ 1.61
<b>24 hours</b>					
	<b>SIP(SP1)</b>	<b>SIP(SP2)</b>	<b>SIP(SP3)</b>	<b>SIP(HyHEL-10)</b>	<b>SIP(L19)</b>
<b>Tumor</b>	1.34 $\pm$ 0.18	0.36 $\pm$ 0.06	5.28 $\pm$ 0.72	0.91 $\pm$ 0.36	16.44 $\pm$ 1.49
<b>Liver</b>	0.62 $\pm$ 0.05	0.27 $\pm$ 0.01	0.82 $\pm$ 0.05	0.20 $\pm$ 0.03	1.24 $\pm$ 0.10
<b>Lung</b>	0.33 $\pm$ 0.03	0.18 $\pm$ 0.03	2.59 $\pm$ 0.10	0.27 $\pm$ 0.11	3.00 $\pm$ 0.36
<b>Spleen</b>	0.40 $\pm$ 0.01	0.21 $\pm$ 0.04	0.73 $\pm$ 0.11	0.19 $\pm$ 0.06	1.12 $\pm$ 0.11
<b>Heart</b>	0.20 $\pm$ 0.01	0.08 $\pm$ 0.01	0.90 $\pm$ 0.03	0.10 $\pm$ 0.03	1.13 $\pm$ 0.10
<b>Kidney</b>	1.49 $\pm$ 0.09	1.00 $\pm$ 0.08	1.86 $\pm$ 0.14	0.36 $\pm$ 0.10	2.12 $\pm$ 0.24
<b>Blood</b>	0.53 $\pm$ 0.04	0.24 $\pm$ 0.05	2.17 $\pm$ 0.08	0.30 $\pm$ 0.10	3.89 $\pm$ 0.37
<b>Intestine</b>	0.15 $\pm$ 0.02	0.07 $\pm$ 0.02	0.50 $\pm$ 0.03	0.10 $\pm$ 0.03	1.35 $\pm$ 0.27
<b>48 hours</b>					
	<b>SIP(SP1)</b>	<b>SIP(SP2)</b>	<b>SIP(SP3)</b>	<b>SIP(HyHEL-10)</b>	<b>SIP(L19)</b>
<b>Tumor</b>	0.51 $\pm$ 0.16	0.09 $\pm$ 0.01	2.71 $\pm$ 0.85	0.28 $\pm$ 0.10	9.73 $\pm$ 0.48
<b>Liver</b>	0.35 $\pm$ 0.02	0.11 $\pm$ 0.01	0.24 $\pm$ 0.03	0.10 $\pm$ 0.03	0.53 $\pm$ 0.03
<b>Lung</b>	0.17 $\pm$ 0.03	0.06 $\pm$ 0.02	0.73 $\pm$ 0.07	0.16 $\pm$ 0.09	0.83 $\pm$ 0.07
<b>Spleen</b>	0.23 $\pm$ 0.01	0.07 $\pm$ 0.01	0.29 $\pm$ 0.01	0.08 $\pm$ 0.02	0.43 $\pm$ 0.05
<b>Heart</b>	0.06 $\pm$ 0.01	0.03 $\pm$ 0.01	0.19 $\pm$ 0.01	0.03 $\pm$ 0.01	0.36 $\pm$ 0.04
<b>Kidney</b>	0.75 $\pm$ 0.06	0.43 $\pm$ 0.04	0.66 $\pm$ 0.06	0.15 $\pm$ 0.04	0.80 $\pm$ 0.03
<b>Blood</b>	0.12 $\pm$ 0.02	0.03 $\pm$ 0.01	0.49 $\pm$ 0.07	0.07 $\pm$ 0.02	1.33 $\pm$ 0.07
<b>Intestine</b>	0.05 $\pm$ 0.004	0.01 $\pm$ 0.004	0.11 $\pm$ 0.02	0.02 $\pm$ 0.01	0.78 $\pm$ 0.09

The negative control antibody SIP(HyHEL-10) and the antibodies SIP(SP1) and SIP(SP2) specific to MMP-1A and MMP-2 respectively, were cleared very rapidly from the blood stream and from most normal organs and did not show a selective accumulation at the site of tumor [Table 2.6 and Fig. 2.20b]. By contrast, both SIP(SP3), specific to MMP-3, and SIP(L19) preferentially localized to the tumor [Table 2.6 and Fig. 2.20b].

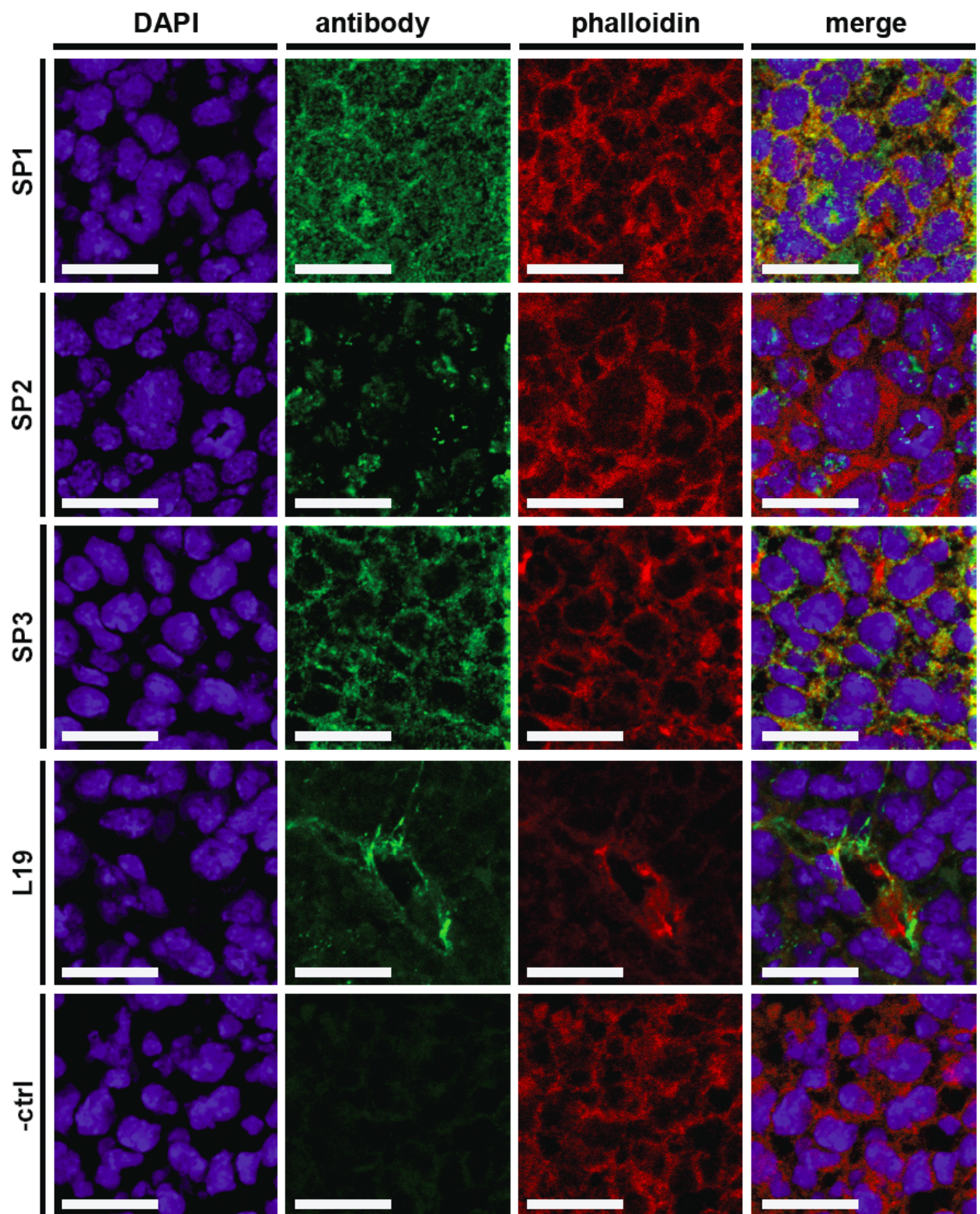


**Figure 2.21: Confocal laser scanning analysis performed on cryosections of murine F9 teratocarcinoma.** MMP-1A, MMP-2, MMP-3 and extradomain B of fibronectin were stained in green, the cytoskeleton was stained in red and cell nuclei were stained in blue using DAPI. Scale bar = 20  $\mu$ m

A more rapid blood clearance profile was observed for SIP(SP1) and SIP(SP2), both carrying a VL domain consisting of the DPL16 germline gene (Pfaffen et al, 2010), compared to SIP(L19) and SIP(SP3), which carried a VL domain based on the DPK22 germline segment (Pfaffen et al, 2010; Borsi et al, 2002). All four antibodies contain a VH domain based on the DP47 germline gene (Villa et al, 2008) and are identical in other portions of the SIP molecule. A comparative analysis of biodistribution studies performed with three SIP antibodies based on DPK22 VL domains and five SIP antibodies based on DPL16 light chains revealed a general trend to faster blood clearance for DPL16-based antibodies [Figure 2.22].

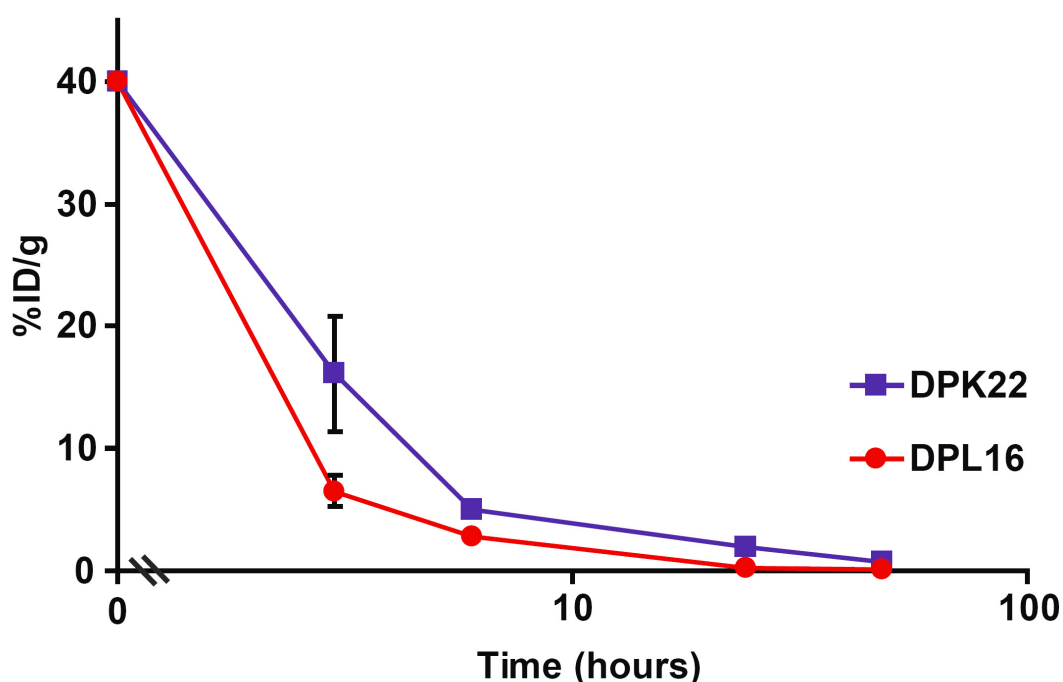


**Figure 2.22: Blood clearance comparison of SIP antibodies containing either a DPL16 (F16, SP1, SP2, P12 and G11) or a DPK22 light chain (SP3, L19, F8).** For all antibodies, %ID/g values at time 0 were set equal to 40%, corresponding to a blood volume of 2.5 ml. The data points were calculated as average of the individual %ID/g values for the SIP antibodies in the two groups. The corresponding biodistribution data for the individual SIPs can be found in the following articles: *Borsi et al, 2002*; *Schliemann et al, 2009*; *El-emir et al, 2007*; *Brack et al, 2006*; *Silacci et al, 2006*; *Villa et al, 2008*.

Thirty minutes after intravenous injection, a more rapid excretion of the SIP(SP2) antibody can be detected, compared to SIP(SP3) and SIP(L19) [Figure 2.23 a]. While clearance via the hepatobiliary route predominates, antibody dehalogenation in the liver leads to the excretion of free radioiodine through the kidneys, as revealed by a gel-filtration analysis of urine [Figure 2.23 b]. We hypothesized that the longer retention of SIP(SP3) and SIP(L19) in the blood could be due to a non-covalent association with plasma components.

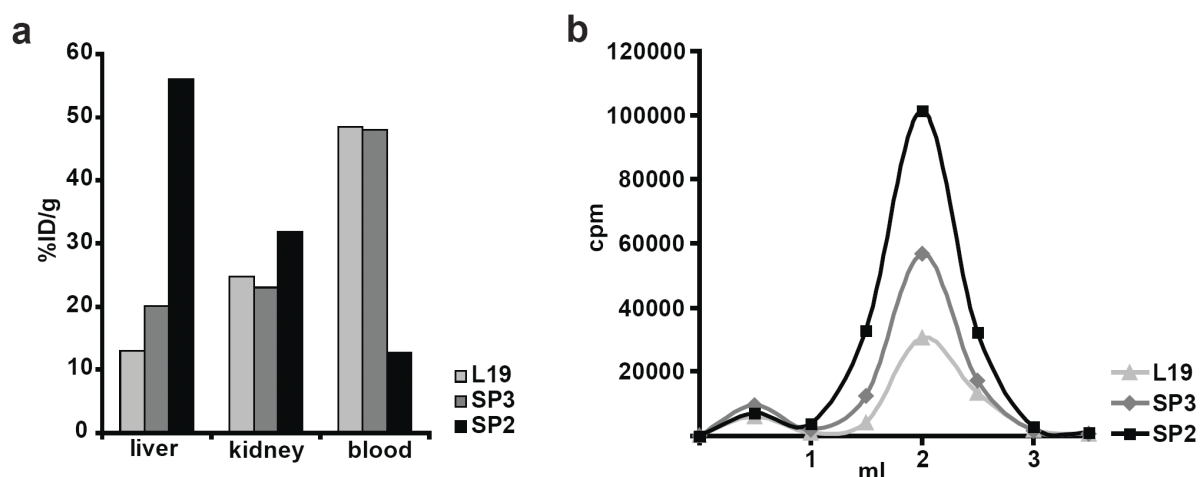


**Figure 2.23: Biodistribution (a) and urine analysis (b) of  $^{125}\text{I}$ -labeled SIP(SP2), SIP(SP3) and SIP(L19) 30 minutes after intravenous injection. Each value corresponds to an average of two animals. a Organ data are expressed in %ID/g tissue, b while radioactivity in urine fractions was measured in counts per minute (cpm).**

**Figure 2.24** reveals that indeed SIP(SP3), but not SIP(SP1) and SIP(SP2), forms a complex with plasma proteins, as shown by real-time interaction analysis on a BIAcore 3000 instrument.



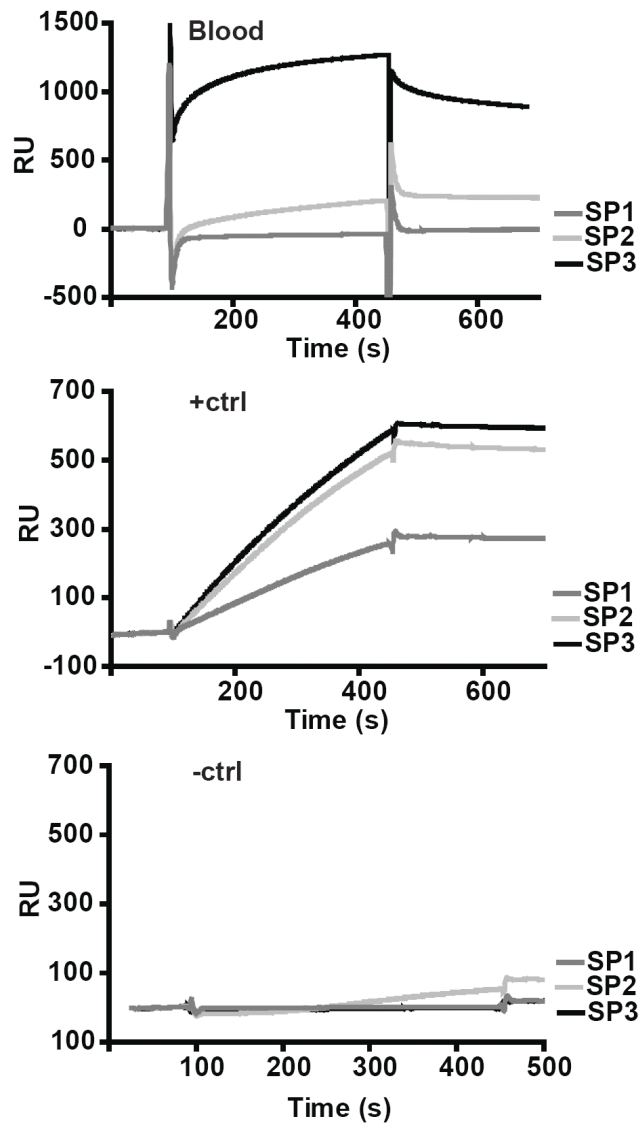


**Figure 2.24: BIAcore sensograms of the murine blood plasma, run onto biosensor chips coated with SIP(SP1), SIP(SP2) and SIP(SP3).** As positive control for SIP immunodetection on BIAcore, rabbit anti-human IgE was used. As negative control, saline solution was flushed over the SIP-coated chip.

### 3 DISCUSSION

This thesis describes the cloning and expression of the catalytic domains of murine MMP-1A, MMP-2 and MMP-3, and their use for the isolation and affinity maturation of human recombinant antibodies. Five monoclonal antibodies (SP1, SP2, SP3, 5E and 9H) with affinities in the low nanomolar range were isolated, which were found to be specific to their cognate antigen (MMP-1A, MMP-2 and MMP-3, respectively). These antibodies were used for a comparative immunofluorescence and immunohistochemical analysis of mouse tissues in health and disease [Figure 2.12 and Figure 2.13].

While several reports on MMP expression in individual organs (healthy and diseased) can be found in the literature (Kuivanen, et al, 2009; Jeffery et al, 2009; Köhrmann et al, 2009; Naka et al, 2008; Kinoshita et al, 2008), to our knowledge no comparative immunohistofluorescence analysis in normal tissues, tumors and arthritic specimens had been reported until now for murine MMP-1A, MMP-2 and MMP-3. Our study revealed that the high-affinity antibodies SP1, SP2 and SP3 exhibit an intense staining of various cancer and arthritis specimens, while display either no staining (MMP-1A) or moderate staining of few normal mouse organs (MMP-2 and MMP-3). In our experience, it is often important to use high-affinity monoclonal antibodies, in order to better assess the relative levels of the antigen of interest in immunofluorescence analysis (Carnemolla et al, 1996; Castellani et al, 2002; Pedretti et al, 2009).

Immunocytochemical analysis of murine F9 teratocarcinoma cells by confocal laser scanning microscopy revealed a cytoplasmatic staining for SP1 specific to MMP-1A and SP3 specific to MMP-3 [Figure 2.14]. By contrast a nuclear localization was observed for MMP-2 in keeping with previous reports (Si-Tayeb et al, 2006). *In vivo*, the MMPs are produced not only by tumor cells, but also by stromal cells (Basset et al, 1990).

Furthermore, this thesis reports the first biodistribution analysis of the tumor targeting performance of radiolabeled high-affinity monoclonal antibodies, specific to three different murine MMPs. While all antibodies strongly stain a variety of tumor sections (Pfaffen et al, 2010), including F9 tumors [Figure 2.20 and Figure 2.21], only the SIP(SP3) and the SIP(9H) antibody, specific to murine MMP-3, exhibited a preferential localization at the tumor site.

The comparative biodistribution analysis of the SP1, SP2, SP3 and L19 antibodies in SIP format was performed in mice bearing murine tumors and was facilitated by the fact that the

EDB has identical sequence in mouse and man (Neri and Bicknell, 2005), thus allowing a characterization of tumor targeting properties in a syngeneic setting. To our knowledge, only one biodistribution study with a monoclonal antibody specific to human membrane-type MMP-1 in a mouse and a rat xenograft cancer model had previously been reported in the literature (Temma et al, 2009), which however exhibited no preferential antibody localization to the tumor, in line with our results.

As mentioned above, the immunohistochemical analysis of the patterns of murine MMP-1A, MMP-2 and MMP-3 expression has shown that these antigens are undetectable in most normal mouse tissues (exception made for liver for MMP-2 and MMP-3, and lung, brain and kidney for MMP-2), but are strongly expressed in the majority of tumors tested, making them suitable candidates for biomolecular anti-cancer pharmacodelivery strategies. In order to qualify for antibody-based tumor targeting applications, an antigen needs to be accessible *in vivo* and also needs to mediate an “immobilization” of the antibody on the neo-plastic lesion. The biodistribution results presented in this thesis indicate that MMP-3 is sufficiently abundant and accessible in F9 tumors to permit a preferential antibody localization at the neoplastic site. This protease is probably anchored to extracellular matrix components via e.g. the NC1 domain of type IV collagen or the laminin-binding domain of agrin, which are structurally similar to tissue inhibitors of metalloproteinases (reviewed in Overall and Lopez-Otin, 2002). MMP-1A and MMP-3 showed a similar cellular localization in F9 tumor cells, but only MMP-3 could be efficiently targeted *in vivo*. By contrast, in this tumor model, the majority of MMP-2 was intracellular and thus not accessible to antibodies *in vivo* [Figure 2.21].

Antibodies were used in SIP format for biodistribution studies. Miniantibody formats have been extensively studied by our group and by other laboratories and appear to provide an ideal compromise between the fast-clearing scFv fragments and the long-lived IgGs (Borsi et al, 2002). Unlike scFv and Fab fragments, antibodies in SIP format are mainly cleared via the hepatobiliary route (Villa, et al, 2008; Borsi et al, 2002), which spares the kidneys for radioimmunotherapy applications. Indeed, <sup>131</sup>I-labeled SIP(L19) and SIP(F16) are currently being investigated in Phase II radioimmunotherapy trials, with a special focus on hematological malignancies (Neri and Bicknell, 2005). Furthermore, these two SIPs labeled with <sup>124</sup>I are being studied in immuno-PET clinical trials.

In line with previous observations made in biodistribution studies with antibodies in IgG, Fab and scFv formats, the results of **Table 2.6** show differences in blood clearance properties among different SIPs, with the L19 and SP3 antibodies being the longest-lived recombinant antibodies in circulation. The reasons for these differences are not obvious, since the

cognate antigens are present at negligibly low concentrations (ng/ml levels or lower) in blood and since all antibodies have a VH domain based on the same (DP47) germline V segment (Pfaffen et al, 2010). Interestingly, both SIP(SP3) and SIP(L19) carry a Vk domain based on the DPK22 germline V segment, while SIP(SP1) and SIP(SP2) have a Vλ domain, based on the DPL16 germline segment. Biodistribution studies revealed that DPL16-based antibodies in SIP format clear more rapidly from the blood compared to antibodies containing DPK22 light chains **[Figure 2.22]**. A previously unsuspected non-covalent binding interaction of SIP(SP3) with serum, clearly revealed by BIAcore analysis **[Figure 2.24]**, may account for the longer residence time of this antibody in the bloodstream **[Fig. 2.20b and Table 2.6]**. Both L19 and SP3 exhibited a long residence time on the tumor *in vivo*, a favorable property for the use of these antibodies as building blocks for the development of targeted anti-cancer biopharmaceuticals.

The selective tumor localization properties of SIP(SP3) suggest that anti-MMP-3 antibodies may be useful for the immuno-PET visualization of this antigen in patients with cancer, but also in other pathologies where MMP-3 is strongly over-expressed (e.g., rheumatoid arthritis). In addition to nuclear medicine applications, it would be conceivable to use anti-MMP-3 antibodies as building blocks for pharmacodelivery applications, in full analogy to antibodies specific to splice isoforms of fibronectin and tenascin-C (Neri and Bicknell, 2005; Borsi et al, 2002; Villa et al, 2008) which have been fused to cytokines, photosensitizers, pro-coagulant factors, enzymes and drugs. Some of these derivatives (most notably, L19-IL2, L19-TNF, F16-IL2, F8-IL10) are currently being investigated in clinical trials. However, since the catalytic domain of MMP-3 displays only an 82% homology between mouse and man, human-specific monoclonal antibodies will be needed for clinical applications.

## 4 MATERIAL AND METHODS

### 4.1 Cell lines

Cell culture media and supplements were purchased from Invitrogen (Basel, Switzerland). The human glioblastoma cell line U87 (HTB-14, ATCC) was cultured in MEM medium, supplemented with 10% fetal calf serum (FCS) and antibiotic–antimycotic at 37°C and 5% CO<sub>2</sub>. The murine melanoma cell line B16 (CRL-6322, ATCC) was cultured in DMEM containing 10% FCS and incubated at 37°C and 5% CO<sub>2</sub>. The human kidney clear cell carcinoma cell line Caki-1 (HTB-46, ATCC), the human ovarian cancer cell line SKOV-3 (HTB-77, ATCC) and the human renal cell carcinoma cell line 786-O (CRL-1932, ATCC) were cultured in RPMI 1640 supplemented with as described above. The human lung cancer cell line H460 (HTB-177, ATCC) was cultured in RPMI medium containing 2 mM glutamine, 10% FCS and antibiotic-antimycotic at 37°C and 5% CO<sub>2</sub>. The murine teratocarcinoma cell line F9 (CRL-1720, ATCC) was cultured in cell culture vessels coated with 0.1% gelatine solution in DMEM containing 10% FCS and antibiotic-antimycotic at 37°C and 5% CO<sub>2</sub>.

## **4.2 Production and characterization of the catalytic domain of MMP-1A, MMP-2 and MMP-3**

### **4.2.1 Cloning and expression of the murine MMP-1A catalytic domain**

The murine MMP-1A catalytic domain (residues 95-280) was isolated from a murine cDNA library (7 day embryo) (Clontech) and cloned into the pQE12 vector (Qiagen) using the restriction sites *EcoRI* and *BglII* and the primers 5'- CCG GAA TTC ATT AAA GAG GAG AAA TTA ACT ATG GCC CCA TAT GCC ATT ACT CAC -3' and 5'- ACT AGA TCT CTA TCA GTG ATG GTG ATG GTG ATG GCC ACC TGG ATG TGG TGT TGT TGC ACC-3'(Eurofins MWG Operon). The protein containing a C-terminal 6 x His-tag was purified with a Ni-NTA agarose (Qiagen) by refolding on the column and dialysis against 50 mM Tris-Cl, 200 mM NaCl, pH 7.4, and stored frozen at -20°C.

### **4.2.2 Cloning and expression of the murine MMP-2 catalytic domain**

The murine MMP-2 catalytic domain lacking three fibronectin type II domains (residues 112-219 and 393-445) was isolated from the full length cDNA clone RAVp968H04129D6 (imaGenes) and was cloned into the pQE12 vector (Qiagen) using the restriction sites *EcoRI* and *BglII*. PCR assembly of the two subunits of the catalytic domain was achieved using primers 5'-CCG GAA TTC ATT AAA GAG GAG AAA TTA ACT ATG AAC TAC AAC TTC TTC CCC CGC AAG CCC-3' and 5'-GCT ATA TCC TTG TTG TCC TTC TCC CAG GGT CCA CAG-3' for residues 112-219, and primers 5'- GGA GAA GGA CAA CAA GAA TAT AGC CTATTC CTC GTG GCA-3' and 5'- ACT AGA TCT CTA TCA GTG ATG GTG ATG GTG ATG GCC ACC ATA GAG CTC CTG GAT CCC CTT GAT GTC- 3' for residues 393-445 (Eurofins MWG Operon). The protein containing a C-terminal 6 x His-tag was purified with Ni-NTA agarose (Qiagen), dialysis against 50 mM Tris-Cl, 200 mM NaCl, pH 7.4, and stored frozen at -20°C.

### **4.2.3 Cloning and expression of the murine MMP-3 catalytic domain**

The murine MMP-3 catalytic domain (residues 100-273) was isolated from a murine cDNA library (eye) (Clontech) and cloned into the pQE12 vector (Qiagen) using the restriction sites *EcoRI* and *BglII* and the primers 5'-CCG GAA TTC ATT AAA GAG GAG AAA TTA ACT ATG TTC AGT ACC TTC CCA GGT TCG-3' and 5'- ACT AGA TCT CTA TCA GTG ATG GTG ATG GTG ATG GCC ACC GAG GAC ATC AGG GGA TGC TGT-3' (Eurofins MWG Operon).

The protein containing a C-terminal 6 x His-tag was purified with Ni-NTA agarose (Qiagen), dialyzed against 50 mM Tris-Cl, 200 mM NaCl, pH 7.4, and stored frozen at -20°C (Scheuermann et al, 2008).

#### **4.2.4 Activity assay for the catalytic domains of MMP-1A MMP-2 and MMP-3**

Forty eight  $\mu$ l of MMP-1A (final concentrations: 0-3000 nM) or MMP-3 (final concentrations: 0-300 nM) in 39 mM Tris-Cl, 156 mM NaCl, 5.6% DMSO, 0.056% Brij-35, 56 mM 2-(N-morpholino) ethanesulfonate, 1.1 mM  $\text{CaCl}_2$ , 22  $\mu$ M  $\text{ZnCl}_2$  at pH 6 were incubated with 10  $\mu$ l of the fluorogenic substrate Mca-Pro-Leu-Gly-Leu-Dpa-Ala-Arg-NH<sub>2</sub> (final concentrations: 1-166  $\mu$ M) (OmniMMP, Biomol). The change of fluorescence signal ( $\lambda_{\text{ex}}$  328 nm;  $\lambda_{\text{em}}$  393 nm) was recorded over 10 min using a SpectraMax Gemini microplate reader (Molecular Devices). The rate of fluorescence signal increase over the time (initial reaction velocity) was plotted versus different substrate concentrations and the  $K_M$  and  $k_{\text{cat}}$  values were obtained by fitting the equation  $v = V_{\text{max}} \times S / (K_M + S)$  and  $k_{\text{cat}} = V_{\text{max}} / E$  ( $v$  = initial velocity,  $S$  = initial substrate concentration,  $V_{\text{max}}$  = maximum rate,  $K_M$  = Michaelis constant,  $k_{\text{cat}}$  = turnover number,  $E$  = enzyme concentration) using Kaleidagraph software (Synergy software) (Netzel-Arnett et al, 1991).

Forty eight  $\mu$ l of MMP-2 (0-780 nM) in 39 mM Tris-Cl, 156 mM NaCl, 5.6% DMSO, 0.056% Brij-35, 56 mM 3-(N-morpholino) propanesulfonic acid, 1.1 mM  $\text{CaCl}_2$ , 22  $\mu$ M  $\text{ZnCl}_2$  at pH 7 were incubated with 10  $\mu$ l of the fluorogenic substrate Mca-Pro-Leu-Gly-Leu-Dpa-Ala-Arg-NH<sub>2</sub> (final concentrations: 1-33  $\mu$ M) (OmniMMP, Biomol). The change of fluorescence signal ( $\lambda_{\text{ex}}$  328 nm;  $\lambda_{\text{em}}$  393 nm) was recorded over 10 min using a SpectraMax Gemini microplate reader (Molecular Devices).  $K_M$  and  $k_{\text{cat}}$  were determined as described above.

## **4.3 Generation and characterization of scFv fragments**

### **4.3.1 Selection of antibodies from the ETH-2-Gold library by phage display**

The recombinant catalytic domains were immobilized on an Immuntube (NUNC) at a final concentration of 50 µg/ml in phosphate buffered saline (PBS). The selections were performed according to standard antibody phage display protocols (Viti et al, 2000).

Bacterial supernatants, containing recombinant antibody fragments, were screened by ELISA as described previously (Viti et al, 2000). Supernatants of clones positive in ELISA were further analyzed by surface plasmon resonance (SPR) real-time interaction analysis on a high density coated antigen-chip, using a BIAcore3000 instrument (BIAcore AB).

### **4.3.2 Sequencing of scFv antibody genes**

Antibodies were sequenced using Big Dye® Terminator v3.1 Cycle Sequencing kit (Applied Biosystems) on an ABI PRISM 3130 Genetic analyzer. Termination reactions were performed using primers Limb3long 5'- CAG GAA ACA GCT ATG ACC ATG ATT AC - 3' (annealing 110 bp upstream the scFv gene) and fdseqlong 5'- GAC GTT AGT AAA TGA ATT TTC TGT ATG AGG - 3' (annealing 100 bp downstream the scFv gene) (Eurofins MWG Operon).

### **4.3.3 Characterization of antibody scFv fragments**

ScFv antibody fragments were expressed in *E.coli* and purified from culture supernatant by affinity chromatography using Protein A Sepharose Fast Flow Resin (GE Healthcare), as described previously (Silacci et al, 2005).

Purified antibodies were analysed by SDS-PAGE and size exclusion chromatography on Superdex 75 HR10/30 columns (Amersham Biosciences), the peak of the monomeric fraction was collected and used for affinity measurement by BIAcore on a low density coated antigen chip as described (Silacci et al, 2006).

### **4.3.4 Construction of affinity maturation libraries**

Affinity maturation libraries were constructed by introducing sequence variability either in the CDR1 loop of heavy (VH) and light chain (VL) or in the CDR2 loop of VH and VL. Antibody



residues are numbered according to Tomlinson and co-workers (Tomlinson et al, 1992). Mutations at positions 31, 31a, 32 (CDR1 of VL) and 31, 32, 33 (CDR1 of VH) or 50, 51, 52 (CDR2 of VL) and 52, 52a, 53 and 56 were introduced by PCR using partially degenerated primers (Eurofins MWG Operon) as described previously (Villa et al, 2008; Silacci et al, 2006).

Phage display selections were done as described before. Briefly, one single round of panning was performed with the recombinant antigen biotinylated with Sulfo-NHS-LC-Biotin (final concentration:  $10^{-7}$  M) (Pierce) eluting bound phage with 100 mM Triethylamine, as described in Silacci *et al.* (Silacci et al, 2005). Induced supernatants of individual clones were screened by ELISA and by surface plasmon resonance analysis on a high-density coated antigen chip.

#### **4.3.5 Immunofluorescence on frozen tissue sections**

Healthy tissues (excised from Sv129 mice), tumor tissues and arthritic tissues (excised from bovine collagen type II induced mice (Trachsel et al, 2007) were embedded in freezing medium (Microm) and stored at  $-80^{\circ}\text{C}$  until sectioned. Tissue sections (10  $\mu\text{m}$ ) were fixed for 10 min with ice-cold acetone, rehydrated with PBS and blocked with 20% FCS in PBS. Purified scFv antibodies (final concentration: 10-20  $\mu\text{g/ml}$ ) containing a myc-tag were added onto the sections. As secondary antibody a rat anti-myc antibody (Genetex) was applied, detected with donkey anti-rat IgG Alexa Fluor 488 antibody (Invitrogen). Nuclei were counterstained with DAPI (Invitrogen). All commercial binding reagents were diluted according to the manufacturer's recommendation. Rinsing with PBS was performed in between all incubation steps. Slides were mounted with Fluorescent mounting medium (Dako) and analyzed with a Zeiss AxioVision 4.7 image analysis software (Carl Zeiss AG).

#### **4.3.6 Immunocytochemistry /confocal laser scanning microscopy with murine F9 teratocarcinoma cells**

Confocal laser scanning microscopy was performed as previously described by our group (Rösli et al, 2009). Briefly, the F9 teratocarcinoma cells were grown on 4.2  $\text{cm}^2$  Falcon cell culture inserts (BD Biosciences). The adherent cells were fixed for 10 min with ice-cold methanol, permeabilized with 0.2% Triton-X100 in PBS and rehydrated in PBS. Purified scFv antibodies (final concentration: 20-30  $\mu\text{g/ml}$ ) containing a myc-tag were added onto the cells. As secondary antibody a rat anti-myc antibody (Genetex) was applied, detected with a donkey anti-rat IgG Alexa Fluor 594 antibody (Invitrogen). Nuclei were counterstained with DAPI (Invitrogen). Rinsing with PBS was performed in between all incubation steps. Slides

were mounted with Fluorescent mounting medium (Dako) and analyzed with a LSM 510 META from Zeiss (Carl Zeiss AG).

#### **4.3.7 Immunohistochemistry on frozen tissue sections**

Healthy tissues (excised from Sv129 mice), tumor tissues and arthritic tissues (excised from bovine collagen type II induced mice (Trachsel et al, 2007) were embedded in freezing medium (Microm) and stored at -80°C until sectioned. Tissue sections (10 µm) were fixed for 10 min with ice-cold acetone, rehydrated with TBS (50 mM Tris, 100 mM NaCl, 0.01% Aprotinin) and blocked with 20% FCS in TBS (Invitrogen). Purified scFv antibodies (final concentration: 10-20 µg/ml) containing a myc-tag were added onto the sections, together with a monoclonal anti-myc antibody 9E10 (AbD Serotec) biotinylated with Sulfo-NHS-LC-Biotin (Pierce) (final concentration: 5 µg/ml). Bound antibodies were detected with a streptavidin-alkaline phosphatase complex (Biospa). All commercial binding reagents were diluted according to the manufacturer's recommendation. Rinsing with TBS was performed in between all incubation steps. Fast Red (Sigma) was used as phosphatase substrate, and sections were counterstained with Gill's hematoxylin No2 (Sigma). Slides were mounted with Glycergel mounting medium (Dako) and analyzed with a Zeiss AxioVision 4.7 image analysis software (Carl Zeiss AG).

## **4.4 GENERATION AND CHARACTERIZATION OF SIP ANTIBODIES**

### **4.4.1 Cloning, expression, and purification of antibodies in the SIP format**

ScFvs were converted into the SIP format by cloning VH and VL into pcDNA3.1 (Invitrogen) using the same strategy as described in (Villa et al, 2008; Zuberbühler et al, 2009). The plasmids were transfected into CHO-S cells (Invitrogen) using Cell Line Nucleofector Kit V (Lonza), following the manufacturer's protocol. Transfectants were grown in RPMI supplemented with 10% FCS and selected by addition of 0.5 mg/ml Geneticin (G418) (Merck Chemicals Ltd). Monoclonal cultures were obtained by fluorescent-activated cell sorting or by limited dilution, as described (Zuberbühler et al, 2009). After 10 to 14 days of selection, cells were brought into suspension, and cultured in PowerCHO-2 CD (Lonza). SIP antibodies were purified from culture medium by affinity chromatography using Protein A Sepharose Fast Flow resin (GE Healthcare), as described in (Zuberbühler et al, 2009).

### **4.4.2 Characterization of the SIP antibodies**

Purified SIP antibodies were analyzed by SDS-PAGE, size exclusion chromatography on Superdex 200 HR10/300 columns (Amersham Biosciences) and by surface plasmon resonance (SPR) measurements on a low density coated antigen chip as described in (Villa et al, 2008) to determine the apparent  $K_D$ .

### **4.4.3 Immunofluorescence analysis of frozen tissue sections**

F9 teratocarcinoma tissues were embedded in freezing medium (Microm) and stored at -80°C until sectioned. Tissue sections (10 µm) were fixed for 10 min with ice-cold acetone, rehydrated with PBS and blocked with 20% FCS in PBS. Biotinylated SIP(L19) (2 µg/ml) (specific to the alternatively-spliced EDB domain of fibronectin, used as positive control antibody of proven tumor targeting properties (Borsi et al, 2002)), purified SIP(HyHEL-10) (2 µg/ml) (specific to hen egg lysozyme, used as negative control antibody) or the purified antibodies scFv(SP1), scFv(SP2) and scFv(SP3) (10 - 20 µg/ml) containing a myc-tag were added onto the sections. As secondary reagents for the scFvs a rat anti-myc antibody (Genetex) and for the SIP(HyHEL-10) a rabbit anti-human IgE (Dako) were applied. The detection was achieved by Streptavidin Alexa Fluor 488 for SIP(L19), goat anti-rabbit IgG Alexa Fluor 488 (Invitrogen) for SIP(HyHEL-10) or donkey anti-rat IgG Alexa Fluor 488

antibody (Invitrogen) for the scFvs, respectively. Nuclei were counterstained with DAPI (Invitrogen). All commercial binding reagents were diluted according to the manufacturer's recommendation. Rinsing with PBS was performed in between all incubation steps. Slides were mounted with Fluorescent mounting medium (Dako) and analyzed with a Zeiss AxioVision 4.7 image analysis software (Carl Zeiss AG).

For laser scanning microscopy analysis all steps were performed as described above. In addition, the cytoskeleton was counterstained with Phalloidin Alexa 647 (Invitrogen). Slides were analyzed with a LSM 510 META from Zeiss (Carl Zeiss AG).

#### **4.4.4 Radioiodination of SIP antibodies**

Antibody radioiodination was performed as previously described (Villa et al, 2008). Briefly, 300 µg of protein was combined with 200 µCi of <sup>125</sup>I (Perkin Elmer) and with filtered chloramine T (Sigma) aqueous solution (5 mg/ml; 0.25 µg of chloramine T per µg of protein was used) for 1 min 45 sec followed by separation from unincorporated iodine using a PD-10 disposable gel filtration column (GE Healthcare). Antibody immunoreactivity after labeling was evaluated by affinity chromatography as previously described (Borsi et al, 2002). Binding reactivity, defined as the ratio between the counts of the eluted antibody and the sum of the counts (flowthrough, wash and eluate), was 79% for the SIP(L19), 62% for the SIP(SP1), 67% for the SIP(SP2), 84% for the SIP(SP3) and 73% for the SIP(HyHEL-10).

#### **4.4.5 Biodistribution of tumor bearing mice with the radiolabeled SIP antibodies**

F9 murine teratocarcinoma cells ( $2 \times 10^7$ ) were implanted s.c. into the left flank of 10- to 12-week-old 129/SvEv mice (Taconic) and tumors were allowed to grow for 8 days. The <sup>125</sup>I-labeled antibody fragment (15 - 20 µg; 3 - 6 µCi) in 100µl saline solution, radiolabeled on the same day, was injected intravenously. Mice were sacrificed 3 hours, 24 hours and 48 hours after injection. Organs were weighed and radioactivity was counted. Three to six animals were used for each time point and each construct. Radioactivity content of representative organs are expressed as the percentage of the injected dose per gram of tissue (%ID/g ± S.E.).

#### **4.4.6 Microautoradiography**

Twenty-four hours after the i.v. injection of radiolabeled antibodies, mice were sacrificed and F9 tumors were embedded and frozen in OTC medium (Thermo Fisher Scientific). Twenty-

micrometer sections were cut, fixed with ice-cold acetone and coated with NBT KODAK autoradiography emulsion (Kodak). After drying, the slides were stored at 4°C in the dark for approximately 4 weeks. The autoradiography emulsions were developed (KODAK developer D-19) for 4 min and fixed (KODAK Eastman Fixer) for 5 min. Finally, slides were rinsed with deionized water and counterstained with hematoxin (Sigma).

#### **4.4.7 Immunofluorescence analysis of *in vivo* injected antibodies**

To investigate the *in vivo* distribution and penetration of the antibodies within the F9 tumors, immunofluorescence staining was performed 24 hours after i.v. injection. Fixed sections (20µm) were incubated with rat anti-mouse CD31 antibody to stain the blood vessels and with rabbit-anti-human IgE antibody for detection of the SIP-antibodies. As secondary antibodies a goat-anti-rat Alexa Fluor-594 (Invitrogen) and donkey anti-rabbit Alexa Fluor 488 (Invitrogen) were used. Nuclei were counterstained with DAPI. All commercial binding reagents were diluted according to the manufacturer's recommendation. Rinsing with PBS was performed in between all incubation steps. Slides were mounted with Fluorescent mounting medium (Dako) and analyzed with a Zeiss AxioVision 4.7 image analysis software (Carl Zeiss AG).

#### **4.4.8 Deglycosylation**

To deglycosylate purified SIP(SP1), 15 µg protein samples were incubated with 500 units of PNGase F (New England Biolabs) for 3 h at 37°C. The resulting product was used directly for SDS-PAGE analysis.

#### **4.4.9 Murine blood plasma analysis by surface plasmon resonance measurements**

Murine blood plasma was analyzed by SPR on a BIAcore 3000 instrument (GE Healthcare), using high density coated SIP antibody chip as described in (Villa et al, 2008). A rabbit anti-human IgE antibody (Dako) (final concentration: 83 µg/ml) and buffered saline solution were used as positive control and as negative control, respectively.

#### **4.4.10 Biodistribution of healthy mice with radiolabeled SIP antibodies**

<sup>125</sup>I-labeled antibody fragments (30 - 40 µg; 3 - 6 µCi) in 200 µl saline solution, radiolabeled immediately prior to use, was injected intravenously. Mice were sacrificed 30 min after injection. Urine was collected and was applied to a disposable gel filtration column (GE Healthcare). Fractions of 500 µl were collected and radioactivity was measured. Organs were excised, weighed and radioactivity was counted. Two animals were used for each construct. Radioactivity content of urine fractions is expressed as counts per minute (cpm). Radioactivity content of representative organs is expressed as the percentage of the injected dose per gram of tissue (%ID/g).

## 5 SUPPLEMENTARY MATERIAL

### 5.1 *scFv*(SP1)

#### 5.1.1 Nucleotide sequence

GAGGTGCAGCTGTTGGAGTCTGGGGGAGGCTTGGTACAGCCTGGGGGGTCCCTGAGA  
CTCTCCTGTGCAGCCTCTGGATTCACCTTTAGC**CGTCAACAT**ATGAGCTGGGTCCGCCA  
GGCTCCAGGGAAGGGGCTGGAGTGGGTCTCAGCTATT**ACTGCGGCGGGTGGTAGG**AC  
ATACTACGCAGACTCCGTGAAGGGCCGGTTCACCATCTCCAGAGACAATTCCAAGAACA  
CGCTGTATCTGCAAATGAACAGCCTGAGAGCCGAGGACACGGCCGTATATTACTGTGC  
GAAA**CATTGCGCTAGTGTTACG**TTTGACTACTGGGGCCAGGGAACCCTGGTCACCGTC  
TCGAGT

**GGTGGAGGCGGTTTCAGGCGGAGGTGGCTCTGGCGGTGGCGGA**

TCGTCTGAGCTGACTCAGGACCCTGCTGTGTCTGTGGCCTTGGGACAGACAGTCAGGA  
TCACATGCCAAGGAGACAGCCTCAGA**CGGTATTAT**GCAAGCTGGTACCAGCAGAAGCC  
AGGACAGGCCCTGTACTTGTTCATCTAT**GGGAAAGCTGGG**CGGCCCTCAGGGATCCCA  
GACCGATTCTCTGGCTCCAGCTCAGGAAACACAGCTTCCCTTGACCATCACTGGGGCTCA  
GGCGGAAGATGAGGCTGACTATTACTGTAACCTCT**TTTCCCTTTGCGCCTTTT**GTGGT  
ATTCGGCGGAGGGACCAAGCTGACCGTCCTAGGCGCGGCCGC**AGAACAAAACTCATC**  
**TCAGAAGAGGATCTGAATGGGGCCGCATAG**

#### 5.1.2 Amino acid sequence

EVQLLESGLVQPGGSLRLSCAASGFTFS**RQH**MSWVRQAPGKGLEWVSAIT**AA**GGRTY  
YADSVKGRFTISRDNKNTLYLQMNSLRAEDTAVYYCAK**HSPSVT**FDYWGGQGLVTVSS

**GGGSGGGSGGGG**

SSELTQDPAVSVALGQTVRITCQGDSL**RYY**ASWYQQKPGQAPVLVIY**GKAG**RPSGIPDRF  
SGSSSGNTASLTITGAQAEDEADYYCNSS**FPFAPF**VVFGGKLTVLGAAA**EQKLISEEDLN**  
GAA-

## 5.2 scFv(5E)

### 5.2.1 Nucleotide sequence

GAGGTGCAGCTGTTGGAGTCTGGGGGAGGCTTGGTACAGCCTGGGGGGTCCCTGAGA  
CTCTCCTGTGCAGCCTCTGGATTCACCTTTAGC **AGGCGTCCT**ATGAGCTGGGTCCGCC  
AGGCTCCAGGGAAGGGGCTGGAGTGGGTCTCAGCTATT **ACTGCGGCG**GGTGGT **AGGA**  
CATACTACGCAGACTCCGTGAAGGGCCGGTTCACCATCTCCAGAGACAATTCCAAGAAC  
ACGCTGTATCTGCAAATGAACAGCCTGAGAGCCGAGGACACGGCCGTATATTACTGTG  
CGAAA **CATTGCGCTAGTGTACG**TTTGACTACTGGGGCCAGGGAACCCTGGTCACCGT  
CTCGAGT

**GGTGGAGGCGGTTTCAGGCGGAGGTGGCTCTGGCGGTGGCGGA**

TCGTCTGAGCTGACTCAGGACCCTGCTGTGTCTGTGGCCTTGGGACAGACAGTCAGGA  
TCACATGCCAAGGAGACAGCCTCAGA **GTTGGTAT**GCAAGCTGGTACCAGCAGAAGCC  
AGGACAGGCCCTGTACTTGTTCATCTAT **GGGAAA****GCTGGG**CGGCCCTCAGGGATCCCA  
GACCGATTCTCTGGCTCCAGCTCAGGAAACACAGCTTCCTTGACCATCACTGGGGCTCA  
GGCGGAAGATGAGGCTGACTATTACTGTAACCTCT **TTTCCCTTTGGGCCTTTT**GTGGT  
ATTCGGCGGAGGGACCAAGCTGACCGTCCTAGGCGCGGCCGC **CAGAACA AAAACTCATC**  
**TCAGAAGAGGATCTGAATGGGGCCGCATAG**

### 5.2.2 Amino acid sequence

EVQLLESGLVQPGGSLRLSCAASGFTFS **RRP**MSWVRQAPGKGLEWVSAI **TAA****GG****R**TY  
YADSVKGRFTISRDN SKNTLYLQMNSLRAEDTAVYYCAK **HSPSVT**FDYWGGQGLTVTVSS

**GGGSGGGSGGGG**

SSELTQDPAVSVALGQTVRITCQGDSL **RWY**ASWYQQKPGQAPVLVIY **GKAG**RPSGIPDR  
FSGSSSGNTASLTITGAQAEDEADYYCNSS **FPFAPF**VVFGGGTKLTVLGAAA **EQKLISEEDL**  
NGAA-



### 5.3 scFv(SP2)

#### 5.3.1 Nucleotide sequence

GAGGTGCAGCTGTTGGAGTCTGGGGGAGGCTTGGTACAGCCTGGGGGGTCCCTGAGA  
CTCTCCTGTGCAGCCTCTGGATTCACCTTTAGCAGGGGGGCTATGAGCTGGGTCCGCC  
AGGCTCCAGGGAAGGGGCTGGAGTGGGTCTCAGCTATTAGTGGTAGTGGTGGTAGCAC  
ATACTACGCAGACTCCGTGAAGGGCCGGTTCACCATCTCCAGAGACAATTCCAAGAACA  
CGCTGTATCTGCAAATGAACAGCCTGAGAGCCGAGGACACGGCCGTATATTACTGTGC  
GAAACATGGGAGTTCGCGGAATTTTGACTACTGGGGCCAGGGAACCCTGGTCACCGTC  
TCGAGT

**GGTGGAGGCGGTTCAAGGCGGAGGTGGCTCTGGCGGTGGCGGA**

TCGTCTGAGCTGACTCAGGACCCTGCTGTGTCTGTGGCCTTGGGACAGACAGTCAGGA  
TCACATGCCAAGGAGACAGCCTCAGACCGAGGCTTGCAAGCTGGTACCAGCAGAAGCC  
AGGACAGGCCCTGTACTTGTTCATCTATGGTAAAAACAACCGGCCCTCAGGGATCCCA  
GACCGATTCTCTGGCTCCAGCTCAGGAAACACAGCTTCCTTGACCATCACTGGGGCTCA  
GGCGGAAGATGAGGCTGACTATTACTGTAACCTCTACGCTTAGTCGGCCCTCTGTG  
GTATTCGGCGGAGGGACCAAGCTGACCGTCCTAGGCGCGGCCGCGAGAACA AAAACTCA  
TCTCAGAAGAGGATCTGAATGGGGCCGCATAG

#### 5.3.2 Amino acid sequence

EVQLLES~~GGGLVQPGGSLRLS~~CAASGFTFSRGAMSWVRQAPGKGLEWVSAISGSGGSTY  
YADSVKGRFTISRDNKNTLYLQMNSLRAEDTAVYYCAKHGSSRNFDYWGQGTLVTVSS

**GGGSGGGSGGGG**

SSELTQDPAVSVALGQTVRITCQGDSLRPLASWYQQKPGQAPVLVIYGKNNRPSGIPDRF  
SGSSSGNTASLTITGAQAEDADYYCNSSLSRPSVVFGGGTKLTVLGAAA  
EQKLISEEDLNGAA-

## 5.4 scFv(SP3)

### 5.4.1 Nucleotide sequence

GAGGTGCAGCTGTTGGAGTCTGGGGGAGGCTTGGTACAGCCTGGGGGGTCCCTGAGA  
CTCTCCTGTGCAGCCTCTGGATTCACCTTTAGCGGCTATGCCATGAGCTGGGTCCGCC  
AGGCTCCAGGGAAGGGGCTGGAGTGGGTCTCAGCTATTAGTGGTAGTGGTGGTAGCAC  
ATACTACGCAGACTCCGTGAAGGGCCGGTTCACCATCTCCAGAGACAATTCCAAGAACA  
CGCTGTATCTGCAAATGAACAGCCTGAGAGCCGAAGACACGGCCGTATATTACTGTGC  
GAAAATTCTTCTTTTCATTTTGACTACTGGGGCCAGGGAACCCTGGTCACCGTCTCGA  
GT

**GGTGGAGGCGGTTTCAGGCGGAGGTGGCTCTGGCGGTGGCGGA**

GAAATTGTGTTGACGCAGTCTCCAGGCACCCTGTCTTTGTCTCCAGGGGAAAGAGCCAC  
CCTCTCCTGCAGGGCCAGTCAGAGTGTTAGCGGGCGGCGGTTAGCCTGGTACCAGCA  
GAAACCTGGCCAGGCTCCCAGGCTCCTCATCTATGGTGCATCCAGCAGGGCCACTGGC  
ATCCCAGACAGGTTTCAGTGGCAGTGGGTCTGGGACAGACTTCACTCTCACCATCAGCA  
GACTGGAGCCTGAAGATTTTGCAGTGTATTACTGTCAGCAGCCGAGGGGTGCTCCGAC  
GACGTTCCGCCAAGGGACCAAGGTGGAAATCAAAGCGGCCGCAGAACAAAACTCATC  
TCAGAAGAGGATCTGAATGGGGCCGCATAG

### 5.4.2 Amino acid sequence

EVQLLESGLVQPGGSLRLSCAASGFTFSGYAMSWVRQAPGKGLEWVSAISGSGGSTY  
YADSVKGRFTISRDNKNTLYLQMNSLRAEDTAVYYCAKISSFHFDYWGQGTLVTVSS

**GGGSGGGSGGGG**

EIVLTQSPGTLSPGERATLSCRASQSVSGRRLAWYQQKPGQAPRLLIYGASSRATGIPDR  
FSGSGSDFTLTISRLEPEDFAVYYCQQPRGAPTTFGQGTKVEIKAAAEQKLISEEDLNGA  
A-

## 5.5 scFv(9H)

### 5.5.1 Nucleotide sequence

GAGGTGCAGCTGTTGGAGTCTGGGGGAGGCTTGGTACAGCCTGGGGGGTCCCTGAGA  
CTCTCCTGTGCAGCCTCTGGATTCACCTTTAGCTTGGATGGCGATGAGCTGGGTCCGCC  
AGGCTCCAGGGAAGGGGCTGGAGTGGGTCTCAGCTATTAGTGGTAGTGGTGGTAGCAC  
ATACTACGCAGACTCCGTGAAGGGCCGGTTCACCATCTCCAGAGACAATTCCAAGAACA  
CGCTGTATCTGCAAATGAACAGCCTGAGAGCCGAAGACACGGCCGTATATTACTGTGC  
GAAAATTCTTCTTTTCATTTTGACTACTGGGGCCAGGGAACCCTGGTCACCGTCTCGA  
GT

**GGTGGAGGCGGTTTCAGGCGGAGGTGGCTCTGGCGGTGGCGGA**

GAAATTGTGTTGACGCAGTCTCCAGGCACCCTGTCTTTGTCTCCAGGGGAAAGAGCCAC  
CCTCTCCTGCAGGGCCAGTCAGAGTGTTAGCAATTCTGGGTTAGCCTGGTACCAGCAG  
AAACCTGGCCAGGCTCCCAGGCTCCTCATCTATGGTGCATCCAGCAGGGCCACTGGCA  
TCCCAGACAGGTTTCAGTGGCAGTGGGTCTGGGACAGACTTCACTCTCACCATCAGCAG  
ACTGGAGCCTGAAGATTTTGCAGTGTATTACTGTCAGCAGCCGAGGGGTGCTCCGACG  
ACGTTCCGCCAAGGGACCAAGGTGGAAATCAAAGCGGCCGCCAGAACA AAAACTCATCT  
CAGAAGAGGATCTGAATGGGGCCGCATAG

### 5.5.2 Amino acid sequence

EVQLLESGLVQPGGSLRLSCAASGFTFSWMAMSWVRQAPGKGLEWVSAISGSGGSTY  
YADSVKGRFTISRDN SKNTLYLQMNSLRAEDTAVYYCAKISSFHFDYWGGQGLTVT

**SSGGGSGGGGSGGGG**

EIVLTQSPGTLSPGERATLSCRASQSVSNSGLAWYQQKPGQAPRLLIYGASSRATGIPDR  
FSGSGSGTDFLTISRLEPEDFAVYYCQQPRGAPTTFGQGTKVEIKAAAEQKLISEEDLNGA  
A-

**CDR1**

**CDR2**

**CDR3**

**MYC-TAG**

**LINKER**

## 6 REFERENCES

- Ahlskog JKJ, Schliemann C, Mårilind J, Qureshi U, Ammar A, Pedley RB, Neri D, Human monoclonal antibodies targeting carbonic anhydrase IX for the molecular imaging of hypoxic regions in solid tumours, *Br. J. Cancer* 101 (2009) 645-657
- Ahmed SH, Clark LL, Pennington WR, Webb CS, Bonnema DD, Leonardi AH, McClure CD, Spinale FG, Zile MR, Matrix metalloproteinases/tissue inhibitors of metalloproteinases—relationship between changes in proteolytic determinants of matrix composition and structural, functional, and clinical manifestations of hypertensive heart disease, *Circulation* 113 (2006) 2089–2096
- Airola K, Johansson N, Kariniemi AL, Kahari VM, Saarialho-Kere UK, Human collagenase-3 is expressed in malignant squamous epithelium of the skin, *J. Invest. Dermatol.* 109 (1997) 225-231
- Albright CF, Graciani N, Han W, Yue E, Stein R, Lai ZH, Diamond M, Dowling R, Grimminger L, Zhang SY, Behrens D, Musselman A, Bruckner R, Zhang MZ, Jiang X, Hu D, Higley A, DiMeo S, Rafalski M, Mandlekar S, Car B, Yeleswaram S, Stern A, Copeland RA, Combs A, Seitz SP, Trainor GL, Taub R, Huang P, Oliff A, Matrix metalloproteinase-activated doxorubicin prodrugs inhibit ht1080 xenograft growth doxorubicin with less toxicity, *Mol. Cancer Ther.* 4 (2005) 751–760
- Basset P, Bellocq JP, Wolf C, Stoll I, Hutin P, Limacher JM, Podhajcer OL, Chenard MP, Rio MC, Chambon P, A novel metalloproteinase gene specifically expressed in stromal cells of breast carcinomas, *Nature* 348 (1990) 699-704
- Bein K, Simons M, Thrombospondin type 1 repeats interact with matrix metalloproteinase 2. Regulation of metalloproteinase activity, *J. Biol. Chem.* 275 (2000) 32167-32173
- Berndorff D, Borkowski S, Sieger S, Rother A, Friebe M, Viti F, Hilger CS, Cyr JE, Dinkelborg LM, Radioimmunotherapy of solid tumors by targeting extra domain B fibronectin: identification of the best-suited radioimmunoconjugate, *Clin. Cancer Res.* 11 (2005) 7053s-7063s
- Bertschinger J, Neri D, Covalent DNA display as a novel tool for directed evolution of proteins in vitro, *Protein Eng. Des. Sel.* 17 (2004) 699-707
- Bes C, Troadec S, Chentouf M, Breton H, Lajoix AD, Heitz F, Gross R, Pluckthun A, Chardes T, PIN-bodies: a new class of antibody-like proteins with CD4 specificity derived from the protein inhibitor of neuronal nitric oxide synthase, *Biochem. Biophys. Res. Commun.* 343 (2006) 334-344
- Binz HK, Amstutz P, Kohl A, Stumpp MT, Briand C, Forrer P, Grutter MG, Pluckthun A, High-affinity binders selected from designed ankyrin repeat protein libraries, *Nat. Biotechnol.* 22 (2004) 575-582
- Biondi ML, Turri O, Leviti S, Seminati R, Cecchini F, Bernini M, Ghilardi G, Guagnellini E, MMP1 and MMP3 polymorphisms in promoter regions and cancer, *Clin. Chem.* 46 (2000) 2023-2024
- Bird RE, Hardman KD, Jacobson JW, Johnson S, Kaufman BM, Lee SM et al, Single-chain antigen-binding proteins, *Science* 242 (1988) 423–426
- Boder ET, Midelfort SK, Wittrup KD, Directed evolution of antibody fragments with monovalent femtomolar antigenbinding affinity, *Proc. Natl. Acad. Sci. USA* 97 (2000) 10701–10705
- Boder ET, Wittrup KD, Optimal screening of surface-displayed polypeptide libraries, *Biotechnol. Prog.* 14 (1998) 55-62
- Borsi L, Balza E, Bestagno M, Castellani P, Carnemolla B, Biro A, Leprini A, Sepulveda J, Burrone O, Neri D, Zardi L. Selective targeting of tumoral vasculature: comparison of different formats of an antibody (L19) to the ED-B domain of fibronectin. *Int. J. Cancer* 102 (2002) 75-85

- Borsi L, Castellani P, Allemanni G, Neri D, Zardi L, Preparation of phage antibodies to the ED-A domain of human fibronectin, *Exp. Cell. Res.* 240 (1998) 244–251
- Bothmann H, Pluckthun A, Selection for a periplasmic factor improving phage display and functional periplasmic expression, *Nat. Biotechnol.* 16 (1998) 376-380
- Brack SS, Silacci M, Birchler M, Neri D, Tumor-targeting properties of novel antibodies specific to the large isoform of tenascin-C, *Clin. Cancer Res.* 12 (2006) 3200-3208
- Brekke OH, Sandlie I, Therapeutic antibodies for human diseases at the dawn of the twenty-first century, *Nat. Rev. Drug Discov.* 2 (2003) 52-62
- Buck TB, Yoshiji H, Harris SR, Bunce OR, Thorgeirsson UP, The effects of sustained elevated levels of circulating tissue inhibitor of metalloproteinases-1 on the development of breast cancer in mice, *Ann. N Y Acad. Sci.* 878 (1999) 732-735
- Burrage PS, Mix KS, Brinckerhoff CE, Matrix metalloproteinases: Role in arthritis. *Front. Biosci.* 11 (2006) 529–543
- C.E. Brinckerhoff, Joint destruction in arthritis: metalloproteinases in the spotlight, *Arthritis Rheum.* 34 (1991) 1073-1075
- Carnemolla B, Neri D, Castellani P, Leprini A, Neri G, Pini A, Winter G, Zardi L, Phage antibodies with pan-species recognition of the oncofetal angiogenesis marker fibronectin ED-B domain, *Int. J. Cancer* 68 (1996) 397-405
- Carter P, Bispecific human IgG by design, *J. Immunol. Methods* 248 (2001) 7–15
- Carter PJ, Potent antibody therapeutics by design, *Nat. Rev. Immunol.* 6 (2006) 343-357
- Castellani P, Borsi L, Carnemolla B, Biro A, Dorcaratto A, Viale GL, Neri D, Zardi L, Differentiation between high- and low-grade astrocytoma using a human recombinant antibody to the extra domain-B of fibronectin, *Am. J. Pathol.* 161 (2002) 1695-1700
- Celiker MY, Ramamurthy N, Xu JW, Wang MS, Jiang YF, Greenwald R, Shi YE, Inhibition of adjuvant-induced arthritis by systemic tissue inhibitor of metalloproteinases 4 gene delivery, *Arthritis Rheum.* 46 (2002) 3361–3368
- Cereghino GP, Cregg JM, Applications of yeast in biotechnology: protein production and genetic analysis, *Curr. Opin. Biotechnol.* 10 (1999) 422-427
- Chames P, Baty D, Antibody engineering and its applications in tumor targeting and intracellular immunization, *FEMS Microbiol. Lett.* 189 (2000) 1–8
- Chames P, Van Regenmortel M, Weiss E, Baty D, Therapeutic antibodies: successes, limitations and hopes for the future, *Br. J. Pharmacol.* 157(2009) 220-233
- Chari RVJ, Targeted delivery of chemotherapeutics: tumor-activated prodrug therapy, *Adv. Drug Deliv. Rev.* 31 (1998) 89–104
- Chen L, MacMillan AM, Chang W, Ezaz-Nikpay K, Lane WS, Verdine GL, Direct identification of the active-site nucleophile in a DNA (cytosine-5)-methyltransferase, *Biochemistry* 30 (1991) 11018-11025
- Chen Y, Wiesmann C, Fuh G, Li B, Christinger HW, McKay P, de Vos AM, Lowman HB, Selection and analysis of an optimized anti-VEGF antibody: crystal structure of an affinity-matured Fab in complex with antigen, *J. Mol. Biol.* 293 (1999) 865-881
- Cho GS, Szostak JW, Directed evolution of ATP binding proteins from a zinc finger domain by using mRNA display, *Chem. Biol.* 13 (2006) 139-147

- Chrastina A, Zavada J, Parkkila S, Kaluz S, Kaluzova M, Rajcani J, Pastorek J, Pastorekova S, Biodistribution and pharmacokinetics of <sup>125</sup>I-labeled monoclonal antibody M75 specific for carbonic anhydrase IX, an intrinsic marker of hypoxia, in nude mice xenografted with human colorectal carcinoma, *Int. J. Cancer* 105 (2003) 873-881
- Cicortas Gunnarsson L, Dexlin L, Karlsson EN, Holst O, Ohlin M, Evolution of a carbohydrate binding module into a proteinspecific binder, *Biomol. Eng.* 23 (2006) 111-117
- Cortez DM, Feldman MD, Mummidi S, Valente AJ, Steffensen B, Vincenti M, Barnes JL, Chandrasekar B, IL-17 stimulates MMP-1 expression in primary human cardiac fibroblasts via p38 MAPK- and ERK1/2-dependent C/EBP- beta, NF-kappaB, and AP-1 activation, *Am. J. Physiol. Heart. Circ. Physiol.* 293 (2007) H3356-3365
- Coussens LM, Fingleton B, Matrisian LM, Matrix metalloproteinase inhibitors and cancer: trials and tribulations, *Science* 295 (2002) 2387-2392
- Dalby PA, Hoess RH, DeGrado WF, Evolution of binding affinity in a WW domain probed by phage display, *Protein Sci.* 9 (2000) 2366-2376
- Davies B, Miles DW, Happerfield LC, Naylor MS, Bobrow LG, Rubens RD, F.R. Balkwill, Activity of type IV collagenases in benign and malignant breast disease, *Br. J. Cancer* 67 (1993) 1126-1131
- Davis JJ, Tkac J, Laurenson S, Ferrigno PK, Peptide aptamers in label-free protein detection. 1. Characterization of the immobilized scaffold, *Anal. Chem.* 79 (2007) 1089-1096
- DeClerck YA, Imren S, Protease inhibitors: role and potential therapeutic use in human cancer, *Eur. J. Cancer* 30A (1994) 2170-2180
- Demartis S, Huber A, Viti F, Lozzi L, Giovanni L, Neri P, Winter G, Neri D, A strategy for the isolation of catalytic activities from repertoires of enzymes displayed on phage, *J. Mol. Biol.* 286 (1999) 617-633
- Devy L, Huang L, Naa L, Yanamandra N, Pieters H, Frans N, Chang E, Tao Q, Vanhove M, Lejeune A, van Gool R, Sexton DJ, Kuang G, Rank D, Hogan S, Pazmany C, Ma YL, Schoonbroodt S, Nixon AE, Ladner RC, Hoet R, Henderikx P, Tenhoor C, Rabbani SA, Valentino ML, Wood CR, Dransfield DT, Selective inhibition of matrix metalloproteinase-14 blocks tumor growth, invasion, and angiogenesis, *Cancer Res.* 69 (2009) 1517-1526
- DiMartino M, Wolff C, High W, Stroup G, Hoffman S, Laydon J, Lee JC, Bertolini D, Galloway WA, Crimmin MJ, Davis M, Davies S, Anti-arthritis activity of hydroxamic acid-based pseudopeptide inhibitors of matrix metalloproteinases and TNF alpha processing, *Inflamm. Res.* 46(1997) 211-215
- Dreher ML, Gherardi E, Skerra A, Milstein C, Colony assays for antibody fragments expressed in bacteria, *J. Immunol. Methods*, 139 (1991) 197-205
- Dufner P, Jermutus L, Minter RR, Harnessing phage and ribosome display for antibody optimization, *Trends Biotechnol.* 24 (2006) 523-529
- Edwards DR, in *Matrix metalloproteinase inhibitors in cancer therapy* (eds Clendennin NJ and Appelt K) 67-84 (Humana Press, Totowa, New Jersey, 2001)
- Egeblad M, Werb Z, New functions for the matrix metalloproteinases in cancer progression, *Nat. Rev. Cancer* 2 (2002) 161-174
- El-Emir E, Dearling JL, Huhlov A, Robson MP, Boxer G, Neri D, van Dongen GA, Trachsel E, Begent RH, Pedley RB, Characterisation and radioimmunotherapy of L19-SIP, an anti-angiogenic antibody against the extra domain B of fibronectin, in colorectal tumour models, *Br. J. Cancer* 96 (2007) 1862-1870
- Ewert S, Huber T, Honegger A, Plückthun A, Biophysical properties of human antibody variable domains, *J. Mol. Biol.* 325 (2003) 531-553

Fei X, Zheng QH, Liu X, Wang JQ, Sun HB, Mock BH et al. Synthesis of radiolabeled binphenylsulfonamide matrix metalloproteinase inhibitors as new potential cancer imaging agents, *Bioorg. Med. Chem. Lett.* 13 (2003) 2217-2222

Feldhaus MJ, Siegel RW, Opresko LK, Coleman JR, Feldhaus JMW, Yeung YA, Cochran JR, Heinzelman P, Colby D, Swers J, Graff C, Wiley HS, Wittrup KD, Flow-cytometric isolation of human antibodies from a nonimmune *Saccharomyces cerevisiae* surface display library, *Nat. Biotechnol.* 21 (2003) 163–170

Fiedler M, Skerra A, Non-antibody scaffolds. In *Handbook of Therapeutic Antibodies*, vol. II. Emerging Developments, Edited by Dubel S. Wiley–VCH (2007) 467-499

Fingleton B, Matrix metalloproteinase inhibitors for cancer therapy: current situation and future prospects, *Expert. Opin. Ther. Targets* 7 (2003) 385-397

Firestone RA, Telan LA, 2005, Enzyme-activated anti-tumor prodrug compounds, US patent 6855689

Fischer N, Leger O, Bispecific antibodies: molecules that enable novel therapeutic strategies, *Pathobiology* 74 (2007) 3–14

Friedman M, Ståhl S, Engineered affinity proteins for tumour-targeting applications, *Biotechnol. Appl. Biochem.* 53 (2009) 1-29

Furrer E, Berdugo M, Stella C, Behar-Cohen F, Gurny R, Feige U, Lichtlen P, Urech DM, Pharmacokinetics and posterior segment biodistribution of ESBA105, an anti-TNF-alpha single-chain antibody, upon topical administration to the rabbit eye, *Invest. Ophthalmol. Vis. Sci.* 50 (2009) 771-778

Furukawa H, Shimojyo R, Ohnishi N, Fukuda H, Kondo A, Affinity selection of target cells from cell surface display libraries: a novel procedure using thermo-responsive magnetic nanoparticles, *Appl. Microbiol. Biotechnol.* 62 (2003) 478–483

Gao C, Mao S, Kaufmann G, Wirsching P, Lerner RA; Janda KD, A method for the generation of combinatorial antibody library using phage pIX phage display, *Proc. Natl. Acad. Sci. U S A* 99 (2002) 12612-12616

Gao C, Mao S, Lo CH, Wirsching P, Lerner RA, Janda KD, Making artificial antibodies: a format for phage display of combinatorial heterodimeric arrays, *Proc. Natl. Acad. Sci. U S A* 96 (1999) 6025-6030

Gherardi E, Pannell R, Milstein C, A single-step procedure for cloning and selection of antibody-secreting hybridomas, *J. Immunol. Methods* 126 (1990) 61–68

Gill DS, Damle NK, Biopharmaceutical drug discovery using novel protein scaffolds, *Curr. Opin. Biotechnol.* 17 (2006) 653-658

Giovannoni L, Viti F, Zardi L, Neri D, Isolation of anti-angiogenesis antibodies from a large combinatorial repertoire by colony filter screening, *Nucleic. Acids Res.* 29 (2001) E27

Glazier A, 1997, Tumor protease activated prodrugs of phosphoramidate mustard analogs with toxification and detoxification functionalities, US patent 5659061

Glennie MJ, McBride HM, Worth AT, Stevenson GT, Preparation and performance of bispecific F(ab' y)2 antibody containing thioether-linked Fab' y fragments, *J. Immunol.* 139 (1987) 2367–2375

Grabulovski D, Kaspar M, Neri D, A novel, non-immunogenic Fyn SH3-derived binding protein with tumor vascular targeting properties, *J. Biol. Chem.* 282 (2007) 3196-3204

Greenwood J, Willis AE, Perham RN, Multiple display of foreign peptides on a filamentous bacteriophage. Peptides from *Plasmodium falciparum* circumsporozoite protein as antigens, *J. Mol. Biol.* 220 (1991) 821-827

Griffiths AD, Williams SC, Hartley O, Tomlinson IM, Waterhouse P, Crosby WL, Kontermann RE, Jones PT, Low NM, Allison TJ, et al, Isolation of high affinity human antibodies directly from large synthetic repertoires, *EMBO J.* 13(1994) 3245-3260

Hamers-Casterman C, Atarhouch T, Muyldermans S, Robinson G, Hamers C, Songa EB et al, Naturally occurring antibodies devoid of light chains. *Nature* 363 (1993) 446-448

Hanes J, Jermutus L, Pluckthun A, Selecting and evolving functional proteins in vitro by ribosome display, *Methods Enzymol.* 328 (2000) 404-430

Harris ED, Jr, Krane SM, An endopeptidase from rheumatoid synovial tissue culture *Biochim Biophys. Acta.* 258 (1972) 566-576

Harris ED, Jr, Krane SM, An endopeptidase from rheumatoid synovial tissue culture, *Biochim. Biophys. Acta.* 258 (1972) 566-576

Hasty KA, Reife RA, Kang AH, Stuart JM, The role of stromelysin in the cartilage destruction that accompanies inflammatory arthritis, *Arthritis Rheum.* 33 (1990) 388-397

Heinis C, Huber A, Demartis S, Bertschinger J, Melkko S, Lozzi L, Neri P, Neri D, Selection of catalytically active biotin ligase and trypsin mutants by phage display, *Protein Eng.* 14 (2001) 1043-1052

Hey T, Fiedler E, Rudolph R, Fiedler M, Artificial, non-antibody binding proteins for pharmaceutical and industrial applications, *Trends Biotechnol.* 23 (2005) 514-522

Hiipakka M, Poikonen K, Saksela K, SH3 domains with high affinity and engineered ligand specificities targeted to HIV-1 Nef, *J. Mol. Biol.* 293(1999)1097-1106

Ho M, Kreitman RJ, Onda M, Pastan I, In vitro antibody evolution targeting germline hot spots to increase activity of an anti-CD22 immunotoxin, *J. Biol. Chem.* 280 (2005) 607-617

Hofheinz RD, al-Batran SE, Hartmann F, Hartung G, Jager D, Renner C, Tanswell P, U. Kunz, A. Amelsberg, H. Kuthan, G. Stehle, Stromal antigen targeting by a humanised monoclonal antibody: an early phase II trial of sibrotuzumab in patients with metastatic colorectal cancer, *Onkologie* 26 (2003) 44-48

Holliger P, Hudson PJ, Engineered antibody fragments and the rise of single domains, *Nat. Biotechnol.* 23 (2005) 1126-1136

Holliger P, Prospero T, Winter G, 'Diabodies': small bivalent and bispecific antibody fragments, *Proc. Natl. Acad. Sci. USA* 90 (1993) 6444-6448

Hoogenboom HR, Griffiths AD, Johnson KS, Chiswell DJ, Hudson P, Winter G, Multi-subunit proteins on the surface of filamentous phage: methodologies for displaying antibody (Fab) heavy and light chains, *Nucleic. Acids. Res.* 19 (1991) 4133-4137

Hoogenboom HR, Selecting and screening recombinant antibody libraries, *Nat. Biotechnol.* 23(2005) 1105-1116

Hoogenboom HR, Winter G, By-passing immunisation. Human antibodies from synthetic repertoires of germline VH gene segments rearranged in vitro, *J. Mol. Biol.* 227 (1992) 381-388

Hu J, Van den Steen PE, Sang QX, Opdenakker G, Matrix metalloproteinase inhibitors as therapy for inflammatory and vascular diseases, *Nat. Rev. Drug Discov.* 6 (2007) 480-498

Hu S, Shively L, Raubitschek A, Sherman M, Williams LE, Wong JY, Shively JE, Wu AM, Minibody: A novel engineered anti-carcinoembryonic antigen antibody fragment (single-chain Fv-CH3) which exhibits rapid, high-level targeting of xenografts, *Cancer Res.* 56 (1996) 3055-3061



- Huang W, Dolmer K, Gettins PG, NMR solution structure of complement-like repeat CR8 from the low density lipoprotein receptor-related protein, *J. Biol. Chem.* 274(1999) 14130-14136
- Iannolo G, Minenkova O, Petruzzelli R, Cesareni G, Modifying filamentous phage capsid, limits size of the major capsid protein, *J. Mol. Biol.* 248 (1995) 835-844
- Ingman T, Tervahartiala T, Ding YL, Tschesche H, Haerian A, Kinane DF, Konttinen YT, Sorsa T, Matrix metalloproteinases and their inhibitors in gingival crevicular fluid and saliva of periodontitis patients, *J. Clin. Periodontol.* 23 (1996) 1127–1132
- Irving RA, Coia G, Roberts A, Nutall SD, Hudson PJ, Ribosome display and affinity maturation: from antibodies to single V-domains and steps towards cancer therapeutics, *J. Immunol. Methods* 248 (2001) 31-45
- Itoh T, Tanioka M, Yoshida H, Yoshioka T, Nishimoto H, Itohara S, Reduced angiogenesis and tumor progression in gelatinase A-deficient mice, *Cancer Res.* 58 (1998) 1048-1051
- Janicki JS, Brower GL, Gardner JD, Chancey AL, Stewart JA, The dynamic interaction between matrix metalloproteinase activity and adverse myocardial remodeling, *Heart. Fail. Rev.* 9 (2004) 33–42
- Janssens S, Lijnen HR, What has been learned about the cardiovascular effects of matrix metalloproteinases from mouse models, *Cardiovasc. Res.* 69 (2006) 585-594
- Jeffery N, McLean MH, El-Omar EM, Murray GI, The matrix metalloproteinase / tissue inhibitor of matrix metalloproteinase profile in colorectal polyp cancers, *Histopathology* 54 (2009) 820-828
- Jespers L, Schon O, Famm K, Winter G, Aggregation resistant domain antibodies selected on phage by heat denaturation, *Nat. Biotechnol.* 22 (2004) 1161-1165
- Jones PT, Dear PH, Foote J, Neuberger MS, Winter G, Replacing the complementarity-determining regions in a human antibody with those from a mouse. *Nature* 321 (1986) 522–525
- Kanamori Y, Matsushima M, Minaguchi T, Kobayashi K, Sagae S, Kudo R, Terakawa N, Nakamura Y, Correlation between expression of the matrix metalloproteinase-1 gene in ovarian cancers and an insertion/deletion polymorphism in its promoter region, *Cancer Res.* 59(1999) 4225-4227
- Kaspar M, Trachsel E, Neri D, The antibody-mediated targeted delivery of interleukin-15 and GM-CSF to the tumor neovasculature inhibits tumor growth and metastasis, *Cancer Res.* 67 (2007) 4940–4948
- Kerkela E, Saarialho-Kere U, Matrix metalloproteinases in tumor progression: focus on basal and squamous cell skin cancer, *Exp. Dermatol.* 12 (2003) 109-125
- Khokha R, Suppression of the tumorigenic and metastatic abilities of murine B16-F10 melanoma cells in vivo by the overexpression of the tissue inhibitor of the metalloproteinases-1, *J Natl. Cancer Inst.* 86 (1994) 299-304
- Kinoshita M, Izumoto S, Hashimoto N, Kishima H, Kagawa N, Hashiba T, Chiba Y, Yoshimine T, Immunohistochemical analysis of adhesion molecules and matrix metalloproteinases in malignant CNS lymphomas: a study comparing primary CNS malignant and CNS intravascular lymphomas, *Brain Tumor Pathol.* 25 (2008) 73-78
- Kirkham PM, Mortari F, Newton JA, Schroeder HW, Jr Immunoglobulin VH clan and family identity predicts variable domain structure and may influence antigen binding, *EMBO J.* 11(1992) 603-609
- Knight CG, F. Willenbrock, G. Murphy, A novel coumarin-labelled peptide for sensitive continuous assays of the matrix metalloproteinases, *FEBS Lett.* 296 (1992) 263-266
- Kohler G, Milestein C, Continuous cultures of fused cell secreting antibody of predefined specificity, *Nature* 256 (2005) 495-497

Köhrmann A, Kammerer U, Kapp M, J. Dietl, J. Anacker, Expression of matrix metalloproteinases (MMPs) in primary human breast cancer and breast cancer cell lines: New findings and review of the literature, *BMC Cancer* 9 (2009) 188

Koide A, Baily CW, Huang X, Koide S, The fibronectin type III domain as scaffold for novel binding proteins, *J. Mol. Biol.* 284 (1998) 1141-1151

Konttinen YT, Ainola M, Valleala H, Ma J, Ida H, Mandelin J, Kinne RW, Santavirta S, Sorsa T, Lopez-Otin C, Takagi M, Analysis of 16 different matrix metalloproteinases (MMP-1 to MMP-20) in the synovial membrane: different profiles in trauma and rheumatoid arthritis, *Ann. Rheum. Dis.* 58 (1999) 691-697

Koop S, Khokha R, Schmidt EE, MacDonald IC, Morris VL, Chambers AF, Groom AC, Overexpression of metalloproteinase inhibitor in B16F10 cells does not affect extravasation but reduces tumor growth, *Cancer Res.* 54 (1994) 4791-4797

Kratz F, Dreves J, Bing G, Stockmar C, Scheuermann K, Lazar P, Unger C, Development and in vitro efficacy of novel MMP2 and MMP9 specific doxorubicin albumin conjugates, *Bioorg. Med. Chem. Lett.* 11 (2001) 2001–2006

Kristensen P, Winter G, Proteolytic selection for protein folding using filamentous bacteriophages, *Fold. Des.* 3 (1998) 321-328

Kuivanen T, Jeskanen L, Kyllönen L, Isaka K, Saarialho-Kere U, Matrix metalloproteinase-26 is present more frequently in squamous cell carcinomas of immunosuppressed compared with immunocompetent patients, *J. Cutan. Pathol.* 36 (2009) 929-936

Kusukawa J, Sasaguri Y, Morimatsu M, Kameyama T, Expression of matrix metalloproteinase-3 in stage I and II squamous cell carcinoma of the oral cavity, *J. Oral Maxillofac. Surg.* 53 (1995) 530-534

Lavoie TB, Drohan WN, Smith-Gill SJ, Experimental analysis by site-directed mutagenesis of somatic mutation effects on affinity and fine specificity in antibodies specific for lysozyme, *J. Immunol.* 148 (1992) 503-513

Lepage M, Dow WC, Melchior M, You Y, Fingleton B, Quarles CC, Pépin C, Gore JC, Matrisian LM, McIntyre JO, Noninvasive detection of matrix metalloproteinase activity in vivo using a novel magnetic resonance imaging contrast agent with a solubility switch, *Mol. Imaging* 6 (2007) 393-403

Ley AC, Markland W, Ladner RC, Obtaining a family of high-affinity, high-specificity protein inhibitors of plasmin and plasma kallikrein, *Mol. Divers.* 2 (1996) 119-124

Liotta LA, Tryggvason K, Garbisa S, Hart I, Foltz CM, Shafie S, Metastatic potential correlates with enzymatic degradation of basement membrane collagen, *Nature* 284 (1980) 67-68

Lipovsek D, Plückthun A, In-vitro protein evolution by ribosome display and mRNA display, *J. Immunol. Methods* 290 (2004) 51-67

Lowman HB, Bass SH, Simpson N, Wells JA, Selecting high-affinity binding proteins by monovalent phage display, *Biochemistry* 30 (1991) 10832-10838

Luttun A, Lutgens E, Manderveld A, Maris K, Collen D, Carmeliet P, Moons L, Loss of matrix metalloproteinase-9 or matrix metalloproteinase-12 protects apolipoprotein E-deficient mice against atherosclerotic media destruction but differentially affects plaque growth, *Circulation* 109 (2004) 1408-1414

Mansour AM, Dreves J, Esser N, Hamada FM, Badary OA, Unger C, Fichtner I, Kratz F, A new approach for the treatment of malignant melanoma: Enhanced antitumor efficacy of an albumin-binding doxorubicin prodrug that is cleaved by matrix metalloproteinase 2, *Cancer Res.* 63 (2003) 4062–4066

- Martel-Pelletier J, McCollum R, Fujimoto N, Obata K, Cloutier JM, Pelletier J-P, Excess of metalloproteases over tissue inhibitor of metalloproteinase may contribute to cartilage degradation in osteoarthritis and rheumatoid arthritis, *Lab. Invest.* 70 (1994) 807-815
- Martel-Pelletier J, Welsch DJ, Pelletier JP, Metalloproteases and inhibitors in arthritic diseases, *Best. Pract. Res. Clin. Rheumatol.* 15 (2001) 805–829
- Mattheakis LC, Bhatt RR, Dower WJ, An in vitro polysome display system for identifying ligands from very large peptide libraries, *Proc. Natl. Acad. Sci. U S A* 91(1994) 9022-9026
- McCafferty J, Griffiths AD, Winter G, Chiswell DJ, Phage antibodies: filamentous phage displaying antibody variable domains, *Nature* 348 (1990) 552-554
- McCawley LJ, Crawford HC, King LE, Jr., Mudgett J, Matrisian LM, A protective role for matrix metalloproteinase-3 in squamous cell carcinoma, *Cancer Res.* 64 (2004) 6965-6972
- McCawley LJ, Wright J, LaFleur BJ, Crawford HC, Matrisian LM, Keratinocyte expression of MMP3 enhances differentiation and prevents tumor establishment, *Am. J. Pathol.* 173 (2008) 1528-1539
- Mengshol JA, Mix KS, Brinckerhoff CE, Matrix metalloproteinases as therapeutic targets in arthritic diseases—bull's-eye or missing the mark, *Arthritis Rheum.* 46 (2002) 13–20
- Miller GK, Naeve GS, S.A. Gaffar, A.L. Epstein, Immunologic and biochemical analysis of TNT-1 and TNT-2 monoclonal antibody binding to histones, *Hybridoma* 12 (1993) 689-698
- Milstein C, Cuello AC, Hybrid hybridomas and their use in immunohistochemistry, *Nature* 305 (1983) 537–540
- Montgomery AM, De Clerck YA, Langley KE, Reisfeld RA, Mueller BM, Melanoma-mediated dissolution of extracellular matrix: contribution of urokinase-dependent and metalloproteinase-dependent proteolytic pathways, *Cancer Res.* 53 (1993) 693-700
- Mott JD, Thomas CL, Rosenbach MT, Takahara K, Greenspan DS, Banda MJ, Post-translational proteolytic processing of procollagen C-terminal proteinase enhancer releases a metalloproteinase inhibitor, *J. Biol. Chem.* 275 (2000) 1384-1390
- Mudgett JS, Hutchinson NI, Chartrain NA, Forsyth AJ, McDonnell J, Singer II, Bayne EK, Flanagan J, D. Kawka, C.F. Shen, K.Stevens, H. Chen, M. Trumbauer, D.M. Visco, Susceptibility of stromelysin 1-deficient mice to collagen-induced arthritis and cartilage destruction, *Arthritis Rheum.* 41 (1998) 110-121
- Murray GI, Duncan ME, O'Neil P, Melvin WT, Fothergill JE, Matrix metalloproteinase-1 is associated with poor prognosis in colorectal cancer, *Nat. Med.* 2 (1996) 461-462
- Nagase H, Woessner JF, Matrix metalloproteinases, *J. Biol. Chem.* 274 (1999) 21491-21494
- Naka T, Kuester D, Boltze C, Schulz TO, Samii A, Herold C, Ostertag H, Roessner A, Expression of matrix metalloproteinases-1, -2 and-9; tissue inhibitors of matrix metalloproteinase-1 and -2; cathepsin B; urokinase plasminogen activator; and plasminogen activator inhibitor, type I in skull base chordoma, *Hum. Pathol.* 39 (2008) 217-223
- Nemunaitis J, Poole C, Primrose J, Rosemurgy A, Malfetano J, Brown P, Berrington A, Cornish A, Lynch K, Rasmussen H, Kerr D, Cox D, Millar A, Combined analysis of studies of the effects of the matrix metalloproteinase inhibitor marimastat on serum tumor markers in advanced cancer: selection of a biologically active and tolerable dose for longer-term studies, *Clin. Cancer Res.* 4 (1998) 1101-1109
- Neri D, Bicknell R, Tumour vascular targeting, *Nat. Rev. Cancer* 5 (2005) 436-446

- Netzel-Arnett S, Mallya SK, Nagase H, Birkedal-Hansen H, Van Wart HE, Continuously recording fluorescent assays optimized for five human matrix metalloproteinases, *Anal. Biochem.* 195 (1991) 86-92
- Netzer KO, Suzuki K, Itoh Y, Hudson BG, Khalifah RG, Comparative analysis of the noncollagenous NC1 domain of type IV collagen: identification of structural features important for assembly, function, and pathogenesis, *Protein Sci.* 7(1998)1340-1351
- Neuberger MS, Williams GT, Mitchell EB, Jouhal SS, Flanagan JG, Rabbitts TH, A hapten-specific chimaeric IgE antibody with human physiological effector function, *Nature* 314 (1985) 268-270
- Newby AC, Pauschinger M, Spinale FG, From tadpole tails to transgenic mice: Metalloproteinases have brought about a metamorphosis in our understanding of cardiovascular disease, *Cardiovas. Res.* 69 (2006) 559-561
- Nilsson F, Kosmehl H, Zardi L, Neri D, Targeted delivery of tissue factor to the ED-B domain of fibronectin, a marker of angiogenesis, mediates the infarction of solid tumors in mice, *Cancer Res.* 61 (2001) 711-716
- Nimjee SM, Rusconi CP, Sullenger BA, Aptamers: an emerging class of therapeutics, *Annu. Rev. Med.* 56 (2005) 555-583
- Norman TC, Smith DL, Sorger PK, Drees BL, O'Rourke SM, Hughes TR, Roberts CJ, Friend SH, Fields S, Murray AW, Genetic selection of peptide inhibitors of biological pathways, *Science* 285 (1999) 591-595
- North CL, Blacklow SC, Structural independence of ligand-binding modules five and six of the LDL receptor, *Biochemistry.* 38 (1999) 3926-3935
- Nuttall SD, Walsh RB, Display scaffolds: protein engineering for novel therapeutics, *Curr. Opin. Pharmacol.* 8 (2008) 609-615
- Osborn JK, Field A, Wilton J, Derbyshire E, Earnshaw JC, Jones PT, Allen D, McCafferty J, Generation of a panel of related human scFv antibodies with high affinities for human CEA, *Immunotechnology* 2 (1996) 181-196
- Overall CM, Kleifeld O, Tumour microenvironment-opinion: Validating matrix metalloproteinases as drug targets and anti-targets for cancer therapy, *Nat. Rev. Cancer* 6 (2006) 227-239
- Overall CM, Lopez-Otin C, Strategies for MMP inhibition in cancer: innovations for the post-trial era, *Nat. Rev. Cancer* 2 (2002) 657-672
- Padlan EA, Anatomy of the antibody molecule, *Mol. Immunol.* 31 (1994) 169-217
- Panni S, Dente L, Cesareni G, In vitro evolution of recognition specificity mediated by SH3 domains reveals target recognition rules, *J. Biol. Chem.* 277 (2002) 21666-21674
- Patel DJ, Suri AK, Jiang F, Jiang L, Fan P, Kumar RA, Nonin S, Structure, recognition and adaptive binding in RNA aptamer complexes, *J. Mol. Biol.* 272 (1997) 645-664
- Pedersen H, Holder S, Sutherlin DP, Schwitter U, King DS, Schultz PG, A method for directed evolution and functional cloning of enzymes, *Proc. Natl. Acad. Sci. U S A* 95 (1998) 10523-10528
- Pedretti M, Soltermann A, Arni S, Weder W, Neri D, Hillinger S, Comparative immunohistochemistry of L19 and F16 in non-small cell lung cancer and mesothelioma: two human antibodies investigated in clinical trials in patients with cancer, *Lung Cancer* 64 (2009) 28-33
- Pfaffen S, Hemmerle T, Weber M, Neri D, Isolation and characterization of human monoclonal antibodies specific to MMP-1A, MMP-2 and MMP-3, *Exp. Cell. Res.* 316 (2010) 836-847

Pini A, Viti F, Santucci A, Carnemolla B, Zardi L, Neri P, Neri D, Design and use of a phage display library. Human antibodies with subnanomolar affinity against a marker of angiogenesis eluted from a two-dimensional gel, *J. Biol. Chem.* 273 (1998) 21769-21776

Polette M, Gilbert N, Stas I, Nawrocki B, Noël A, Remacle A, Stetler-Stevenson WG, Birembaut P, Foidart M, Gelatinase A expression and localization in human breast cancers. An in situ hybridization study and immunohistochemical detection using confocal microscopy, *Virchows. Arch.* 424 (1994) 641-645

Rajpal A, Beyaz N, Haber L, Cappuccilli G, Yee H, Bhatt RR, Takeuchi T, Lerner RA, Crea R, A general method for greatly improving the affinity of antibodies by using combinatorial libraries, *Proc. Natl. Acad. Sci. U S A* 102 (2005) 8466-8471

Rauchenberger R, Borges E, Thomassen-Wolf E, Rom E, Adar R, Yaniv Y, Malka M, Chumakov I, Kotzer S, Resnitzky D et al, Human combinatorial Fab library yielding specific and functional antibodies against the human fibroblast growth factor receptor 3, *J. Biol. Chem.* 278 (2003) 38194-38205

Rodriguez-Lopez J, Perez-Pampin E, Gomez-Reino JJ, Gonzalez A, Regulatory polymorphisms in extracellular matrix protease genes and susceptibility to rheumatoid arthritis: A case-control study, *Arthritis Res. Ther.* 8 (2006)

Rodriguez-Manzaneque JC, Lane TF, Ortega MA, Hynes RO, Lawler J, Iruela-Arispe ML, Thrombospondin-1 suppresses spontaneous tumor growth and inhibits activation of matrix metalloproteinase-9 and mobilization of vascular endothelial growth factor, *Proc. Natl. Acad. Sci. U S A* 98 (2001) 12485-12490

Roesli C, Borgia B, Schliemann C, Gunthert M, Wunderli-Allenspach H, Giavazzi R, Neri D, Comparative analysis of the membrane proteome of closely related metastatic and nonmetastatic tumor cells, *Cancer Res.* 69 (2009) 5406-5414

Rothe A, Hosse RJ, Power BE, Ribosome display for improved biotherapeutic molecules, *Expert. Opin. Biol. Ther.* 6 (2006) 177-187

Rybak JN, Trachsel E, Scheuermann J, Neri D, Ligand-based vascular targeting of disease, *ChemMedChem* 2 (2007) 22-40

Scherer RL, McIntyre JO, Matrisian LM, Imaging matrix metalloproteinases in cancer, *Cancer Metastasis Rev.* 27 (2008) 679-690

Scheuermann J, Dumelin CE, Melkko S, Zhang Y, Mannocci L, Jaggi M, Sobek J, Neri D, DNA-encoded chemical libraries for the discovery of MMP-3 inhibitors, *Bioconjugate Chem.* 19 (2008) 778-785

Schliemann C, Neri D, Antibody-based targeting of the tumor vasculature, *Biochim. Biophys. Acta.* 1776 (2007) 175-192

Schliemann C, Palumbo A, Zuberbühler K, Villa A, Kaspar M, Trachsel E, Klapper W, Menssen HD, Neri D, Complete eradication of human B-cell lymphoma xenografts using rituximab in combination with the immunocytokine L19-IL2, *Blood* 113 (2008) 2275-2283

Schmitz U, Versmold A, Kaufmann P, Frank HG, Phage display: a molecular tool for the generation of antibodies, *Placenta* 21 (2000) S106-112

Schrama D, Reisfeld RA, Becker JC, Antibody targeted drugs as cancer therapeutics, *Nat. Rev. Drug. Discov.* 5 (2006) 147-159

Shima I, Sasaguri Y, Kusukawa J, Yamana H, Fujita H, Kakegawa T, Morimatsu M, Production of matrix metalloproteinase-2 and metalloproteinase-3 related to malignant behavior of esophageal carcinoma: a clinicopathologic study, *Cancer* 70 (1992) 2747-2753

- Silacci M, Brack S, Schirru G, Mårilind J, Ettore A, Merlo A, Viti F, Neri D, Design, construction and characterization of a large synthetic human antibody phage display library, *Proteomics* 5 (2005) 2340-2350
- Silacci M, Brack SS, Späth N, Buck A, Hillinger S, Arni S, Weder W, Zardi L, Neri D, Human monoclonal antibodies to domain C of tenascin-C selectively target solid tumors in vivo, *Protein Eng. Des. Sel.* 19 (2006) 471-478
- Silence J, Lupu F, Collen D, Lijnen HR, Persistence of atherosclerotic plaque but reduced aneurysm formation in mice with stromelysin-1 (MMP-3) gene inactivation, *Arterioscler. Thromb. Vasc. Biol.* 21 (2001) 1440-1445
- Silverman J, Liu Q, To W, Duguay A, Alba BM, Smith R, Rivas A, Li P, Le H et al. Multivalent avimer proteins evolved by exon shuffling of a family of human receptor domains, *Nat. Biotechnol.* 23 (2005) 1556-1561
- Si-Tayeb K, Monvoisin A, Mazzocco C, Lepreux S, Decossas M, Cubel G, Taras D, Blanc JF, Robinson DR, Rosenbaum J, Matrix metalloproteinase 3 is present in the cell nucleus and is involved in apoptosis, *Am. J. Pathol.* 169 (2006) 1390-1401
- Skerra A, Alternative non-antibody scaffolds for molecular recognition, *Curr. Opin. Biotechnol.* 18 (2007) 295-304. Epub 2007 Jul 20
- Skerra A, Dreher ML Winter G, Filter screening of antibody Fab Fragments secreted from individual bacterial clones: specific detection of antigen binding with a two-membrane system, *Anal. Biochem.* 196 (1991)151–155
- Skerra A, Lipocalins as a scaffold, *Biochim. Biophys. Acta*, 1482 (2000) 337-350
- Smith GP, Filamentous fusion phage: novel expression vectors that display cloned antigens on virion surface, *Science* 228 (1985) 1315-1317
- Sorsa T, Tjaderhane L, Salo T, Matrix metalloproteinases (MMPs) in oral diseases, *Oral Dis.* 10 (2004) 311–318
- Somerville RP, Oblander SA, Apte SS, Matrix metalloproteinases: old dogs with new tricks, *Genome Biol.* 4:216doi:10.1186/gb-2003-4-6-216
- Sottrup-Jensen L, Birkedal-Hansen H, Human fibroblast collagenase-alpha-macroglobulin interactions. Localization of cleavage sites in the bait regions of five mammalian alpha-macroglobulins, *J. Biol. Chem.* 264 (1989) 393-401
- Sternlicht MD, Werb Z, How matrix metalloproteinases regulate cell behavior, *Annu. Rev. Cell Dev. Biol.* 17 (2001) 463-516
- Stetler-Stevenson WG, Progelatinase A activation during tumor cell invasion, *Invasion Metastasis*, 14 (1994) 259-268
- Street HH, Goris ML, Fisher GA, Wessels BW, Cho C, Hernandez C, Zhu HJ, Zhang Y, Nangiana JS, Shan JS, Roberts K, Knox SJ, Phase I study of 131I-chimeric(ch) TNT-1/B monoclonal antibody for the treatment of advanced colon cancer, *Cancer Biother. Radiopharm.* 21 (2006) 243-256
- Takeha S, Fujiyama Y, Bamba T, Sorsa T, Nagura H, Ohtani H, Stromal expression of MMP-9 and urokinase receptor is inversely associated with liver metastasis and with infiltrating growth in human colorectal cancer: a novel approach from immune/inflammatory aspect, *Jpn. J. Cancer. Res.* 88 (1997) 72-81
- Tawfik DS, Griffiths AD, Man-made cell-like compartments for molecular evolution, *Nat. Biotechnol.* 16 (1998) 652-656

- Temma T, Sano K, Kuge Y, Kamihashi J, Takai N, Ogawa Y, Saji H, Development of a radiolabeled probe for detecting membrane type-1 matrix metalloproteinase on malignant tumors, *Biol. Pharm. Bull.* 32 (2009) 1272-1277
- Tomlinson IM, Walter G, Marks JD, Llewelyn MB, Winter G, The repertoire of human germline VH sequences reveals about fifty groups of VH segments with different hypervariable loops, *J. Mol. Biol.* 227 (1992) 776-798
- Trachsel E, Bootz F, Silacci M, Kaspar M, Kosmehl H, Neri D, Antibody-mediated delivery of IL-10 inhibits the progression of established collagen-induced arthritis, *Arthritis Res. Ther.* 9 (2007) R9
- Tsuruda T, Costello-Boerrigter LC, Burnett JC, Matrix metalloproteinases: Pathways of induction by bioactive molecules, *Heart Failure Rev.* 9 (2004) 53-61
- Vartak DG, Gemeinhart RA, Matrix metalloproteases: underutilized targets for drug delivery, *J. Drug. Target.* 15 (2007) 1-20
- Villa A, Trachsel E, Kaspar M, Schliemann C, Som mavilla R, Rybak JN, Rösli C, Borsi L, Neri D, A high-affinity human monoclonal antibody specific to the alternatively spliced EDA domain of fibronectin efficiently targets tumor neo-vasculature in vivo, *Int. J. Cancer* 122 (2008) 2405-13
- Vincenti MP, Brinckerhoff CE, Transcriptional regulation of collagenase (MMP-1, MMP-13) genes in arthritis: integration of complex signaling pathways for the recruitment of gene-specific transcription factors, *Arthritis Res.* 4 (2002) 157-164
- Viti F, Nilsson F, Demartis S, Huber A, Neri D, Design and use of phage display libraries for the selection of antibodies and enzymes, *Methods Enzymol.* 326 (2000) 480-505
- Wang GY, Bergman MR, Nguyen AP, Turcato S, Swigart PM, Rodrigo MC, Simpson PC, Karliner JS, Lovett DH, Baker AJ, Cardiac transgenic matrix metalloproteinase-2 expression directly induces impaired contractility, *Cardiovasc. Res.* 69 (2006) 688-696
- Ward ES, Gussow D, Griffiths AD, Jones PT, Winter G, Binding activities of a repertoire of single immunoglobulin variable domains secreted from *Escherichia coli*, *Nature* 341 (1989) 544-546
- Weiner LM, Fully human therapeutic monoclonal antibodies, *J. Immunother.* 29 (2006) 1-9
- Weissleder R, Ntziachristos V, Shedding light onto live molecular targets, *Nature Med.* 1 (2003) 123-128
- Weissleder R, Tung CH, Mahmood U, Bogdanov A Jr, In vivo imaging of tumors with protease-activated near-infrared fluorescent probes, *Nat Biotechnol.* 17 (1999) 375-378
- Werb Z, ECM and cell surface proteolysis: regulating cellular ecology, *Cell* 91 (1997) 439-442
- Whittaker M, Floyd CD, Brown P, Gearing AJ, Design and therapeutic application of matrix metalloproteinase inhibitors, *Chem. Rev.* 99 (1999) 2735-76
- Winter G, Milstein C, Man-made antibodies, *Nature* 349 (1991) 293-299
- Wong JY, Chu DZ, Williams LE, Yamauchi DM, Ikle DN, Kwok CS, Liu A, Wilczynski S, Colcher D, Yazaki PJ, Shively JE, Wu AM, Raubitschek AA, Pilot trial evaluating an 123I-labeled 80-kilodalton engineered anticarcinoembryonic antigen antibody fragment (cT84.66 minibody) in patients with colorectal cancer, *Clin. Cancer Res.* 10 (2004) 5014-5021
- Wu AM, Yazaki PJ, Designer genes: recombinant antibody fragments for biological imaging, *Q. J. Nucl. Med.* 44 (2000) 268-283.
- Yang W, Arai S, Gorrin-Rivas MJ, Mori A, Onodera H, Imamura M, Human macrophage metalloelastase gene expression in colorectal carcinoma and its clinicopathologic significance, *Cancer* 91(2001) 1277-1283

Yang Z, Strickland DK, Bornstein P, Extracellular matrix metalloproteinase 2 levels are regulated by the low density lipoprotein-related scavenger receptor and thrombospondin 2, *J. Biol. Chem.* 276 (2001) 8403-8408

Ye S, Dhillon S, Turner SJ, Bateman AC, Theaker JM, Pickering RM, Day I, Howell WM, Invasiveness of cutaneous malignant melanoma is influenced by matrix metalloproteinase 1 gene polymorphism, *Cancer Res.* 61 (2001) 1296-1298

Ye S, Eriksson P, Hamsten A, Kurkinen M, Humphries SE, Henney AM, Progression of coronary atherosclerosis is associated with a common genetic variant of the human stromelysin-1 promoter which results in reduced gene expression, *J. Biol. Chem.* 271(1996) 13055-13060

Yelton DE, Rosok MJ, Cruz G, Cosand WL, Bajorath J, Hellström I, Hellström KE, Huse WD, Glaser SM, Affinity maturation of the BR96 anti-carcinoma antibody by codon-based mutagenesis, *J. Immunol.* 155 (1995) 1994-2004

Yoshihara Y, Nakamura H, Obata K, Yamada H, Hayakawa T, Fujikawa K, Okada Y, Matrix metalloproteinases and tissue inhibitors of metalloproteinases in synovial fluids from patients with rheumatoid arthritis or osteoarthritis, *Ann. Rheum. Dis.* 59 (2000) 455-461

Yoshiji H, Harris SR, Raso E, Gomez DE, Lindsay CK, Shibuya M, Sinha CC, Thorgeirsson UP, Mammary carcinoma cells over-expressing tissue inhibitor of metalloproteinases-1 show enhanced vascular endothelial growth factor expression, *Int. J. Cancer* 75 (1998) 81-87

Yu W-H, Woessner JF Jr., McNeish JD, Stamenkovic I, CD44 anchors the assembly of matrilysin/MMP-7 with heparin-binding epidermal growth factor precursor and ErbB4 and regulates female productive organ remodeling, *Genes Dev.* 16 (2002) 307-323

Zheng QH, Fei X, Liu X, Wang JQ, Bin SH, Mock, BH, et al., Synthesis and preliminary biological evaluation of MMP inhibitor radiotracers [<sup>11</sup>C]methyl-halo-CGS 27023A analogs, new potential PET breast cancer imaging agents. *Nucl. Med. Biol.* 7 (2002) 761-770

Zhu Y, Spitz MR, Lei L, Mills GB, Wu X, A single nucleotide polymorphism in the matrix metalloproteinase-1 promoter enhances lung cancer susceptibility, *Cancer Res.* 61 (2001) 7825-7829

Zuberbühler K, Palumbo A, Bacci C, Giovannoni L, Somavilla R, Kaspar M, Trachsel E, Neri D, A general method for the selection of high-level scFv and IgG antibody expression by stably transfected mammalian cells, *Protein Eng. Des. Sel.* 22 (2009) 169-174



## 7 ABBREVIATIONS

<b>%ID/g</b>	percent injected dose per gram
<b>°C</b>	Celsius
<b>µg</b>	microgram
<b>5E</b>	antibody specific to MMP-1A
<b>786-O</b>	human renal cell carcinoma cell line
<b>9H</b>	antibody specific to MMP-3
<b>A</b>	adenosine
<b>A375</b>	human melanoma cell line
<b>B16</b>	murine melanoma cell line
<b>BiTE</b>	bispecific single chain variable fragment fused by a peptide linker
<b>Brij</b>	polyalkylglycoether
<b>C</b>	catalytic domain
<b>Caki-1</b>	human kidney clear cell carcinoma cell line
<b>CD31</b>	cluster of differentiation molecule, PECAM-1
<b>cDNA</b>	complementary DNA
<b>CDR</b>	complementary determining region
<b>CHO</b>	chinese hamster ovary cell line
<b>cpm</b>	counts per minute
<b>ctrl</b>	control
<b>dAb</b>	domain antibody
<b>DAF</b>	decay accelerating factor
<b>DAPI</b>	4',6-Diamidin-2-phenylindol
<b>DARPin</b>	designed ankyrin repeat proteins
<b>dg</b>	deglycosylated
<b>DMEM</b>	Dulbecco's modified Eagle medium
<b>DMSO</b>	dimethyl sulfoxid
<b>DNA</b>	desoxyribonucleic acid
<b>E</b>	initial enzyme concentration
<b>E. coli</b>	Escherichia coli
<b>ECM</b>	extracellular matrix
<b>EDB</b>	extra-domain B of fibronectin
<b>ELISA</b>	enzyme-linked immunosorbent assay
<b>EMMPRIN</b>	extracellular matrix metalloproteinase inducer

<b>EMT</b>	epithelial mesenchymal transmission
<b>F9</b>	murine teratocarcinoma cell line
<b>Fab</b>	fragment antigen binding
<b>FACS</b>	fluorescent activated cell sorting
<b>FCS</b>	fetal calf serum
<b>FDA</b>	food and drug administration
<b>G</b>	guanine
<b>Gd</b>	Gadolinium
<b>GPI</b>	glycosyl phosphatidyl inositol
<b>H</b>	hinge region
<b>h</b>	hours
<b>H460</b>	human lung carcinoma cell line
<b>HAE</b>	hereditary angioedema
<b>HcAb</b>	heavy chain antibody
<b>HCC</b>	hepatocellular carcinoma
<b>HP</b>	hemopexin-like domain
<b>HyHel-10</b>	antibody specific to hen egg lysozyme
<b>i.v.</b>	intravenous
<b>IgG</b>	Immunoglobuline G
<b>IL</b>	interleukine
<b><math>k_{cat}</math></b>	turnover number
<b><math>K_D</math></b>	dissociation constant
<b>kDa</b>	kilo dalton
<b>keV</b>	kilo electron volt
<b><math>K_M</math></b>	Michaelis-Menten constant
<b><math>k_{on}</math></b>	kinetic association constant
<b><math>k_{off}</math></b>	kinetic dissociation constant
<b>L19</b>	antibody specific to the extra-domain B of fibronectin, currently in clinical trials
<b>M</b>	molar
<b>M</b>	molecular weight marker
<b>mAb</b>	monoclonal antibody
<b>MEM</b>	minimum essential medium Eagle
<b>min</b>	minutes
<b>ml</b>	milliliter
<b>MMP</b>	matrix metalloproteinase
<b>MMP-1</b>	matrix metalloproteinase 1

<b>MMP-1A</b>	matrix metalloproteinase 1A
<b>MMP-2</b>	matrix metalloproteinase 2
<b>MMP-3</b>	matrix metalloproteinase 3
<b>MMPI</b>	matrix metalloproteinase inhibitor
<b>MRI</b>	magnetic resonance imaging
<b>mRNA</b>	messenger ribonucleic acid
<b>MT- MMP</b>	membrane type matrix metalloproteinase
<b>ng</b>	nanogram
<b>Ni-NTA</b>	Nickel Nitrilo-triacetic Acid
<b>nM</b>	nanomolar
<b>nm</b>	nanometer
<b>NR</b>	non-reducing conditions
<b>NTA</b>	Nickel Nitrilo-triacetic Acid
<b>OIM</b>	optical imaging
<b>P</b>	propeptide
<b>PBS</b>	phosphate buffered saline
<b>pcDNA3.1</b>	mammalian expression vector
<b>PCR</b>	polymerase chain reaction
<b>PET</b>	positron emission tomography
<b>pHEN-1</b>	phagemid vector
<b>pQE12</b>	bacterial expression vector
<b>proMMP</b>	inactive zymogen
<b>R</b>	reducing conditions
<b>RCC</b>	renal cell carcinoma cell line
<b>RNA</b>	ribonucleic acid
<b>rpm</b>	rounds per minute
<b>RPMI</b>	Roswell Park Memorial Institute medium
<b>RT</b>	room temperature
<b>RT-PCR</b>	reverse transcriptase polymerase chain reaction
<b>S</b>	initial substrate concentration
<b>s</b>	second
<b>scFv</b>	single chain variable fragment (antibody fragment)
<b>sdAb</b>	single domain antibody
<b>SDS-PAGE</b>	sodium dodecylsulfate polyacrylamide gel electrophoresis
<b>S.E.</b>	standard error
<b>SIP</b>	small immuno protein
<b>SKOV-3</b>	human ovarian carcinoma cell line

<b>SNP</b>	single nucleotide polymorphism
<b>SP</b>	signal peptide
<b>SP1</b>	antibody specific to MMP-1A
<b>SP2</b>	antibody specific to MMP-2
<b>SP3</b>	antibody specific to MMP-3
<b>SPECT</b>	single photon emission computed tomography
<b>SPR</b>	surface plasmon resonance
<b>TBS</b>	Tris buffered saline
<b>TEA</b>	triethylamine
<b>TG-1</b>	termite group 1 bacteria
<b>TIMP</b>	tissue inhibitor of matrix metalloproteinases
<b>Tris-CI</b>	Tris(hydroxymethyl)-aminomethan
<b>U87</b>	human glioblastoma multiforma cell line
<b>v</b>	initial velocity
<b>VEGF</b>	vascular endothelial growth factor
<b>VEGF-R2</b>	vascular endothelial growth factor receptor 2
<b>VH</b>	variable heavy chain
<b>VL</b>	variable light chain

## 8 CURRICULUM VITAE

Stefanie PFAFFEN



### PERSONAL INFORMATION

---

Date of birth                May 29, 1980, Visp (VS), Switzerland

Nationality                 Swiss

Marital Status             Unmarried

Languages                 German                     native  
                                  English                     fluent  
                                  French                     good knowledge  
                                  Italian                     basic knowledge

Business address         Institute of Pharmaceutical Sciences  
                                  ETH Zurich  
                                  Wolfgang-Pauli-Str. 10  
                                  8093 Zurich  
                                  Switzerland  
                                  Phone: +41 44 633 74 18  
                                  Fax:     +41 44 633 13 58  
                                  stefanie.pfaffen@pharma.ethz.ch

Home address             Riedhofstr. 57  
                                  8049 Zurich  
                                  Switzerland  
                                  Phone: +41 43 343 13 24  
                                  Mobile: +41 79 694 99 83

### EDUCATION

---

2006-present             **PhD thesis** in the group of Prof. Dr. Dario Neri on the topic  
                                  “**Human monoclonal antibodies for the targeting of matrix metalloproteinases**”  
                                  Institute of Pharmaceutical Sciences, ETH Zurich, Switzerland

2006-present             Member of the PhD student program Cancer Network Zurich (CNZ)

2000-2005                 Studies in Pharmaceutical Sciences, ETH Zurich, Switzerland  
                                  Graduated:     **Eidg. Dipl. Apotheker ETH**  
   **Diploma of Pharmaceutical Sciences**  
   (average mark: 5.7 / 6.0)

2004                         **Diploma thesis** in the group of Prof. Dr. Dario Neri on the topic  
                                  “**Optimization of the *in vivo* biotinylation technology for the discovery of accessible tissue-specific markers**”  
                                  Institute of Pharmaceutical Sciences, ETH Zurich, Switzerland

1995-2000                      **Swiss Matura B**, Kollegium Spiritus Sanctus, Brig, Switzerland

## **WORK EXPERIENCE**

---

2008                              Organization of the 3<sup>rd</sup> Experimental Course on Antibody Phage Technology including a demonstration on the colony picking robot  
Institute of Pharmaceutical Sciences, ETH Zurich

2006-2009                      Supervision of two master students and practical training of a biology technician during my PhD

2006-2009                      Teaching of practical courses “Medicinal chemistry” and “Anatomy of the rat” for pharmacy students,  
Institute of Pharmaceutical Sciences, ETH Zurich

2006-2009                      Saturday’s service as **pharmacist**, Tödi-Apotheke, Zurich  
(D. Schorno)

2005                              **Pharmacist**, Tödi-Apotheke, Zurich

2004-2005                      Practical course, Tödi-Apotheke, Zurich

2000-2004                      Saturday’s and Sunday’s service as organist, Stalden (VS)

## **AWARDS**

---

2005                              ETH medal for the diploma thesis

2000                              Award of the LONZA group (Visp) for the best Matura mark in chemistry (6.0 / 6.0)

## **RESEARCH FELLOWSHIPS**

---

2006-2007                      Research fellowship of the Roche Research Foundation for the 1<sup>st</sup> year salary as PhD student

## **PUBLICATIONS**

---

**Pfaffen S**, Hemmerle T, Weber M, Neri D, Isolation and characterization of human monoclonal antibodies specific to MMP-1A, MMP-2 and MMP-3, *Exp. Cell Res.* **316** (2010) 836-847

**Pfaffen S**, Frey K, Stutz I, Roesli C, Neri D, Tumor targeting properties of antibodies specific to MMP-1A, MMP-2 and MMP-3”, *Eur. J. Nucl. Med. Mol. Imaging* (2010) *in press*

Sgier D, Zuberbühler K, **Pfaffen S**, Neri D, Isolation and characterization of an inhibitory human monoclonal antibody specific to the urokinase-type activator uPA, *Protein Eng. Des. Sel.* (2010) *in press*

## **PRESENTATIONS AND POSTERS**

---

Oral presentation at the students' retreat of the Cancer Network Zurich (CNZ), March 2009

Oral presentation at the „Doktorandentag“ of the Institute of Pharmaceutical Sciences, ETH Zurich, September 2008

Poster at the students' retreat of the Cancer Network Zurich (CNZ), January 2008

Oral presentation at the students' retreat of the Cancer Network Zurich (CNZ), 2007

## **PERSONAL INTERESTS**

---

Snowboarding, swimming, playing the piano, reading

## **REFERENCES**

---

### **Prof. Dr. Dario Neri**

Institute of Pharmaceutical Sciences  
ETH Zurich  
Wolfgang-Pauli-Str. 10  
8093 Zurich, Switzerland

[neri@pharma.ethz.ch](mailto:neri@pharma.ethz.ch)

Phone: +41 44 633 74 01  
+41 44 633 74 02 (secretary)

### **Daniel Schorno**

Eidg. Dipl. Apotheker ETH  
Tödi-Apotheke  
Pharmacie Internationale  
Bleicherweg / Tödistr. 46  
8002 Zurich, Switzerland

[toedi-apotheke@ovan.ch](mailto:toedi-apotheke@ovan.ch)

Phone: +41 44 201 37 47

## 9 ACKNOWLEDGEMENTS

First I would like to express my gratitude to Prof. Dario Neri for giving me the opportunity to perform my Ph.D. studies in his laboratory and for supporting me throughout these four years. Despite his immense workload, Prof. Dario Neri always found the time for discussing my projects and providing valuable assistance.

I am grateful to Prof. Roger Schibli who kindly accepted to be my co-examiner.

Special thank goes to former and current lab members of the Neri lab for the warm working atmosphere. I would like to especially thank Dr. Julia Ahlskog and Dr. Alessandra Villa for introducing me to the phage display and protein engineering technology, to Katharina Frey for her great assistance in animal studies, to Dr. Jörg Scheuermann for his help with the MMP activity assay and to Dr. Christoph Rösli for his assistance with the laser scanning microscope.

I would like to thank my master students Marcel Weber and Teresa Hemmerle and my biology technician apprentice Irène Frey for their contribution to my work.

Finally, I would like to thank my parents and my sister for their love and great support during my whole studies. A whole-hearted thank-you goes to Dragan who encouraged me every day with his enthusiasm and his humor and his helpful suggestions in respect of research.